MODELING AND OPTIMIZATION OF WIRE ELECTRO DISCHARGE MACHINING (WEDM) OF AL 7075

Submitted by

KINGSHUK MANDAL

DOCTOR OF PHILOSOPHY (Engineering)

DEPARTMENT OF PRODUCTION ENGINEERING

FACULTY COUNCIL OF ENGINEERING & TECHNOLOGY

JADAVPUR UNIVERSITY

KOLKATA-700032 INDIA

2023

JADAVPUR UNIVERSITY

KOLKATA-700032

Index No. 210/16/E

Registration No. 1021616001

TITLE OF THE Ph.D. (Engg.) THESIS:

Modeling and Optimization of Wire Electro Discharge Machining (WEDM) of Al 7075

NAME, INSTITUTE & DESIGNATIONS OF THE SUPERVISORS:

(i) Professor (Dr.) Soumya Sarkar
Professor, Department of Production Engineering,
Jadavpur University,
Kolkata – 700032, West Bengal, INDIA.

(ii) Professor (Dr.) Souren Mitra
Professor, Department of Production Engineering,
Jadavpur University,
Kolkata – 700032, West Bengal, INDIA.

(iii) Professor (Dr.) Dipankar Bose
Professor, Department of Mechanical Engineering,
National Institute of Technical Teachers' Training and Research (NITTTR),
Kolkata – 700106, West Bengal, INDIA.

PUBLICATIONS IN WEDM

(a) List of international refereed journals:

1. "Influence of dielectric conductivity on corner error in wire electrical discharge machining of Al 7075 alloy", Proceedings of the Institute of Mechanical Engineers, Part C: Journal of Mechanical Engineering Science, (2021), Vol. 235(20), pp. 5043-5056.
2. "Experimental investigation of process parameters in WEDM of Al 7075 alloy", Manufacturing Review, (2020), Vol. 7(30), pp. 1-9.
3. "Statistical analysis of process parameters and multi-objective optimization in wire electrical discharge machining of Al 7075 using weight-based constrained algorithm", International Journal on Interactive Design and Manufacturing, (2022), https://doi.org/10.1007/s12008-022-01120-8.
4. "Impact of dielectric conductivity and other process parameters on machining characteristics in WEDM of al 6065 alloy", Journal of Advanced Manufacturing Systems, (2022), https://doi.org/10.1142/S0219686723500415.
5. "Multi-Attribute Optimization in WEDM of Light Metal Alloy" Materials Today: Proceedings, (2019), Vol. 18(7), pp. 3492–3500.
6. "Parametric analysis and GRA approach in WEDM of Al 7075 alloy", Materials Today: Proceedings, (2020), Vol. 26(2), pp. 660–664.
7. "MOGA approach in WEDM of advanced aluminium alloy" Materials Today: Proceedings, (2020), Vol. 26(2), pp. 887-890.
8. "Surface roughness and surface topography evaluation of Al 6065-T6 alloy using wire electro-discharge machining (wire EDM)", Advances in Materials Processing and Technologies, (2020), Vol. 6(1), pp. 75-83.

(b) List of international conferences:

1. "Surface roughness and surface topography evaluation of aluminum alloy using Wire Electro Discharge Machining (wire-EDM) process",20th Edition of International Conference on Advances in Materials and processing Technologies (AMPT-2017), 11th -14th December 2017, VIT University- Chennai, INDIA.
2. "Analysis of wire-EDM input parameters on kerf width and surface integrity for Al 6061 alloy", International Conference on Energy, Materials and Information

Technology (ICEMIT-2017), 23rd -24th December 2017, Amity University Ranchi, City Campus, Ranchi, INDIA.

3. "Multi-Attribute Optimization in WEDM of Light Metal Alloy" 9th International Conference of Materials Processing and Characterization (ICMPC-2019), 8th – 10th March 2019, Gokaraju Rangaraju Institute of Engineering and Technology (GRIET), Hyderabad, Telangana.
4. "Influence of the variable process parameters on high conductive new generation aluminum alloy in WEDM" 40th International MATADOR Conference on Advanced Manufacturing, 8-10th July 2019, Sailing International Hotel, Hangzhou-310023, China.
5. "Parametric analysis and GRA approach in WEDM of Al 7075 alloy", 10th International Conference of Materials Processing and Characterization (ICMPC-2020), 21st – 23rd February 2020, GLA University Mathura, Uttar Pradesh, India.
6. "Analysis of Surface Roughness and Topography of Aluminum Alloy (Al 7075) Machined by WEDM" International Conference on Advancements in Mechanical Engineering (ICAME 2020), 16-18th January 2020, Aliah University, Kolkata.

(c) List of book chapters:

1. Book title: Innovation in Materials Science and Engineering
   Chapter name: "Analysis of Wire-EDM Input Parameters on Kerf Width and Surface Integrity for Al 6061 Alloy"
   ISBN: 978-981-13-2943-2
   Publisher: Springer Nature Singapore
2. Book title: Machine Learning Applications in Non-Conventional Machining Processes
   Chapter name: "Multi-Objective Optimization in WEDM of Al 7075 Alloy Using TOPSIS and GRA Method"
   ISBN: 9781799836247
   Publisher: IGI Global

(d) List of patents: NIL

Statement of Originality

I Kingshuk Mandal registered on 5th February 2016 do hereby declare that this thesis entitled "Modeling and Optimization of Wire Electro Discharge Machining (WEDM) of Al 7075" contains literature survey and original research work done by the undersigned candidate as part of doctoral studies.

All information in this thesis have been obtained and presented in accordance with existing academic rules and ethical conduct. I declare that, as required by these rules and conduct, I have fully cited and referred all materials and results that are not original to this work.

I also declare that I have checked this thesis as per the "Policy on Anti Plagiarism, Jadavpur University, 2019", and the level of similarity as checked by iThenticate software is **4%.**

……. Date: 23.06.2023
Kingshuk Mandal

Certified by Supervisor(s):
(Signature with date and seal)

1. Professor (Dr.) Soumya Sarkar, Production Engineering Department, Jadavpur University, Kolkata-700032.

2. Professor (Dr.) Souren Mitra, Production Engineering Department, Jadavpur University, Kolkata-700032.

3. Professor (Dr.) Dipankar Bose, Mechanical Engineering Department, NITTTR-Kolkata, Kolkata-700106.

CERTIFICATE FROM THE SUPERVISORS

*This is to certify that the thesis entitled "**Modeling and Optimization of Wire Electro Discharge Machining (WEDM) of Al 7075**" submitted by Shri. Kingshuk Mandal, who got his name registered on 5th February 2016 for the award of Ph.D. (Engg.) degree of Jadavpur University is absolutely based upon his own work under the supervision of Professor Soumya Sarkar, Professor Souren Mitra and Professor Dipankar Bose that neither this thesis nor any part of the thesis has been submitted for any degree/diploma or any other academic award anywhere before.*

---	---	---
Signature of the Supervisor and date with official seal	Signature of the Supervisor and date with official seal	Signature of the Supervisor and date with official seal
Prof. (Dr.) Soumya Sarkar Prod. Engg. Dept. Jadavpur University Kolkata-700032.	Prof. (Dr.) Souren Mitra Prod. Engg. Dept. Jadavpur University Kolkata-700032.	Prof. (Dr.) Dipankar Bose Mech. Engg. Dept. NITTTR-Kolkata Kolkata-700106.

PREFACE

Wire electro-discharge machining (WEDM) has been found to be an incredible non-conventional machining process. This proficient machining technique can machine any kind of electrically conductive material, irrespective of its chemical and mechanical properties. This advanced machining process is capable of manufacturing intricate shapes and sizes with a decent surface quality that is very difficult to produce by conventional methods. Since the introduction of this advanced process, WEDM has grown from a simple means of making tool and die to the best alternative for producing micro-scale parts with precise dimensional accuracy and surface quality. Some other common applications of WEDM include fabrication of stamping and extrusion tools and dies, fixtures and gauges, prototypes, manufacturing of cam wheels and grinding wheel form tools. However, further enhancements are still required to meet the growing demand for products with high precision and accuracy in those sectors of manufacturing. Therefore, the results in achieving good surface quality and accuracy of parts have become the most desirable performances in this process.

In WEDM, the material erosion mechanism occurred due to the melting and evaporation of material. Heat generation in plasma channel takes place due to the avalanched motion of electrons. A spark is formed between the electrode (wire) and the workpiece through dielectric liquid (deionized water). The electrical conductivity of the dielectric liquid plays a crucial role in determining the material removal in WEDM. The conductivity of the dielectric liquid directly determines the sustainability of the plasma channel in inter electrode gap (IEG). It is a common fact that the cutting speed increases in WEDM when the electrical conductivity of the dielectric increases. It plays a very important role when materials to be machined having higher conductivity (more than conventional materials like steel and alloys).

During machining in WEDM, the electrode (wire) naturally bends like a parabola, which makes the electrode lose its ideal straight position as the wire is thin and flexible due to gap force. This wire deflection from the ideal straight position while machining is termed "wire bending" or "wire lag." Hence, the corner error presence in the curved profile is increased. This wire bending effect creates a dimensional inaccuracy on the work surface to be machined; this, for some specific applications, becomes undesirable. There is no such method for the exact measurement of the exact value of wire bending or wire lag under various machining conditions. Still, now it is a major obstruction towards accuracy improvement in WEDM products.

In the present research, multipass cutting followed by single-pass cutting has been carried out on an Al 7075 work piece. An experimental investigation was carried out for parametric analysis of various important response factors, including "cutting speed," "corner error," "surface roughness," and "overcut." Mathematical models are developed by using non-linear regression techniques for analysis. Finally, optimization is also carried out to find the optimum parametric combination for various process requirements. Total research work mainly divided into three major phases. The phases of research work are given as follows:

Phase-I

- To study the major influencing factors and their ranges by conducting pilot (preliminary) experiments.
- To find out the appropriate conductivity setting that is suitable for efficient machining of Al 7075.

Phase-II

- To study the influence of dielectric conductivity in single pass (rough) cutting operation.
- To study the impact of four independent process parameters like open circuit voltage (V_{OC}), pulse on time (T_{ON}), pulse frequency (f_P) and servo sensitivity (S_C) on corner accuracy and surface finish.
- To prepare an optimal chart for efficient machining of Al 7075 this is very useful for shop floor operator.

Phase-III

- To develop a new machining strategy for rough and trim cutting operation.
- To carry out three successive trim cuts over the rough cut to enhance the dimensional accuracy and surface quality.
- To study the comparative performance of corner accuracy and surface finish in different cutting condition (i.e., rough & trim).
- To study the surface topography and surface characteristics of rough and trim cut surfaces.

The entire thesis has various purposes, and in order to demonstrate each objective, the thesis is divided into seven chapters, from Chapter 1 to Chapter 7.

In Chapter-1, general introduction and basic principle of Wire Electrical Discharge Machining Process are elaborately explained. Additionally, chemical properties, mechanical property, special applications of Al 7075 alloy are also described.

Review of past literature, existing knowledge gap, objectives of present research work is given in the Chapter-2. WEDM areas are categorized into three major groups' namely process parameter analysis, parametric modelling and optimization and the last one is accuracy and surface quality improvement. In the context of present research study above three areas are reviewed.

Chapter-3 deals with the structural and operational features of WEDM system. Hardware unit and software are the main features in a WEDM system. Hardware unit consists of machine tool unit, power supply unit and dielectric supply unit whereas software is used for part programming. Additionally, some important machining features like single pass, multipass cutting and wire diameter compensation are also highlighted in this chapter.

In Chapter-4, preliminary investigation of machining parameters at default conductivity setting has been carried out to determine the major influencing factor for machining of Al 7075. In this chapter, influence of seven control factors such as pulse on time (T_{on}), arc on time (A_{on}), pulse off time (T_{off}), arc off time (A_{off}), servo sensitivity (S_c), wire tension (W_t) and servo voltage (S_v) on machining speed (V_c), corner error (C_e) and surface roughness (R_a) has been reported.

Chapter-5 deals with the parametric analysis based on Taguchi Methodology of various important response factors, including cutting speed, corner error, surface roughness and overcut. Additionally, influence of dielectric conductivity has been studied through developed mathematical models. Three different set of experiments in three different conductivity setting have carried out using L_9 orthogonal array. Four independent control factors open circuit voltage, pulse on time, pulse frequency and servo sensitivity have been studied to establish the trends of variation of all important machining criteria keeping other control factors constant. Nonlinear regression technique is used to predict the responses for any arbitrary level of dielectric conductivity. Apart from this, an attempt has been made to optimize the WEDM process using constrained Pareto algorithm. Instead of regular approach to finding the optimal solution among the limited combination of input factors used in the experimental study; all possible combinations have been explored to find out the optimal solution. For this purpose regression models are used to predict response factors. Then the

required optimal combinations are searched out from all these combinations by using the constrained Pareto algorithm.

In Chapter-6, a new machining strategy has been developed for rough and trim cutting operations. The improvement of corner accuracy and surface finish through successive three trim cutting operations has also been investigated. Total four different set of experiments have been carried out for rough and trim cutting operations. Trim cutting process parameters i.e. $(T_{ON})_1$, $(T_{ON})_2$, $(T_{ON})_3$ & $(WO)_{E1}$, $(WO)_{E2}$, $(WO)_{E3}$ are varied in trim cutting set of experiments. It is perceived that the number of passes improved the corner accuracy and surface finish. It is also observed that the accuracy and finish are not only depends on the number of passes but also considerably influenced by the trim cutting process parameters.

Chapter-7 contains the summary and general conclusions of the entire research work. At the end of this chapter, some future scope of research area is mentioned.

The present research findings will give a new path to the modern manufacturing industries. The original and practical research work in the area of dielectric conductivity and multi pass cutting are useful to the present manufacturing industries and R&D organization to revolutionize the domain of accuracy and precision in the field of WEDM.

ACKNOWLEDGEMENT

Research work throughout last few years help me a lot to gain some new understanding and precious experience. The valuable work leading to the doctorate of philosophy (PhD) is impossible without help and support from many people and organization. At the very beginning, I would like to convey my warm gratitude and enthusiastic admiration to my PhD supervisors Professor (Dr.) Soumya Sarkar and Professor (Dr.) Souren Mitra, Production Engineering Department, Jadavpur University, Kolkata for their passionate guidance, valuable suggestions and constant support which are very much essential for the completion of my research work. I am so much grateful to both of them for their constant inspiration and consisting support through the inevitable ups and downs during the research and of course continuous caring to focus and giving some fruitful advice in all aspects of my entire research. I always appreciate their contributions of valuable time, new ideas and keen interest to make my research experience fertile and motivating. And of course, it is an honour to me to be their PhD student.

I would like to express my deepest gratitude for the inspiration, encouragement and guidance that I received from my other PhD supervisor Professor (Dr.) Dipankar Bose, NITTTR-Kolkata for successful completion of this thesis.

My sincere appreciation and thanks to Professor (Dr.) Bijoy Bhattacharyya, HOD Production Engineering, for his generous assistance and support in every stage of my research work. Thanks to other faculty members especially Professor B. Sarkar, Professor A. S. Kuar, Professor A. K. Dutta, Associate Professor S. K. Debnath and Associate Professor B. R. Sarkar of Production Engineering Department, for extending all kind of help.

I also express my deep respect to Dr. Mukandar Sekh, Assistant Professor of Aliah University, Kolkata. I am greatly thankful to him for allowing me to complete my PhD work. I also acknowledge the co-operation and encouragement to Mr. Biswanath Das, Mr. Anwar Sadat Ali, Mr. Sukamal Manna and Mr. Safirul Seikh of Aliah University for their cooperation.

Author gratefully acknowledges the Centre of Advanced Study (CAS) –Phase V Programme of the University Grants Commission (UGC), New Delhi for their support, and Department of Production Engineering, Jadavpur University for providing the laboratory facilities. I also acknowledge the financial assistance provided by Jadavpur University under State

Government Departmental Fellowship Scheme and centre of excellence scholarship funded by TEQIP-III of Jadavpur University during the course of research study. Thanks are also extended to FET office and research section for their cordial assistance and administrative supports.

I would like to convey my deepest and heartfelt thanks to my seniors, juniors and my fellow colleagues Dr. Nilanjan Roy, Dr. Abhishek Sen, Dr. Subhrajit Debnath, Dr. Sandip Kunar, Dr. Debal Pramanik, Mr. Subham Biswas, Md. Sahjahan Biswas, Mr. Dhrubajoti Bannerjee, Mr. Arka Mandal, Mr. Pritthiraj Roy, Dr. Koushik Mishra, Mr. Sudip Santra, Mr. Dhiraj Kumar, Mr. Santosh Kumar whose whole hearted support and cooperation in all spheres of activities during my entire tenure will remain in my memory.

Although it could not simply be expressed by words, I would like to thank my father Mr. Mahadeb Mandal and mother Mrs. Sabitri Mandal for their belief in education and endless support for education, uncle Mr. Sadananda Mandal & Mr. Joydeb mandal and aunty Mrs. Purnima Mandal & Mrs. Shiuli Mandal for their warm wishes, little brothers (Mithu, Bittu, Guddu & Jhanu) and all the family members for their constant encouragement and support in the pursuit of this research work, without their understanding none of this would have been possible. Author is also thankful to late grandfather Mr. Mahanta Gope Mandal and grandmother Mrs. Malati Gope Mandal who always encouraged for higher studies.

Last, but not the least, there are limitless worth names, which deserve mention here, but it could not be possible to include in this section due to space constraints. I acknowledge their valuable contribution with gratitude.

Kingshuk Mandal Date: 23.06.2023

VITA

The author, Kingshuk Mandal, son of Mr. Mahadeb Mandal and Mrs. Sabitri Mandal, was born on 20th February 1988 in Bankura, West Bengal. He passed Secondary Examination under West Bengal Board of Secondary Education from Dhanara High School, Ranibandh, Bankura in 2003 and Higher Secondary under West Bengal Council of Higher Secondary Education from Saldiha High School, Indpur, Bankura in 2006.

The author completed his graduation in Mechanical Engineering in 2010 from Mallabhum Institute Technology (MIT) under Maulana Abul Kalam Azad University of Technology (formerly known as West Bengal University of Technology), West Bengal with first class. Author received his post-graduation degree in Mechanical Engineering (Specialization: Manufacturing Technology) from National Institute of Technical Teachers' Training and Research, Kolkata under the same (aforementioned) university with first class in the year 2012. Then he joined in Camellia Institute of Engineering (Madhyamgram campus) as Assistant Professor in September 2012. After that he joined in Hooghly Engineering & Technology College (Hooghly) as Assistant Professor in March 2014. Later on he joined in Production Engineering Department, Jadavpur University as a Research Fellow under, "State Government Fellowship Scheme." After that he joined "TEQIP-III (CoE)" Fellowship Programme in this department. He has done his research work in the area of wire electro discharge machining (WEDM) of various engineering materials during the research period. Author has published 8 research papers in international referred journals and also presented 6 research papers in reputed international conferences related to WEDM in INDIA and abroad. Author also published 2 research articles as book chapter on WEDM.

DEDICATION

Every challenging work needs self-efforts as well as guidance of elders especially those who were very closed to our heart.

My humble effort I dedicate to my sweet and loving

Father & Mother,

Whose affections, love, encouragement and prays of day and night make me able to get such success and honour,

Along with all hard working and respected Teachers.

TABLE OF CONTENTS

LIST OF TABLES

LIST OF FIGURES

Chapter-1
Introduction

1.1 Introduction

Applications of advanced light metal aluminium alloys in manufacturing and production fields are increasing day by day. Scientists are developing such kinds of advanced alloys to meet the needs of industries. These advanced light metals can withstand high temperatures, shocks, fatigue, and corrosion. Intensive research works on such materials have been carried out to improve their strength, hardness, toughness and other mechanical properties. It is very difficult to find a tool material that can efficiently machine such an advanced aluminium alloy in a conventional way. It is, therefore, extremely essential to find a new machining method to deal with the problem that has been created due to the development of materials. Hence, extensive research work has been carried out for a long time to develop an advanced machining method that is not affected by the properties of the workpiece material and can be machined effectively and efficiently. Again, it is too difficult to produce complex shapes and sizes on hard to machine materials by using conventional machining techniques. On the other hand, precision, finish, and accuracy of such complex miniature parts are difficult to maintain in traditional machining techniques. To accomplish these needs, different types of advanced machining methods have been developed to overcome such problems. Generally, advanced machining processes are categorized as electro-mechanical, thermo-electrical, electro-chemical, and pure thermal processes. Electro discharge machining (EDM) and wire electro discharge machining (WEDM) are non-traditional thermo-electrical machining processes. Under such circumstances, WEDM is the most useful and widely accepted machining technique for efficient manufacturing of precision jobs. This is a non-contact material removal process where the wire electrode continuously moves in the vertical direction. Initially, WEDM was used in the tool and die making industries. Later on, it grows up at a highly accelerated rate and becomes non-dominated in the conductive materials machining area. Today, WEDM can produce small micro parts and miniatures with high precision, high accuracy, and a fine surface finish.

Cutting speed or machining velocity, corner accuracy, surface roughness, dimensional deviations, and taper angle are highly demanding day by day from the beginning of WEDM. However, corner error, dimensional inaccuracy, and surface irregularities are the major causes of cutting uncertainty that are still impeding the accuracy and quality features of the product in various applications of WEDM. To improve the accuracy and quality

characteristics of the product, the selection of input factors and strategy of machining play a very important role. The conductivity of the dielectric liquid is one of the most crucial parameters in determining the cutting speed (in terms of productivity), corner error (accuracy feature) and surface roughness (quality feature) during machining. A thorough investigation of dielectric conductivity is required to achieve higher production efficiency and precise finishing. Different materials have different thermal and electrical properties. As a result, the conductivity setting for one material cannot be used to machine the other material. By changing the dielectric conductivity setting, the production rate can improve, whereas, multi-pass cutting (skim or trim cut followed by rough cut) is used to improve the accuracy and precision of the product. Dimensional tolerance and corner inaccuracy in the workpiece are eliminated by single or multiple trim cutting operations according to demand.

1.2 Wire electro discharge machining (WEDM)

Wire electro discharge machining (WEDM) is a thermo-electrical non-traditional machining process where material is removed due to a series of isolated sparks rapidly occurring between the wire electrode and workpiece material. The process is carried out under a dielectric medium (generally deionised water). The number of sparks and the power of each spark are regulated by controlling the machining input parameters. By modifying the process parameters, material removal rate (MRR), corner accuracy, electrode wear rate (EWR), surface finish, and the resulting dimensional error can be controlled.

It is supposed that WEDM is an efficient machining process. With the help of constant research, machine control systems and pulse generators are significantly improved and provide a higher material removal rate. It has resulted in the improvement of the machining process, reducing machining time and dimensional error, improving surface finish, machining speed, and widening the application area. This process has become very popular in industries for a wide range of precision manufacturing.

1.2.1 Material removal mechanism in WEDM

Material removal mechanisms in electro discharge machining (EDM) and wire electro discharge machining (WEDM) are the same. In this process, electrical energy is converted into thermal energy and removes the material from the electrodes (workpiece and tool). In

this machining process, workpiece and tool must be electrically conductive. Generally, wire electrode is connected to the negative terminal (anode) and the workpiece is connected to the positive terminal (cathode). A marginal gap is maintained to apply the potential difference between the electrodes. Depending upon the applied potential difference, an electric field is established between the tool and the job. As the electric field is established, free electrons from the tool surface undergo transformations to create the electrostatic force. If the bonding energy of the tool material is lower, then the free electrons from the tool surface are emitted. The emission of electrons from the tool surface is known as the "cold emission process." Cold emitted electrons are then accelerated towards the work surface through the dielectric medium. Accelerated electrons gain kinetic energy through collisions with dielectric molecules. This collision may result in ionisation of a dielectric that depends upon the bonding energy of each molecule and the energy contained in each electron. Due to the particle collisions, a huge number of positively charged and negatively charged ions are generated. This process continuously occurs and increases the concentration of ions in the inter electrode gap (IEG). As the concentration of ions and electrons increases in the spark gap, matter existing in the gap creates a channel that is known as “plasma channel”. The resistance of this plasma channel is very low. Thus, suddenly, a huge number of electrons will flow from the wire surface towards the workpiece, and reversibly, ions will rapidly move from the work surface to the wire electrode. This process is known as "avalanche motion of electrons." This rapid moving process is visible with open eyes and is seen as a spark. Therefore, electrical energy is conveyed as thermal energy by the spark. The fast moving electrons are then struck on the job surface, and reversibly high speed ions are struck on the wire surface. Hence, the KE (kinetic energy) of the ions and electrons is converted into thermal energy or heat flux and impacts on the job and tool surface. A temperature rise of more than 10,000°C can result from such intense localised heat. At this high temperature, melting and evaporation of material take place. Initially, molten material is not completely removed from the electrode surface. It is partially flashed away from the workpiece and tool. When the potential difference between job and tool is withstood, the plasma channel is no longer sustained in the IEG. It generates a shock wave when the plasma channel collapses in the spark gap and defecate the molten materials from the machining zone. The evacuated molten material creates globules, craters, micro-voids, micro-cracks, etc. around the location

of the spark. As a result, the removal of material in WEDM occurred due to the shock wave formed by the collapse of the plasma channel. Schematic diagram of the discharge channel that occurred during machining is shown in Figure 1.1.

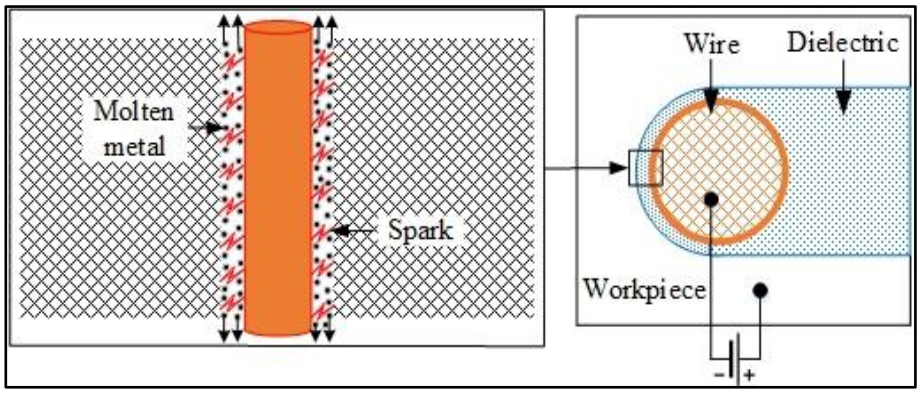

Figure 1.1 Schematic representation of discharge channel in WEDM

1.2.2 Applications

WEDM is widely used in aviation, aerospace, turbine blade, nuclear reactor and automobile industries. It is taking a monopoly position in tool & die making industries for its renounced accuracy features after machining. Minimal set up times mark it a smart method for limited run production of complex geometrics such as modified gear geometries with low aspect ratio. Due to the high proficiency, it is broadly used to manufacture the intricate parts like stepper motor parts, complex gear profile, cam wheel, stator of AC/DC motor etc.

Generally, complicated shapes like taper can be easily formed in WEDM with high accuracy and surface finish which eradicates much complex grinding operations in conventional way. WEDM is a very essential and apposite machining method to machine any electrically conductive materials. More interesting thing is that the material properties like density, hardness, plasticity, strength, brittleness, malleability etc. are not changed after WEDM process. In addition, other applications are given in following:

(i) Prototype production.

(ii) Automotive and aviation parts like engine cylinder, gears, blades, wheel casting etc.

(iii) Manufacturing medical devices for implantations.

(iv) Small and deep-hole making for gun barrels.

(v) Blanking punches in press tool industries.

(vi) Extrusion dies in tool and die making industries.

(vii) Orthopaedic and diagnostic device manufacturing.

(viii) Miniature part production.

(ix) Manufacturing turbine blades and titanium needles.

(x) Internal small gears production and so on.

1.2.3 Types and properties of wire electrode used in WEDM

Wire electrode is the core of the WEDM system. It is very easy to select the wire electrode used in WEDM as its choices are limited to brass and copper. As in the case of WEDM, high speed, high accuracy, high precision, and high quality products are increasing day by day to improve productivity and quality. A single metallic wire electrode cannot fulfil the criteria. That is why the selection of an appropriate wire electrode in WEDM is important. Generally, brass or copper wire is extensively used as a tool electrode. In the early days of WEDM, pure copper wire was extensively used. It was replaced by brass due to its high cost and low strength. Later on, different elements like chromium and aluminium were mixed with brass to improve the quality and strength of the wire. Afterward, the brass wire was coated with zinc and utilized to machine the advanced materials. Along with the current distinction of manufacturing and production field applications, there is an increasing demand for wire with high performance to replace the conventional copper or brass electrode. Generally, physical, mechanical, thermal, and electrical properties are required to be verified while choosing the electrodes. Although high performance wires are categorised on the basis of current carrying capacity, i.e., electrical and thermal conductivity, heat withstand capability, strength, and sparking ability, These wire electrodes are commonly made of zinc coated with a composite, diffusion annealed steel, or metal alloy core. Sometimes the core element of electrodes is made with copper-brass alloys having small amounts of chromium or concentrated zinc. General guidelines for the selection of wire electrode to overcome the above mentioned troubleshooting are shown in Table 1.1.

Table 1.1 General guideline for wire electrode selection

Challenges	Solutions	Types of wire electrode
To reduce the wire breakage and gap short	➢ Use large diameter electrode ➢ Decrease the wire tension during rough cutting operation	❖ Coated wire (Steel core) ❖ Al or Mg alloy
To increase the machining speed or material removal rate	➢ Use large diameter wire ➢ Increase pulse power ➢ Increase electrical conductivity of the wire	❖ Coated brass wire ❖ Coated copper wire
To cut the complex shapes and tapers	➢ Increase strength and ductility ➢ Better flushing	❖ Diffusion annealed copper wire ❖ Zinc coated brass electrode
To cut the high strength thick work piece (More than 50 mm)	➢ Use large diameter electrode ➢ Higher flushing ➢ Increase tensile strength of the wire electrode	❖ Coated steel core wire ❖ Diffusion annealed brass wire ❖ Molybdenum wire
To increase the precision and accuracy	➢ Small diameter electrode ➢ Increase fracture resistance ➢ Optimum flushing	❖ Tungsten wire ❖ Molybdenum wire ❖ Coated steel wire

1.2.4 Role of dielectric in WEDM

In WEDM, dielectric fluid has several main functions and plays a significant role in machining. It works as an isolator to avoid the gap between the wire electrode and the workpiece. Generally, the dielectric fluid is electrically non-conductive, although it acts as a conductive medium at a specific potential difference to accomplish high current density in the plasma channel. Under this potential difference, dielectric liquid reaches the breakdown voltage and molecules start breaking into cations (positively charged ions) and anions (negatively charged ions) in the inter electrode gap (IEG). Dielectric liquid is also used to cool down the electrode surface, i.e., the wire and work piece, and create a counter pressure to expand the plasma channel. Apart from this, dielectric fluid is used to eliminate particles and debris after the discharge process from the machining zone with the help of pressurised flushing. It also protects the wire electrode from short-circuits, interrupted machining, and destruction of the job.

The dielectric fluid is continuously circulated through the machining gap. This circulation process is carried out by an external pumping system that is mounted beside the dielectric tank. Used dielectric filters by wound cotton yarn cartridges or diatomaceous earth filters to take out the debris and metal particles. For general application, the allowable pore size of the filters is 10 microns. However, for high precision and fine finish applications, the filter pore size less than 5 microns is used. After the filtration process, fresh dielectric is sent to the dielectric chamber and stored in the tank. Variations of dielectric that are used in EDM and WEDM are shown in Figure 1.2.

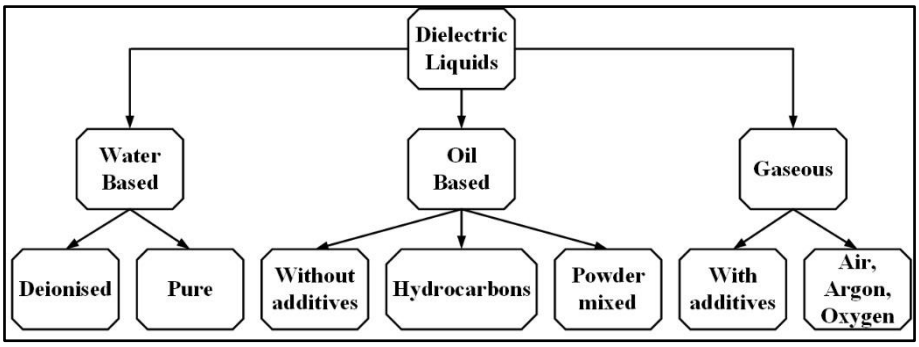

Figure 1.2 Types of dielectric used in electro discharge machining

1.3 Al 7075 alloy: Specialty and applications

Different types of aluminium alloy play a vital role in different engineering and manufacturing applications. Al 7075 is one of the most widely used aluminium alloy and occupied an extensive area of the aluminium industry. Al 7075 is aluminium based new generation lightweight metal with zinc as a secondary alloying element. The other metallic and non-metallic components like copper, magnesium, and silicon are also present. The main important properties of this light metal are high thermal and electrical conductivity, high temperature resistance, high hardness, and small wear rate. The main attractiveness of Al 7075 is that it is comparatively light in weight, high strength, and corrosion-free high performance material. Table 1.2 and Table 1.3 give chemical compositions and mechanical properties of Al 7075.

Table 1.2 Chemical compositions of Al 7075 alloy

Compositions	Al	Zn	Mg	Cu	Si	Others
Weight %	90.00	4.35	3.17	2.23	0.14	0.11

Table 1.3 Mechanical properties of Al 7075 alloy

Density (gm/cm^3)	Melting point (^oC)	Elastic Modulus (GPa)	Tensile properties			Fatigue strength (MPa)	Hardness (BHN)	Conductivity	
			Yield strength (MPa)	Tensile strength (MPa)	Percentage elongation			Thermal (W/m-K)	Electrical (M-S/m)
2.81	635	71.7	505	572	11	170	150	130	19.2

Among the light metals, Al 7075 has become extensively important in present day manufacturing industries due to its high capability to resist temperature and stress corrosion cracking. Aluminum based light metal alloys are substituting candidates for replacing steel and other iron based alloys for structural applications in high temperature ranges. It is comparatively light in weight and corrosion resistant to water, salt, and other environmental factors. This alloy has remarkable applications in space shuttle, medical industries, and aircraft industries due to its excellent mechanical properties. This alloy exhibits good performance in laboratory tests as well as in the work field. Missile parts, bike frames, terrain vehicle sprockets, aircraft fittings, and gear keys are some examples of the applications.

Chapter-2

Literature Review and Objectives of the Present Research

2.1 Review of past literature in the area of WEDM

In the year 1770, Sir Joseph Priestley first observed material erosion by electric spark. Although, in that time it is not used for machining materials. Later on, in 1943 two Russian physicists Dr. B. R Lazarenko and N. I. Lazarenko first introduced spark erosion process to machine materials. Afterward, Rudoroff patented this work for contribution in the field of electro spark machine. In the year 1950, Lazarenko build up a controlled electrical spark machine known as electrical discharge machining (EDM) to brought major evaluation in the manufacturing field. Popularity of this machining process is rapidly increased when industries implicit its process capabilities. In the end of 1960s, numerical control (NC) process is invented to improve the performance of EDM.

In late of 1960s, a newly developed system known as wire electrical discharge machining (WEDM) is manifested by replacing the tool electrode used in EDM. D. H. Dulebohn first introduced an optical line follower system in 1974 to monitor the profile of the component to be machined. Later on, a great invention is added in WEDM to improve the process capability of the system known as computer numerical control (CNC). Now, CNC-WEDM becomes non-dominated for different manufacturing industries to generate intricate shape and widely used for rapid machining. Many research works have been carried out in WEDM to mark it inexpensive and cost effective machining technique in present condition. Although this machining process is limited and only applicable for electrically conductive materials. Different research works have been under going to overcome such problems and try to find an effective solution to machine poorly conductive materials. However, in past literature, many works are exhibited on low conductive ceramics, metal matrix composites (MMC) in the field of WEDM to increase its process capabilities.

Research work in WEDM is broadly classified as state of art of the process and recent advancement, parametric analysis, modelling and optimization, accuracy and quality improvement. In following of this chapter, four major areas i.e. state of art and recent advancement of the process, parametric analysis, process modelling and optimization, quality and accuracy improvement of the process have been covered.

2.1.1 Review on state-of-art and recent advancement of the process

Wire electro discharge machining (WEDM) is an indispensable technology used in a wide range of manufacturing industries. Continuous advancements in technology and scientific knowledge have led to improved technology of material removal process. This not only improved the efficiency of the WEDM process but also enlarged the application area of WEDM. The development of advanced engineering materials and the need for complex three-dimensionally shaped components have made WEDM an important manufacturing process. From the beginning, several attempts are made to improve the machining conditions, performance characteristics and wire electrode properties of the WEDM process. However, selection of optimum machining parameters for obtaining higher accuracy and better surface characteristics is a challenging task in WEDM due to the presence of a large number of process variables and complicated stochastic process mechanisms.

Rajurkar and Wang (1997) emphasized the significance of advanced monitoring and control systems in die-sink electrical discharge machining (EDM) and wire electrical discharge machining (WEDM). The authors introduced a pulse power generator and servo system to effectively manage the discharge gap and analyse the characteristics of the discharge pulses during the EDM and WEDM processes. Rajurkar and Wang concluded that the integration of these monitoring and control technologies resulted in significant improvements in the overall performance of both the EDM and WEDM processes.

Puri and Bhattacharyya (2003) provided an overview of the vibrational behaviour of the wire in wire electrical discharge machining (WEDM) and introduced an analytical method for solving the equation governing wire-tool vibration. Their study focused on investigating the specific effects of wire vibration in WEDM, considering multiple spark discharges. By analysing the wire-tool vibration equation, the authors found that different stresses acting on the wire have an impact on the maximum vibration amplitude. It is also observed that the maximum amplitude of wire vibration changes in relation to the ratio of "the height of a job" to "the span of the wire between the guides." This trend is thoroughly studied and reported in this work. The research conducted by Puri and Bhattacharyya sheds light on the understanding of wire vibration in WEDM. Their analytical approach provides insights into the factors influencing wire vibration and the relationship between vibration amplitude and the geometric parameters of the machining setup.

Yan et al. (2004) proposed three key techniques of making prototype CNC micro-wire EDM. These techniques involve the development of an open architecture CNC system with submicrometer resolution, a two-axis linear motor stage, a wire transport system and a power supply system. The proposed CNC system features an open architecture human machine interface, modularity and DSP-based control. The wire transport system is presented to guarantee smooth wire transport and a constant tension value. The power supply system consists of a low energy discharge circuit and an iso-frequency pulse generator. Pulse states are classified as open circuit, normal spark and abnormal discharge by the level of gap voltage and discharge current. Experimental results demonstrate that the prototype Micro-Wire-EDM machine has the potential to manufacture micro-mechanism parts.

Kumar et al. (2010) introduced the concept of additive mixed wire electrical discharge machining (AWEDM) and explored potential future research trends in this field. They highlighted wire electrical discharge machining (WEDM) as a modern machining technology used to create intricate shapes from tough materials. The authors emphasized that AWEDM represents an innovative approach to enhancing the WEDM process. It is widely employed in noncontact machining and has progressed from its initial applications in tool and die fabrication to microscale machining. The study also placed significant emphasis on evaluating the machining performance and surface treatments associated with AWEDM. By examining these aspects, the researchers aimed to gain insights into the effectiveness and possibilities of AWEDM in various industrial applications.

Kumar et al. (2012) used two types of wire electrodes i.e. brass electrodes and the latest coated electrodes in WEDM. These coated electrodes are developed to meet specific requirements and increased productivity in machining. By using coated electrodes, the machining performance and accuracy levels are increased. The selection of the appropriate wire electrode is crucial to achieving higher taper angles, an improved surface finish and minimal errors. The authors carried out experiments using various types of wires, including pure brass wire, zinc-enriched brass wire, diffusion-annealed wires and alpha-phase coated wire. The results showed that these high performance wires significantly improved productivity in wire electrical discharge machining (WEDM). However, it is important to acknowledge certain limitations associated with these wires, such as their high cost, potential flaking, issues with straightness and the possibility of causing damage to the scrap chopper.

Additionally, it is also to be noted that these high-performance wires may not be universally applicable to all types of WEDM machines.

Ayesta et al. (2016) studied fatigue life of nickel-based Inconel 718 alloy produced through wire electrical discharge machining (WEDM). The objective of this work is to evaluate the capabilities of WEDM by comparing it with the grinding process. The study encompassed surface analysis, metallographic examinations, residual stress analysis, fractography and axial fatigue tests. The results indicated that the utilization of WEDM with the latest machine generation have a negative impact on fatigue strength at high fatigue cycles, reducing it by approximately 10% compared to ground specimens. However, no significant differences are observed between ground and WEDM samples at low fatigue cycles. These findings have implications for considering the feasibility of employing the WEDM process in the manufacturing of disc turbine blades.

Zhang et al. (2020) focused on two crucial performance indicators, namely energy consumption and machining accuracy, in the context of environmentally-friendly operations in WEDM. The research specifically addressed the impact of energy consumption and geometric errors resulting from thermal deformation. The authors proposed a hybrid technique of WEDM combined with magnetic field (MF) assistance to improve machining performance. Through a series of experiments on Inconel 718, the authors investigated thermal deformation and energy consumption in both MF-assisted WEDM and conventional WEDM. The analysis encompassed the effects of the magnetic field on thermal deformation, discharge waveforms, surface integrity and energy consumption. The findings revealed that the hybrid technique of MF-assisted WEDM offered numerous advantages and demonstrated significant potential for applications in the field of environmentally conscious precision manufacturing.

Kavimani et al. (2020) carried out extensive research on magnesium-based metal matrix composites in wire electrical-discharge machining (WEDM). In this research, a combined approach of Taguchi grey relational analysis (GRA) and principal component analysis (PCA) is employed. The objective of this work is to identify the optimal process parameters that can maximize the material removal rate and minimize the surface roughness. Taguchi's L27 orthogonal array is used to conduct the experiments. Key control factors considered in the study, weight percentage of reinforcement, doping percentage, pulse on time, pulse off time and wire feed rate. Through the analysis of variance (ANOVA), it is determined that the

weight percentage and distribution percentage have a significant impact on material removal rate and surface roughness. The optimal parameter settings yielded a maximum material removal rate of 14.9 mm^3/min and a minimum surface roughness of 2.04 μm. This research provides valuable insights for enhancing the WEDM process of magnesium-based metal matrix composites, aiming for improved material removal rates and surface quality.

Chaudhari et al. (2020) employed the central composite design of response surface methodology to optimize the wire electrical discharge machining (WEDM) process parameters for pure titanium. The utilization of central composite design and response surface methodology allows for a systematic approach to parameter optimization in WEDM. The study focused on identifying the input process variables, namely pulse on time, discharge current, and pulse off time, while considering surface roughness and material removal rate as the output variables. An analysis of variance (ANOVA) is used to assess the significance of various factors on the response variables. To obtain an optimal parameter setting that maximizes cutting rate while reducing surface roughness for pure titanium, grey relational analysis (GRA) is applied. After implementing the GRA technique, optimized process parameters are determined as a pulse on time of 6 μs, pulse off time of 4 μs and discharge current of 6 Amp. The GRA analysis demonstrated a very close relationship at the optimal condition, as confirmed during the validation trial. This study provides valuable insights into optimizing the WEDM process for pure titanium, considering both cutting rate and surface roughness.

Devarasiddappa et al. (2020) carried out an experimental investigation on wire electrical discharge machining (WEDM) of Ti6Al4V. The study employed the Taguchi L16 orthogonal array design technique to plan the experiments, considering four variable process parameters: pulse on time, pulse off time, current and wire speed, each at four different levels. A notable aspect of this work is the utilization of reusable wire technology to minimize the surface roughness of Ti6Al4V products during experimentation. Process optimization is carried out using a modified teaching-learning-based optimization (M-TLBO) algorithm. The study also introduced a novel technique called fitness curve fitting, which enabled the determination of the global optimal solution for surface roughness (i.e., the minimum value). The proposed M-TLBO algorithm demonstrated high accuracy and consistency across multiple runs. The mean fitness value is recorded as 3.751 μm, with a standard deviation of 0.006417. This research contributes to the field of WEDM by focusing on the machining of Ti6Al4V and addressing

the minimization of surface roughness. The use of reusable wire technology, along with the M-TLBO algorithm and fitness curve fitting technique, provides effective approaches for optimizing the WEDM process and achieving improved surface quality.

Chaudhari et al. (2020) investigated the impact of wire electrical discharge machining (WEDM) process parameters on surface morphology of nitinol shape memory alloy (SMA). A comprehensive analysis of the surface using scanning electron microscopy (SEM) and energy-dispersive X-ray spectroscopy (EDX) are carried out to obtain a three-dimensional (3D) surface characterization. The results from the 3D surface analysis revealed that the surface roughness is higher at the top of the work surface and lower at the bottom. The authors also performed surface morphology testing on the machined samples at the optimal parameter settings. The analysis revealed the presence of microcracks, micropores and recast globules, with their occurrence being most prominent at high discharge energy levels. Furthermore, the EDX analysis indicated that the machined surface is free of molybdenum, which confirmed the absence of the tool electrode material on the machined surface. The findings provide valuable insights into optimizing the machining process for nitinol and understanding the resulting surface characteristics, contributing to the advancement of WEDM techniques in the fabrication of nitinol-based components.

Sharma et al. (2021) examined the surface integrity of aero-engine components by investigating the morphology, topography, recast layer thickness and roughness parameters of the machined surface. The researchers observed that a better surface morphology, smoother topography, lower roughness values and minimum recast layer thickness are achieved by employing a combination of low pulse duration, high pulse off period and high servo voltage in the wire electrical discharge machining (WEDM) process. Response Surface Methodology (RSM) is employed to statistically model the process. The developed mathematical models are then used for optimization using the Teaching-Learning-Based Optimization (TLBO) algorithm. Through this optimization process, Pareto optimal solutions are obtained, focusing on achieving lower roughness values and higher material removal rates. Microscopic investigations revealed the presence of a significant number of melted droplets, micro-holes and craters on the WEDM surface. The findings of this study contribute to understanding the surface integrity of aero-engine components in relation to WEDM. The utilization of RSM-TLBO algorithms enables the optimization of process parameters to attain improved surface

characteristics. This research highlights the importance of proper parameter selection and flushing techniques to enhance the surface quality of WEDM components.

Ishfaq et al. (2021) conducted an experimental study focusing on seven process variables in wire electrical discharge machining (WEDM) and their impact on responses. The experimental findings indicated that there are differences in corner errors between the top and bottom faces. Specifically, wire tension, off-time and flushing pressure have a significant impact on the angular error at the top face. These factors contributed 25.5%, 12%, and 15.6%, respectively. Conversely, open voltage, pulse on time, wire feed rate and flushing pressure are the main factors affecting the angular error at the bottom face. These variables contributed 28.5%, 15.3%, 13.2% and 10.7%, respectively. Regarding surface finish and material removal rate, the prime control variable is pulse longevity. It contributed 51% to the surface finish and 88% to the material removal rate. This research work provides insights into the influence of various process variables on different responses in WEDM. The findings highlight the specific variables that have the most significant impact on corner errors, angular errors, surface finish and material removal rate. This knowledge can be useful in optimizing the WEDM process and improving overall machining performance.

Sibalija et al. (2021) carried out an experimental study on wire electrical discharge machining (WEDM) for processing Inconel 625. This study focused on investigating the major process variables of WEDM, including pulse-on time, pulse-off time, servo voltage, and wire feed rate, to evaluate several important aspects of the process. The objectives of this work are to reduce the gap current and surface roughness while increasing the cutting speed. The researchers performed experiments to examine the significance of the WEDM parameters on the response variables. Subsequently, an advanced statistical technique is employed to find out the correlations among the outputs and inputs. The Bayesian regularized neural network is utilized to create the models for analysis. This research work contributes to the understanding and optimization of WEDM for Inconel 625.

Zhang et al. (2022) applied transverse magnetic field (TMF) to improve uniformity of discharge point distribution and reduce distortion during the WEDM-LS process for thin-walled components. The authors begin by demonstrating the generation mechanism of this distortion behaviour and the impact of the TMF on distortion through theoretical analysis. To gain further insight into the distortion behaviour in the TMF-WEDM process, the researchers established a novel thermo-physical model that considers the discharge point distribution.

This model enables the simulation of temperature fields, residual stress fields and distortion profiles. A series of Taguchi experiments is conducted to investigate the influence of various process parameters, such as pulse discharge energy (pulse on time, pulse off time, and current) and magnetic field strength. A comparative analysis of the simulated and experimental results is carried out to verify the accuracy of the thermo-physical model. This study reveals that the application of a transverse magnetic field significantly improves the longitudinal distribution's uniformity. This improvement leads to significant reductions of 32.77% in distortion and 22.68% in the formation of recast layers.

Wang et al. (2023) investigated the causes of wire breakage in wire electrical discharge machining (WEDM). Firstly, by observing the wire after discharges and using finite element method, a complete thermal model considering both latent heat and flushing efficiency is built. Using the simulation results and experimental data, the researchers determined the heat partition ratio of the wire through inverse fitting, finding it to be 46.74%. The reduction in cross-sectional area resulted in increased stress levels exceeding the ultimate tensile strength (UTS) of the wire, ultimately leading to wire breakage. These findings provide a deeper understanding of the influence of discharge accumulation on wire breakage in WEDM. The research contributes to the identification of factors contributing to wire breakage, adding a new dimension to mitigate this issue and improve the overall performance and reliability of the WEDM process.

2.1.2 Review on parametric analysis

Several research works have been carried out to find the influence of WEDM process parameters on machining criteria. Different researchers studies and tried to figure out the major influencing factors on cutting speed, material removal rate, surface roughness, corner inaccuracy , taper deviation, dimensional tolerance, overcut etc. It is evident that the WEDM input factors controlled by a large number of parameters such as open circuit voltage, pulse on time, arc on time, pulse off time, arc off time, peak current, servo voltage, wire tension, servo sensitivity, wire feed rate, pulse frequency, pulse power etc. Variation of aforementioned process parameters have concise effects on performance measured i.e. cutting speed, MRR, surface finish etc. So far, many researchers are involved to find out the exact significance of previously mentioned process parameter on different response criteria. In this section, review of past literature on parametric analysis in WEDM has been discussed.

An experimental investigation in WEDM of Al_2O_3 particulate reinforced composite carried out by Liao et al. (1996). The authors performed coarse and fine cutting to investigate the surface morphology of the machined component. It is observe that under these two different cutting conditions, surface roughness is not varied significantly but topography found intrinsically different. Besides that, surface bending also observed in fine cut surface. It is believed that this is happening due to the wire shifting while machining.

Prohaszka et al. (1997) presented the necessities of wire electrode materials, which lead to the development of WEDM performance. Experimental result shows that the machinability of hard to machine material is intensely depended upon the electrode material used. The choice of appropriate wire material and its dimensions reflect the performance of WEDM process has been discussed in the work.

Borsellino et al. (1999) studied the correlation between process factors and quality characteristics of the WEDM specimen. Experimentation is carried out on tempered and high-speed steel to investigate the influence of duty factor, pulse on time and tensile strength of the wire. Authors' executed the importance of these process parameters on material removal rate (MRR) and surface roughness (R_a).

Gokler and Ozanozgu (2000) have been carried out experimental investigation to find the influence of process parameters on surface finish in WEDM. The aim of this research study is to select the prominent cutting and appropriate offset parameter combination in order to get desired surface finish. A series of experiments carried out in different series of steel e.g. grade 1040, 2379 and 2738 with a variable thickness of 30 mm, 60mm and 80mm. Authors claimed that experimental outcomes are useful for industries and most suitable to acquire the necessary surface finish to machining the aforesaid steel alloys.

The effects of dielectric conductivity in WEDM of sintered carbide are performed by Kim and Kruth (2001). Experimental results showed that low conductivity gives the higher material removal rate as the inter electrode gap (IEG) for that material reduced. Four extra repetitive finish cuts on the rough cut contour are performed to acquire the precision and fine surface finish. It is found that appropriate conductivity setting and number of finish cut remarkably improved the surface finish.

Guo et al. (2002) investigated the machinability of Al 6061 based particle reinforced MMC (Al_2O_3) in WEDM. An orthogonal experimental design has been used to conduct the

experiments. It is perceived that the electrical process parameters have little impact on surface finish and it always generates coarse surface. However, machining parameters played a significant role to determined cutting velocity. It is also reported that blind feeding reduced the pulse energy, resulted unstable machining and frequently wire breakage. It is recommended by the authors for effective machining of Al_2O_3, high voltage, pulse on time and current are always desirable.

Tosun and Cogun (2003) analysed the influence of cutting parameters on MRR, average surface roughness and wire wear rate (WWR). Experimentation is conducted by varying the process parameter, such as open circuit voltage, pulse on time, flushing pressure and wire feed rate. Brass wire with a diameter of 250 micron and AISI 4140 steel is used as tool electrode and workpiece material. The variations of responses with input factor have been modelled by using regression technique and the level of importance is determined by analysis of variance (ANOVA). Based on ANOVA results and F-test, authors demand that the most effective parameter on WWR is open circuit voltage and pulse on time.

Kozak et al. (2004) demonstrated theoretical and experimental study in WEDM of low conductive silicon nitride (Si_3N_4). It is observed that the electrical resistance between electrodes varied while machining and it directly depends upon the clamping position of the workpiece. By varying, the clamping positions i.e. changing the total resistance between electrodes, MRR and surface roughness regulates. To minimize the energy loss between electrodes, workpiece is coated with silver foil. Due to this silver coating, voltage drop between wire and workpiece reduced, thereby energy losses in spark also reduced and enhanced the material removal rate and increase the productivity.

Sarkar et al. (2005) described the parametric analysis of the -titanium aluminide super alloy in WEDM. To evaluate the surface finish and dimensional deviation of this beneficial material, extensive research work was carried out by the authors. It is observed that the above response factors are fully independent of pulse off time and a newly developed term incorporated as an input factor is dimensional shift. For adverse cutting conditions, these aspects are very important to achieve better machining stability and high accuracy without negotiating the dimensional deviation and surface finish.

Ozdemir and Ozek (2006) performed the machinability of GGG40 (nodular cast iron) in WEDM. Four independent process parameters pulse on time, current, wire feed and gap voltages are investigated on machining performance such as cutting rate and surface

roughness. Increasing current and pulse on time cutting velocity increases but deep and shallow discharge craters are produced in the machined surface. Authors identified three different zones in rough regime of machined sample: white layer, bulk metal and decarburised layer. Finally, variation of cutting rate and surface finish was mathematically modelled by regression technique.

Han et al. (2007) analysed the effect of input factors on surface finish for skim cutting operation. Discharge current, polarity, pulse interval, pulse on time, dielectric and material are chosen as process variables. It is observed that the surface finish improved as the current and pulse duration both is decreased. Authors also found when discharge energy per pulse is constant, short and long pulse produced same effects on surface finish but surface topography become asymmetrical. However, in case of MRR, short pulse discharge contained more current and eroded more material than long one and enhanced the MRR.

Aspinwall et al. (2008) investigated the workpiece surface integrity with the aid of minimum damage pulse generator technology. Multiple finish cut followed by trim cut are performed on Ti-6Al-4V and Inconel 718 workpiece. Result shows that average recast layer thickness during rough cut is less than 11 μm whereas no significant recast layer or damage is found after several trim cuts. Similarly, substantial variation of micro hardness is not observed in work surface.

Somashekhar et al. (2010) performed an experimental investigation in μ-WEDM of pure aluminum. Influence of capacitance, gap voltage and feed rate on MRR, surface finish and overcut have been performed. ANOVA has been carried out to identify the level of importance of each factor on output responses. Finally, regression analysis is also accomplished to establish the machining performance and process criteria yield.

Shah et al. (2011) performed an inclusive analysis on the influence of workpiece thickness with other significant process variables on major critical factors in WEDM of tungsten carbide (WC). Three most important performance considered by authors are MRR, kerf-gap and surface roughness.

Selvakumar et al. (2014) described the influence of process parameters on the output responses based on signal to noise (S/N) ratio in the Taguchi method. A single-pass cutting operation is carried out on an Al 5053 workpiece while considering pulse on time, peak current, pulse off time, and wire tension as process parameters. Machining speed and surface

roughness are considered as response criteria. On the basis of the S/N ratio, optimal parameter settings to maximise the machining speed and minimise the surface roughness are obtained.

Sharma et al. (2015) investigated the influence of WEDM process parameters on high strength, low alloy (HSLA) steel. Overcut is chosen as the response criteria and models the process using response surface methodology. Optimization has been carried out by a genetic algorithm (GA) for HSLA steel. Optimal parameter settings for this alloy are peak current of 180 amps, pulse on time of 117 µs, wire tension of 6 games, pulse off time of 50 µs, and gap voltage of 49 volts.

Yu et al. (2015) fabricated millimetre-scale groove array structure on Al 5083 alloy substrate with the aid of high speed WEDM. Authors studied the effects of V-shaped groove on wettability and sliding properties of the sub surface. The results exhibited that V-shaped groove array with hierarchical structure shows the decent superamphiphobicity property after a liquid solution immersion. After removing the oxide-layers and performing basic mechanical test, surface structure of Al substrate showed same superamphiphobic properties. The high-speed WEDM technique is much effective and efficient to build up 3D surface. Outcome of the study is appropriate for industrial manufacturing of long-lasting superamphiphobic Al sub-surfaces with anisotropic sliding.

Soundararajan et al. (2016) studied the machinability of squeeze cast A413 alloy through WEDM. Experimentations are systematically conducted by using rotatable central composite design. Mathematical models are developed to predict the results and confirmatory experiments carried out to verify the additivity of the models. It is found that the predicted values from the models are close enough to the experimental results. The average % of error for MRR and surface roughness in response surface methodology is around 7.30% and 3.00%. Significance of process parameters are checked by using ANOVA and multi objective optimization is carried out by using desirability function analysis to get the optimum process appearance.

Kumar et al. (2016) studied the influence of WEDM process parameters such as electrode material, pulse off time and pulse on time on surface roughness, electrode wire rate (EWR) and MRR. Machining is performed on Al-B_4C composite material to investigate the process factors on performance characteristics. Composite material used in this work is made by stir casting process with 5% of B_4C and Al 6061as a matrix material. Based on the ANOVA

results, authors' claims that current is the most dominating factor to evaluate the surface roughness and MRR while electrode material played a significant role to determine the EWR.

Samanta et al. (2016) carried out experimental investigation on die steel material in WEDM of varying job height. Job thickness is a crucial factor to determine corner error, surface roughness, dimensional deviation, kerf width and machining speed. Authors have considered the workpiece thickness as an input factor and the other process parameters are selected as duty factor, peak current and pulse on time. It has been seen that the surface finish deteriorates as the job thickness increased and highly influenced by pulse parameter settings. Duty factor and pulse parameter setting frequently effect on material removal rate. Increasing the pulse on time MRR also increases.

Gong et al. (2017) focused to improve surface finish of Ti6Al4V workpiece using multiple cuts (trim cut followed by main cut) in low speed WEDM. Authors claims that surface roughness obtained after three successive trim cut are 0.67 µm. During multiple trim cutting operations, parameter levels are modified and wire offset values are varied to achieve better surface finish. In addition, SEM analysis also carried out to identify the fusing structure, irregular droplets, craters etc. present in the machined surface.

Bisaria et al. (2019) presented the influence of WEDM parameters namely, spark energy, spark frequency, and peak current on surface finish, avg. cutting velocity, and surface integrity aspects of Nimonic C-263 superalloy with the aid of one-parameter-at-a-time (OPAT) method. Authors claim that surface roughness and avg. cutting rate are increases as the spark energy, peak current are reverse trend with the spark frequency. Additionally, surface integrity features, elemental composition and phase analysis of Nimonic C-263 are also considered in this study.

Phate et al. (2019) considered finding the most beneficial level of process parameters in WEDM of AlSiC (20%) composite using a Taguchi-based hybrid grey-fuzzy grade (GFG). Grey-fuzzy reasoning grade (GFRG) is pooled with fuzzy logic and is used to comprehend the grey-fuzzy reasoning grade (GFRG). The most reasonable input parameters for AlSiCp20 machining, according to the authors, are T_{on} (108 µs), T_{off} (56 µs), WFR (4 m/min), and IP (11 amps).

Mandal et al. (2020) carried out an experimental investigation to select the appropriate process parameter in WEDM of Al 7075. The authors found that the most influential factors

in determining the machining speed, corner error and surface roughness for this alloy are pulse on time, arc on time, pulse off time, servo sensitivity, wire tension and servo voltage.

Straka et al. (2021) presented a research work on identifying the influence of several technological process parameters and material properties of the workpiece on geometrical inaccuracies of the machined profile that arises in WEDM using CuZn37 electrode. It is very difficult to maintain accuracies in a narrow tolerance field. To overcome such probles, authors developed an algorithm for simulation that includes empirically mathematical models. The necessary parameter settings can be predicted with this algorithm when required dimensions and material properties of job and wire electrode are known.

Machining characteristics of particle reinforced metal matrix composite (PR-MMC) in micro-WEDM is introduced by Chen et al. (2021). Authors carried out steadily machining of 65 vol.% SiCp/Al composite with high efficiency and better surface finish. Additionally, influence of process factors on MRR and surface finish is also investigated. Experimental outcome shows that MRR increases with increase of T_{on} and W_t and decrease with T_{off} and S_v. On other hand, surface finish improved with increase of Ton, Sv and decrease of T_{off}.

2.1.3 Review on process modeling and optimization

Selecting the optimal parametric combination in WEDM to achieve superior productivity and other accuracy features is a difficult task. Process parameter optimization becomes more complex due to the presence of a large number of machining parameters and a deceptive stochastic process mechanism in WEDM. In the past, researchers attempted to model the process using various techniques and then optimised them using several optimization methods. In this section, the author reviewed numerous strategies for modelling and optimization used in WEDM.

Spedding and Wang (1997) made an attempt to optimise the WEDM process by modelling the process factors using feed-forward back propagation artificial neural networks (BPANN) and then characterised the machined surface based on time series analysis. The authors identify optimal parametric combinations for surface roughness and waviness. It is found that the machining speed of the process significantly increases as the surface roughness and waviness increase. Finally, surface profiles are characterised by a three-group classification scheme.

Liao et al. (1997) recommended a method to determine the optimal parameter setting in WEDM and established a mathematical model through a regression technique. The feasible direction method is employed by the authors to solve the optimization problem in the WEDM process. In this work, six important control factors are selected as: pulse on time, pulse off time, table feed rate, flushing pressure, wire tension, and wire velocity. The effects of these control factors on MRR, gap width, surface roughness, discharge frequency, and spark gap voltage are resolute.

Speeding and Wang (1997a) proposed a mathematical modeling technique in WEDM through combine approach i.e. response surface methodology and ANN. The pulse duration, pulse gap, wire tension and the flushing pressure are selected as input factors to determine the machining speed, surface finish and waviness.

Han et al. (2002) developed a high accuracy simulation scheme in WEDM to solve the reverse problem by using parametric programming. Parametric programming is the way of searching to find the optimum parametric combinations that minimize or maximize the value of the estimated function. It has been found, simulated result of geometric shape and depth of cut tremendously consistent with the experimental results. The error of this coincidence is less than of 1.5 μm. Adaptive control is then used for coordination of the system, which can automatically generates the optimal machining order in high precision WEDM.

Tosun (2003) performed experimental investigation in WEDM of AISI 4140 steel material. 0.25 mm dia. brass wires with 10 mm thick workpiece are used to conduct the experiments. The variations of surface roughness and cutting parameters were modeled by using regression technique. The importance of cutting parameters on the performance output is determined based on ANOVA. Finally, multi performance optimization is carried out on developed mathematical model to obtain the optimal solution.

Tosun et al. (2003) established a mathematical model between surface roughness and cutting variables, known as pulse on time, open circuit voltage, dielectric pressure and wire feed using regression technique. Power function is found the best-fitted model among the several function used. The most interesting thing is that the surface finish estimated without conducting any kind of experiments via proposed model.

Hewidy et al. (2005) conducted experimental investigation on Inconel 601 alloy material with WEDM. To correlate the relation between various process factors and outputs during

machining of Inconel 601, regression based mathematical model is employed. In this work, different process factors such as, duty factor, current, flushing pressure and wire tension are correlated with MRR, surface finish and wear ratio.

Newman and Allen (2005) introduced how to use STEP-NC compliant information model to support WEDM-CAD into CNC process chain. A STEP-NC compliant WEDM works on Java, object oriented database management (DBMS) based system and employed to demonstrate the information model. This models is based on part 13 of ISO 14649 standard that is devoted for WEDM process. In the subpart 10 of that standard, specify the overall machining information. This information model is used to identified the structure and define additional model known as unified modelling language (UML).

Sarkar et al. (2005) carried out a single-pass cutting operation in WEDM to evaluate the optimum process criteria for gamma titanium aluminide. A cascade-forward back-propagation neural network based on Bayesian regularisation is being developed to model the machining input variables. Three major response factors: wire offset, machining speed, and surface roughness are considered as performance criteria for this super alloy. A mathematical model is used to predict the response factors as a function of different machining parameters such as pulse parameters, servo reference voltage, current, dielectric flow rate, etc. Verification experiments have been carried out to verify the validity of the mathematical model, and finally, optimal parametric combinations are found using an advanced optimisation technique.

Chiang et al. (2006) proposed an effective optimization approach in WEDM of particulate reinforced Al2O3 composite. Machining of Al2O3 is inadequate, and handling of process parameters is also complicated. Multi-objective optimization of the process parameters for this material is performed by using grey relation analysis (GRA). Two major performance characteristics, surface removal rate and surface roughness, are considered to optimise the machining parameters such as discharge time, cutting radius of the job, arc off time, discharge current, flow rate, and wire speed. The authors claim that performance characteristics are significantly improved by this approach.

Mahapatra and Patnaik (2006) optimized the WEDM process using Taguchi based optimization technique. Nonlinear regression method is used to model the process parameters. This mathematical modeled are used to optimize the WEDM process. Optimum result recommended for two different parameter setting to maximize cutting speed and

minimize surface roughness. Authors considered some interactions parameters for depth analysis of linear factors in the process. Predicted and confirmatory experimental results are close enough and the percentage of prediction error for MRR is 4.026% and for surface roughness is 1.53%. Authors conclude that the percentage of error can be reduced if more number of interactions is considered during experimental stage.

Ramakrishnan and Karunamoorthy (2008) developed ANN models and proposed a multi attribute optimization technique in WEDM of Inconel 718. Designs of experiments are planned by Taguchi method and L_9 orthogonal array is used to conduct the experiments. Multi response signal to noise ratio (MRSN) based parametric design of Taguchi method has been concurrently used to optimize the response criteria. It is an extended version of Taguchi's variable design approach where SN values of the outputs are optimized. The valedictory experiments are carried out to verify the developed mathematical models and significant improvements are observed in the optimized results.

Prasad and Krishna (2009) developed a RSM based mathematical model to optimize the WEDM process. Material removal rate and surface roughness are the most important response that decides the performance of the machining process. It is seen that the effect of input variables on MRR and surface finish are opposite in manner i.e. if MRR increases surface finish degrades or vice versa. To resolve such problem, multi objective optimization techniques are employed. Non-dominated shorting genetic algorithm (NSGA) based multi objective optimization has been employed to obtained the optimal result for MRR and surface roughness and generates the Pareto optimal set of solutions.

Chen et al. (2010) analysed the variation of machining speed and surface roughness in WEDM of pure tungsten. An integrated BPNN and simulated annealing technique are proposed to optimize the parameter settings during machining. Total eighteen numbers of experiments have been conducted to train the neural network and also used to predict the machining velocity and surface roughness in different cutting conditions. Optimized results obtained from the proposed algorithm are showing that BPNN is an efficient tool to optimize WEDM process while machining tungsten.

Sarkar et al. (2010) proposed an integrated approach of optimization in WEDM with facilitation of ANN modeling. Influence of four process factors namely flow rate, wire offset value, current and pulse duration on machining speed, surface finish and dimensional shift have been investigated in multi pass cutting condition. Two different ANN models, one is

Bayesian regularization and another is early stopping method have been developed and compared both of them. Pareto optimization technique is used to search out the maximum cutting velocity with desire surface finish in skim cutting operation.

Sadeghi et al. (2011) carried out experimental investigation to find the influencing factors in WEDM while machining AISI D5/DIN 1.2601 steel (X165CrMoV12). Two key response parameters MRR and surface roughness are measured to determine the productivity and quality of the product. Experimental plan is designed by Taguchi method and modeled the process by using nonlinear regression technique. Tabu search optimization algorithm is employed to minimize the weight sum of the responses. Efficiency and ability of the algorithm is verified by confirmatory experiments.

Goswami and Kumar (2014) proposed a utility-based multi-objective optimization of Nimonic-80A in WEDM. An experimental plan executed by using Taguchi's robust technique. The influence of three major process parameters, namely pulse on time, pulse off time, and peak current, on MRR and surface roughness is investigated. Multi-objective optimization using a utility approach offers the combined optimization of both output responses to illuminate the mean of the process.

Kumar et al. (2015) carried out experimental investigation and optimizations of process variables such as current, feed rate, pulse on time and weight percentage of B_4C on different response parameters. The specimen Al 6061 reinforced with 5% (wt) of SiC and 0, 5, 10% (wt) of B4C is prepared for machining with the aid of stir casting process. The optimal parameter setting is 12 amps current, 5% B_4C, 100 µsec of pulse on time and 6 m/min wire feed rate to machine this material. It has been found that pulse on time is the most effective parameter with percentage of contribution of 96.19%.

Gopalakrishnan et al. (2017) investigated machining capabilities of AA7075 MMC in WEDM. An attempt is made to improve the performance characteristics of WEDM process by increasing MRR and decreasing surface roughness. It has been observed that surface finish and MRR are the function of machining process parameters. Four independent process factors such as pulse on time, pulse off time, discharge current and servo feed are considered by the authors. Additionally, major influencing factors are recognised by ANOVA and optimized the process using PSO.

Kumar et al. (2018) studied spark gap and surface characteristics in WEDM of aluminium based MMC. The Box–Behnken's design is utilized to plan the experimentations, and RSM is used for developing quadratic models for selected responses. This research study recommends an optimal process setting such as T_{on} is 0.75 µs, T_{off} is 16 µs, S_V is 35 V, I_p is 120 A, W_t is 1200 g, and WFR is 10 m/min for effective machining of Al/SiCp-MMC.

Mandal et al. (2019) carried out multi-objective optimization in WEDM of light metal alloy. Entropy based TOPSIS method is utilised to convert the several response parameters into a single parameter for optimization. The optimal outcome shows that the best process parameters settings can be pulse on time (1.1 µs), pulse off time (20 µs), flushing pressure (9 kg/cm2) and servo voltage (20 volt).

An effort is made by Phate et al. (2019) to find the optimal cutting condition in WEDM of Al/S_iC_p MMC. Modeling and prediction of process parameters are carried out by using dimensional analysis (DA) and artificial neural network (ANN). From the experimental results, it is found that the T_{on}, thermal conductivity, coefficient of thermal expansion, WFR and W_t are the most effective process parameters. Additionally, to find out the accuracy of the articulated DA and ANN models, correlation-coefficient is calculated. From the results, it is clear that both are competent to predict the surface roughness value and the material removal rate.

Thangaraj et al. (2020) applied Taguchi grey relational analysis (TGRA) based multi-criteria decision making to find the best parameter setting in WEDM of titanium alloy. It is very significant approach to establish multi-criteria decision making to figure out the optimal parameter setting. The optimal parameter setting of prescribed method is servo gap voltage (70 V), peak current (15 A) and duty factor (0.6).

Multi-objective optimization in WEDM of Al 7075 alloy is carried out by Mandal et al. (2020). GRA based optimization technique is employed to find the optimal parameter setting for machining Al 7075. ANOVA is carried out to find the major influencing factors and it is observed that the most dominating factors and their contributions are T_{on} (52%) and T_{off} (27%). The optimal parameter settings obtained from GRA is T_{on} = 0.2 µs, T_{off} = 40 µs, F_p = 12 kg/cm^2, and S_v = 80 V.

Chaudhari et al. (2021) studied machining characteristics of NiTi shape memory alloy in WEDM. A combine approach of RSM and heat transfer search algorithm is used to optimize

the process. An optimal process criterion yields with maximum material removal rate and microharness of 1.49 mm^3/sec and 462.52 HVN, when surface roughness obtained 0.11 µm. Additionally, Pareto plots are generated to indicate the trade-offs between the selected input and response variables.

Goyal et al. (2021) introduced adaptive neuro-fuzzy inference system (ANFIS) and NSGA-II algorithm to create model and optimize the WEDM process. The influence of process factor such as Ton, Toff, Ip and WFR on MRR and WWR is investigated during machining of Ti6Al4V alloy. The optimal results obtained from NSGA-II within acceptance limit and comprehended an improvement of MRR and WWR (percentage errors are 6.784% and 7.589%).

2.1.4 Review on accuracy and surface quality improvement

Different forces are generated in the inter electrode gap (IEG) due to plasma erosion and collapsing of bubbles while machining in WEDM. Force generated due to rapid formation of gas bubbles within the machining zone termed as gap force. As the cylindrical electrode used in WEDM is thin and flexible, it is bent due to high pressure generated by gap force and the wire lost the ideal straight position and making parabolic shape. Apart from this, some other major contributing factors like electrostatic force, hydraulic force and electromagnetic force also generated to deflect the wire positions. This dispensed force is not constant due to volatile nature of the plasma channel and random nature of sparking. The wire fluctuates and displaced from the straight position as the time is varied and produced uninterrupted vibration. This constant vibration is the main source of inaccuracy and surface undulations presence in WEDM as it has potential influence on kerf deviations and dimensional tolerance along the thickness direction. However, instantaneous position of the wire electrode is the function of time but average displacement is constant for a particular machining situation. This mean displacement of wire is known as wire lag and it is the main source of dimensional error in WEDM. This section gives a brief review of past literature in area of accuracy and surface quality in WEDM.

Hsue et al. (1999) estimated a model to predict the MRR during geometrical cutting in WEDM. Authors considered wire deflection with transmuted exponential trajectory of electrode centre. Authors also calculate the MRR and spark frequency for better understanding of the process. It is perceived that the predicted MRR and measured frequency radically dropped as the electrode take turn in corner and the quantity spill in the corner peak

directly depend on angle of corner being cut. It is also investigated that rapid escalation of gap voltage during corner cutting will affect the MRR. It is suggested that jet pressure must be reduced while finishing the corner edge otherwise overlapped kerf will be induced in the corner and more leakage of dielectric liquid takes place.

Lin et al. (2001) exhibited how to reduce the corner inaccuracy presence in the machined parts. A fuzzy approach is introduced to decrease the corner error via retrenchment of wire deflection by increasing pulse interval. It is conclude that the corner inaccuracy presence in rough cut can be reduced up to 50% whereas process time increases not more than 10% irrespective to the normal machining time.

Kunieda and Furudate (2001) introduce a newly developed dry WEDM process. In this process, dielectric liquid is replaced by gas to increase the machining efficiency. With dry WEDM process, machining accuracy, surface roughness, kerf gap, dimensional error etc. can be reduced. Authors presented another major advantage of this process; electrolyte corrosion free job can be manufactured.

Han et al. (2002) developed a simulation method to reproduce the discharge phenomenon accurately in WEDM. Location of discharge, material removed from the workpiece and vibration analysis is considered to search out the simulation results. Some ambiguous factors like explosive force, ignition delay time, dielectric permittivity and damping coefficient are challenging to quantify experimentally. Authors searched the effects of such unclarified factor using parametric programing technique and recognise the optimal parameter settings to obtained best accuracy results.

Puri and Bhattacharyya (2003) carried out an extensive research work on wire lag phenomenon in WEDM. The trend of geometrical error presence in the workpiece and the influence of control variables on wire lag are demonstrated by the authors. Total twenty seven numbers of experiments are conducted for rough cutting operation to figure out the geometrical inaccuracy, surface finish and cutting speed. Trim cutting operation also carried out by the authors to eliminate the maximum inaccuracy present in the profile.

Sato and Shibata (2004) proposed a useful method to improve the accuracy in WEDM by using off time control strategy. It is found that the precision of this technique increased when the effects of off time control on wire vibration is taken into consideration. It seems that the identification mark can be lost in surface finish by using this technique. This proposed

method is very much useful because the method can be apply for any height workpiece machining without varying the process factors. Apart from that, method is not only useful for making concave shapes but also efficient to produce convex shapes. Authors claim that, the method is significantly useful for precision manufacturing in WEDM process.

Yan and Huang (2004) presented close loop wire tension control to reduce the corner inaccuracy of WEDM manufacturing parts. OSA (one step ahead) and proportional integral controller (PIC) are used to inspect the vibrant performance of the wire tensioning system. Experimental finding claims that the geometrical error during corner cutting can reduce 50% approximately and taper presence in the workpiece significantly eliminate.

Sanchez et al. (2004) proposed a new hybrid computer-integrated technique to improve the corner accuracy. Authors combine the experimental results and the numerical simulation values. Based on a technical catalogue and a user friendly database, applied process permits the user to choose the optimum cutting condition, by editing wire cutting command or by path modification. The validation of the propose system is verified through a sequence of case studies and the result shows that significant improvements of accuracy and efficiency with respect to the commonly used knowledge.

Takino et al. (2005) carried out high quality machining of smoothly polished single crystal silicon in WEDM to obtained fine surface quality. Different types of mask is employed to the smooth surface before machining and it is found that the resin mask is quiet effective to obtained the smooth surface finish after machining. Surface finish during rough cutting operation is far better in water medium rather than in oil medium. However, cracks and other defects presence in the rough cut surface can successfully eliminate and produced a fine surface in oil medium. Authors conclude that rough cutting in water medium is better whereas finish cutting in oil medium improve the surface quality.

Sanchez et al. (2007a) have been studied generation of corner geometry in rough and trim cutting operation. Authors correct the corner error of the workpiece by controlling material removal rate during machining. It is conclude by the authors that machining velocity limitations in skim cut can be an achievable approach to correct the material removed to make a precise corner.

Han et al. (2007a) described a simulation method for WEDM of corner cutting during single pass cutting operation. Authors simulate the wire vibration due to different reaction force

acting on the electrode. Authors also established a geometrical model for electrode path and numerical controlled path and carried out an experimental investigation on both of them. Finally, authors verify the feasibility of the simulation method compared them. It has been observed that simulation results and experimental values are closed enough.

Dodun et al. (2009) presented an extensive work to improve the accuracy during corner cutting of thin parts in WEDM. Permanent bending in sharp corner leads to significant deviation from the predefined programmed path. This deviation of corner edge directly depends on magnetic properties of the material being machined and some other factors. Authors mainly focused to establish a means for characterizing this corner shape. Furthermore, authors quantify the impacts of some other factors like corner angle and job thickness on corner deviation.

Lin and Liao (2009) propose an effective wire radius compensation method to improve the precision of wire electro discharge machine. A modified Denavit–Hartenberg (D–H notation) is employed to generate the NC data equation for wire radius compensation. A 4×4 homogeneous transformation matrix is employed to construct the design surface. The modified D–H notation is then applied to originate the machine's skill matrix and also to generate the preferred wire location matrices. Finally, to validate the proposed methodology, top and bottom basic curve are generated by commercial WEDM process. The outcomes showed that the modules manufactured by proposed wire-radius compensation technique, more geometrically correct than the conventional WEDM compensation process.

Wang et al. (2009) carried out an experimental investigation in dry WEDM to improve the surface quality. The authors present a new approach known as gas-liquid combined multiple cut (Single pass cutting is processed in deionised water, semi-finish operation in liquid or gas medium and the final finishing is in gas medium). Six machining factors namely, pulse on time, pulse off time, wire offset, peak current, wire feed and wire length are chosen in dry and wet condition to investigate surface roughness, straightness and material removal rate. Authors conclude that the multi pass cutting in dry condition can improve surface finish significantly.

Sarkar et al. (2011) carried out an extensive research work in depth understanding of wire lag phenomenon to enhance the profile accuracy in WEDM. An analytical model is developed to measure the gap force as well as wire deflection at any machining condition. Impacts of these two important factors are verified by conducting experiments on cylindrical job. Authors'

claims that inaccuracy presence during profile cutting can be eliminated by wire lag compensation technique. It is conclude that the research finding are very much useful to better understanding the wire lag and gap force phenomena in the area of high precision WEDM.

Hoang et al. (2013) demonstrate how to improve the thermal efficiency. Effects of external vibration on productivity and accuracy in micro WEDM process also carried out by the authors. It is observed that the pulse discharge become more effective when external vibration applied. From the experimental results it is also found that the external vibration on the workpiece is more effective rather than electrode. Machining efficiency increases 2.5 times when vibration assisted to the workpiece whereas productivity increases 1.5 times when external vibration applied on the wire electrode.

A magnetic abrasive finishing operation (MAF) is employed to remove the recast layer and also to improve the surface quality of cylindrical specimen in WEDM of aluminium alloy by Amineh et al. (2013). Three level full factorial designs is considered to study the linear speed, working gap, abrasive particle size and finishing time on surface finish and recast layer thickness. Experimental outcome showed the impact of MAF process is very much effective to eliminate the recast layer and surface roughness improvement.

Selvakumar et al. (2016) presented the trim cutting operation to reduce the corner error and enhancing the accuracy of the geometric profile. Authors considered three different factors in rough cutting operation to analysis the volumetric removal rate, surface finish and corner accuracy. Authors conclude that trim cutting is the most suitable strategy to eliminate the die corner error than parameters modification strategy. It is better to carried out machining at higher pulse parameter setting during rough cutting operation to achieved higher productivity. Whereas lower pulse parameters settings in first cut is better for minimizing the corner error and surface roughness when productivity is less important.

Werner (2016) implemented a novel method to improve the accuracy of a curvilinear profile in WEDM. Author developed a nominal geometric model using CAD/CAM system. Distributions of machining deviations are measured by coordinate measuring machine (CMM). This measuring information is used to modify the geometric model and to correct the machined programme. Again, machining is carried out and repetition of measurements conducted to verify the developed model for generation of curvilinear profiles.

Mouralova et al. (2016) analysed the effects of cutting velocity on craters formed in WEDM of 16MnCr5 steel surface. Metallographic study is carried out on electrode as well as workpiece surface to observe the diffusion subsurface damages and microscopic slides presence the surface. A comprehensive study is carried out on brass wire to measure the wear rate produced by the cutting process and also its degradation in terms of the quality and the chemical elements and its composition of surface.

Chen et al. (2017) proposed non-circular parametric curve interpolation algorithm to generate parametric curves such as involutes, Archimedes spirals, cycloids, and parabolas etc. in WEDM. This algorithm based on unit arc length increment method (UALI). Authors compared simulation and experimental results obtain from algorithm. Simulated and experimental outcomes exhibit close enough. Additionally, accuracy of the interpolation algorithm is also analysed.

Mouralova et al. (2018) try to find the key parameters of machine setup to manufacture high-precision components with essential surface quality. For this purpose, surface topography analysis is made using scanning electron microscopy (SEM). Chemical composition of the machined surface is recognised by EDX analysis. In addition, colour filtered and unfiltered images of surfaces taken by 3D profilometer. In this study authors exposed the optimal machining parameters settings to get best quality machined surface is V_g =70 V, T_{on}=6 μs, T_{off}=50 μs, I_p =25 A and WFR=14 m/min.

Mandal et al. (2019) comprehensively studied the evolution of the surface finish of Al 6065-T6 alloy using brass coated (φ=0.25 mm) wire electrode in WEDM. Two successive finished cuts followed by rough cut are performed to improve of the surface quality of machined product. For this purpose, two different wire offsets are considered as 70 μm and 120 μm while other process parameters remain unchanged. The average surface finish value obtained in single pass operation is over 2.5 μm, whereas it reduced upto 1.0 μm after final finish cutting operation.

Farooq et al. (2020) broadly studied influence of significant process parameters, such as pulse on-off time, servo voltage and wire feed rate. Geometrical accuracies and corner radius are considered as response criteria for concave and convex profiles. Optimal combination of process factors is capable of resulting in lowest geometric deviation is 0.25% overcut in case of convex profile whereas 0.236% undercut in case of concave profiles and corner radius is approximately 0.106 mm.

Kirwan et al. (2021) modified machining G-code to compensate the wire lag in sharp corners. Initially, authors are investigated the influence of surface feed rate on profile accuracy and it is observed that surface feed significantly effects on wire lag and profile accuracy. For this purpose, mathematical model of wire lag compensation is developed and verified by experimental investigation. It is also found that the developed model can predict the wire lag or corner error within ±10% of the experimental value.

Trim offset approach in WEDM for precision manufacturing of turbine wheel slots is carried out by Sharma et al. (2021). The generated slot profile has been demonstrated with average roughness of 0.65 μm, accuracy within ±5 μm, minimum hardness alteration (34.87 Hv) and small recast layer (<5 μm) using B-150 wire electrode and satisfied the necessary requirements of turbine industries. Authors conclude that WEDM trim-offset approach is more advantageous with respect to wire electrochemical machining (W-ECM), and of course it should be useful for researchers those are working in Precision machining industries'.

2.2 Existing knowledge gap to outline the research objectives

Majority of the past research work is carried out to find out the appropriate input process parameters that control the performance characteristics in WEDM. It is very important to select, an appropriate process parameter and their levels when material to be machined is particularly uncommon. Generally, speaking parameter settings given in the instruction manual provided by machine manufacturer are suitable for conventional material machining. However, to machine advanced alloy or hard to machine materials, prescribed parameter settings given in the manual cannot fulfil the requirements for optimum machining. For that reason, customized parameter setting is needed for efficient machining of such materials. Al 7075 is the most beneficial aluminum based difficult to machine material that cannot effectively be machined by conventional parameter settings. The dielectric conductivity that is suitable for WEDM of steel and other conventional materials is not expected to be suitable for machining of high conductive new generation Al 7075 alloy. Influence of electrical conductivity of the dielectric on machining of Al 7075 alloy has not been studied. Besides, influence of dielectric conductivity on corner accuracy and surface characteristics for this alloy is not reported so far by any researchers. Multipass cutting operation in appropriate conductivity setting to enhance the corner accuracy and surface finish simultaneously have not been reported so far for this material.

2.3 Objectives of present research

Keeping in view of the above mentioned requirements and research gaps found from the study of past literatures, the objects of the current research work are as follows:

A. To explore the influence of different process parameters including dielectric conductivity and find out the appropriate conductivity setting that is suitable for efficient machining of Al 7075 in rough cutting.

B. To carry out the process optimization in single pass (rough) cutting operation and develop an appropriate technical guideline for optimal machining of this new generation material.

C. To explore the influence of various process parameters in multipass cutting operation of Al 7075 and to improve the corner accuracy and surface finish by a suitable optimization technique.

D. To integrate the rough and trim cutting operation in a single optimization strategy to find out the best machining strategy for given machining requirement.

E. To study the surface morphology and topography for single and multipass cutting operations.

Chapter-3

Structural and Functional Features of EX-40 WEDM System

For effective control of the machining parameters and prosperous utilization of the WEDM system in material machining, all the features of the CNC-WEDM system are required to be detailed in the study. There are three major features in the EX-40 WEDM system known as the hardware unit, software, and operational features. The hardware unit is associated with the power supply, machine control unit, dielectric supply unit, cooling system, etc. Software is used to control the axis movement, parameter settings, and wire driving system. Functional or operational features are subdivided into single-pass cutting, taper cutting, multi-pass cutting, and wire diameter compensation. In this section, the structural and functional features of the EX-40 WEDM system are elaborately explained.

3.1 Hardware unit and software used in EX 40 WEDM system

The EX-40 WEDM system is incorporated with various sub systems. The entire WEDM system is -

a. Machine tool unit
b. Dielectric liquid supply unit
c. Power supply unit.

The three units mentioned above are divided into several subsystems. A schematic diagram of the WEDM system is given in Figure 3.1. The pictorial view of the WEDM setup used to perform the experiments is shown in Figure 3.2. As already said, the major unit of WEDM is associated with several subsystems. These sub-systems are elaborately explained here:

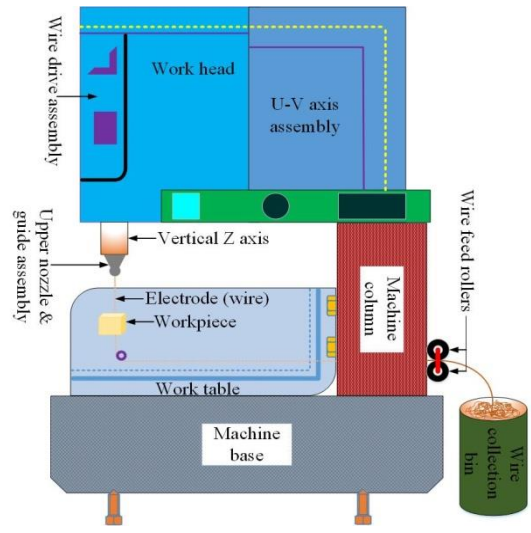

Figure 3.1 Schematic representation of hardware unit in WEDM system

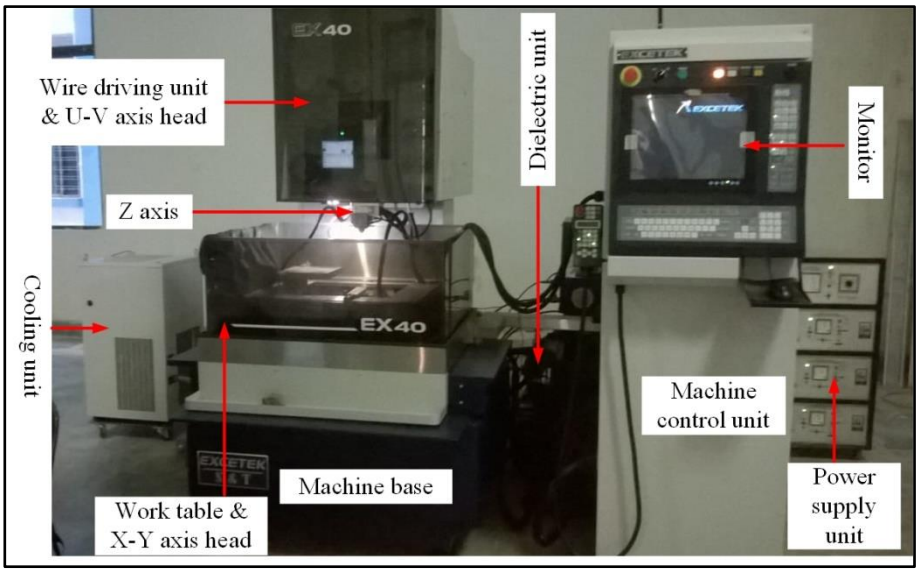

Figure 3.2 Photographic view of the WEDM system used for experimentation

3.1.1 Structure of EX 40 WEDM

WEDM system controls the motion of worktable and the wire driving system during profile cutting. It mainly divided into the following subsystems:

i. Work table (also known as X-Y table) where the job is fastened
ii. The auxiliary table unit i.e. U-V axis (parallel to the X-Y axis)
iii. Vertical Z-axis control unit (perpendicular to the X-Y or U-V axis)
iv. Wire drive and feeding mechanism

i. Work table (also known as X-Y table)

The workpiece mounting table where the job is clamped is also known as the X-Y table. This X-Y table is associated with two metal bridges, which are attached to the base of the machine to hold the workpiece. Common clamping devices are used to fix the flat jobs on the worktable; otherwise, external fixture arrangements are required to hold the intricate workpiece. The table moves along the X and Y axis with a step variation of 0.1 m by means of an AC stepper motor. The job must be clamped on the worktable and ensure electrical contact before starting the machining. The general specifications of the machine are revealed in Table 3.1.

Table 3.1 General specifications of EX-40 WEDM (Flushing type)

Specification	V50
Machine weight	3200 Kg
Table travel of XY	500×300 mm
Table travel of UV	120×120 mm
Z axis travel	260 mm
Maximum workpiece size	850×600×255 mm
Maximum workpiece weight	600 Kg
Wire diameter	0.1~0.3 mm
Dimension of installation	2330×2545×2080 mm
Maximum taper angle	± 26°/100 mm

ii. The auxiliary axes (U-V axis motion control unit)

In the WEDM system, the lower flushing guide is fixed, whereas the upper nozzle guide can move along the U-V axis, which is parallel to the X-Y table. An upper nozzle guide is mounted on the quill. The quill is driven by an AC stepper motor with a minimum step variation of 0.1 µm. The main purpose of the auxiliary head, i.e., U-V axes, is to produce a taper profile and generate an intricate contour. As stated earlier, the lower flushing nozzle is stationary, and the upper nozzle is supported by a U-V axis that can transversely move along the U and V axis. During taper cutting, the wire electrode has to be tilted. This tilting can be achieved by moving the upper nozzle guide along the U-V axis with respect to the X-Y axis. The required taper angle is attained by synchronised movement of the worktable (i.e., X-Y axis) and U-V axis along the predefined programmed path kept in the controller. The maximum travel length of the U-V axis is given in Table 3.1.

iii. Vertical Z-axis control unit

The vertical Z-axis is associated with the upper nozzle guide along with the quill. This vertical axis is driven by an AC stepper motor. The Z-axis quill moves vertically upward and downward. This movement is provided to adjust the gap between the upper and lower flushing nozzles depending upon workpiece thickness. Manual movement of the Z-axis is done by using a joystick, and the position of the Z-axis is prepared according to the dimension of the job to be accommodated with variable thickness. A joystick is used for manual movement of the Z-axis. The moving guide, i.e., the upper nozzle guide, is used to

direct the wire electrode vertically downward. A schematic diagram of the worktable head assembly, X-Y and U-V axis assemblies, and vertical Z-axis arrangement of the machine is shown in Figure 3.3.

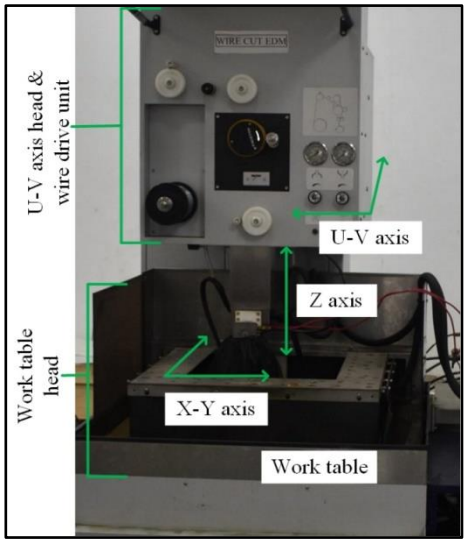

Figure 3.3 Photographic views of the worktable head and X-Y-Z-U-V axis assembly

iv. Wire driving mechanism

A tool electrode (thin wire) is wound on a spool and the spool is mounted on a wire drive plate in the hardware unit. Wire is continuously supplied from the wire spool and it travels through the job to provide fresh and new wire electrodes onto the machining area, and finally, consumed wires go to the wire accumulating bin. A thin wire is held in between two small wire guides to give a smooth and straight movement during machining. The upper wire guide delivers the thin wire from the spool onto the machining region, and the consumed wire moves along in a vertically downward direction via the lower nozzle guide in the system. Generally, a diamond coating is applied to the wire guide orifice to prevent wear and tear and to maintain accuracy.0.3 m clearance gap is allowed between the wire-guide and the nozzle-orifice. The lower nozzle is commonly fixed, whereas the upper nozzle is supported by a U-V axis head, which is moved transversely along the U-V axes with respect to the lower nozzle guide. The position of the vertical Z-axis can be varied by moving the auxiliary head (quill). Conventional wire-guides are manufactured from brass, and special guides are made from an alloy material with a diamond insert. Such a wire guide can machine a diverse range of jobs with varying workpiece heights. To fulfil such demands, an extensive range of wire speeds is essential. Therefore, to accomplish the different working necessities, a unique wire driving system is required with a choice of different wire speeds. The wire must be kept in a tight and

straight condition to provide a smooth drive and also to attain the necessary accuracy of the product. To fulfil this need, a uniform arrangement in the driving system provides an appropriate tension on the wire. Electrode wire passes through a sequence of rollers (idlers) and some wheels to provide a uniform wire tension and also to provide a constant speed in the machining zone. The schematic diagram of the wire driving unit is given in Figure 3.4.

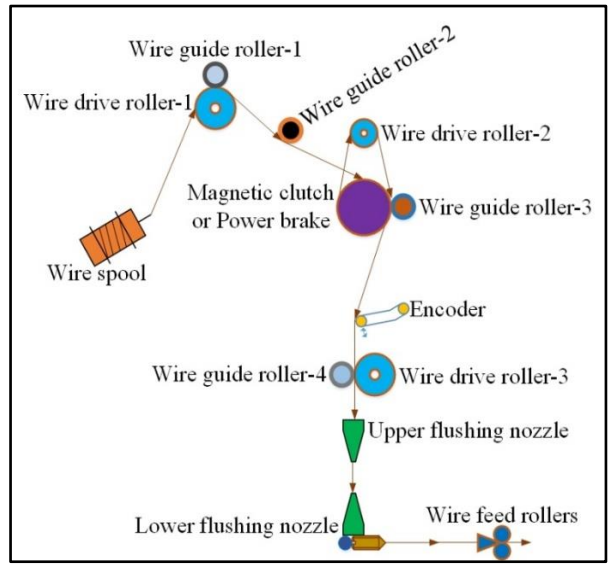

Figure 3.4 Schematic representation of wire tension control system

A Cartesian coordinate positioning system is used in the wire drive system. The function of this system is computer numerical control based. Sometimes, automated wire threading is carried out in this system to minimize the operational time. Product accuracy is mainly controlled by this system. A photographic view of the wire tension control system is exhibited in Figure 3.5.

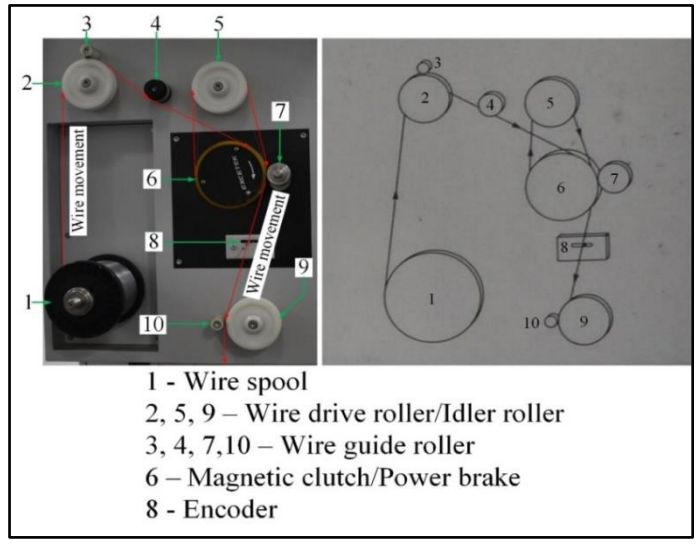

Figure 3.5 Photographic view of the wire tension control system of EX-40 WEDM

3.1.2 Dielectric supply and cooling unit in EX-40 WEDM

Dielectric is one of the most crucial factors in WEDM and it plays an important role in determining the material removal rate and surface finish. It has different functions in the process. Dielectric isolates the wire electrode from the workpiece to achieve the high current density in the plasma channel. Initially, it rapidly ionises when it reaches the required potential difference and then breaks down and works as a cooling agent. It cools down electrode surfaces, i.e., wire as well as job surfaces, and exerts a counter pressure in the inter-electrode gap to expand the plasma channel. Flushing with dielectric removes the debris particles after machining and avoids the particle linkage that causes process disturbance by short circuit and surface damage of the electrode.

Two types of dielectric are used in WEDM; deionized water and hydrocarbon compounds (also known as dielectric oil). In this work, deionised water is used as a dielectric liquid. During machining, contaminated water from the machining tray goes through a fine strainer provided above the contaminated water tank, helping to separate the large eroded particles. The filter pump sucks the contaminated water from the storage tank and delivers it via paper filters to clean up the water. This clean water is stored in the clean water tank. The dielectric recirculation system used in the EX-40 WEDM system is shown in Figure 3.6.

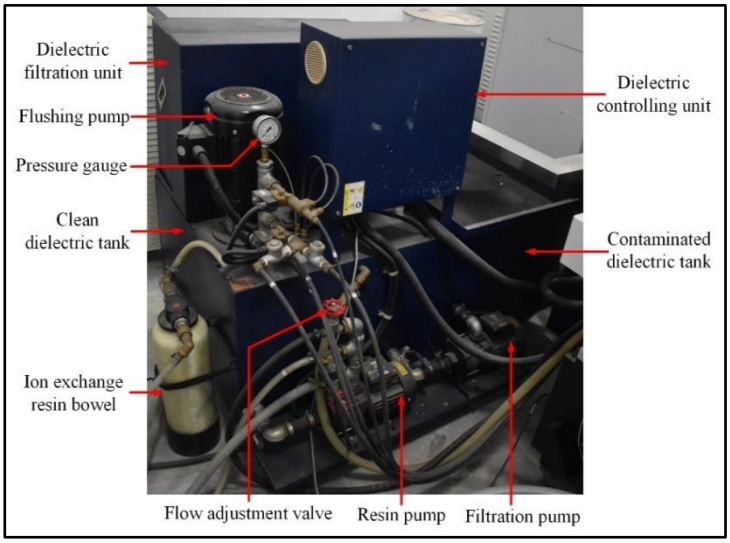

Figure 3.6 Dielectric recirculation system used in EX-40 WEDM

Filter cartridges are required to be changed when the filters are unable to clean the contaminated water. The filter pump sucks contaminated water from the storage water tank and delivers it to the filter cartridge. Contaminated water is then cleaned by the filter

cartridge and the water coming out of the filtration chamber is supplied to the clean water storage tank.

The chiller pump/resin pump sucks the clean water from the storage tank and then passes it through the chiller unit. A refrigeration chiller maintains the water temperature according to the requirements. This cool water coming out of the chilling unit is then delivered to the fresh water storage tank. The chiller unit used in the EX-40 WEDM system is exhibited in Figure 3.7. A solenoid operated delivery unit is in the chiller pump to supply fresh water into the resin chamber. This solenoid operated valve is open when the conductivity of the dielectric reaches above the prescribed limit. The main function of the resin chamber is to maintain the level of conductivity. The resin chamber and filter cartridge used in the WEDM system are given in Figure 3.8. The details of the dielectric supply unit are highlighted in Table 3.2.

Table 3.2 Details of dielectric supply unit

Water filtration system	V50
Dielectric fluid	De-ionized water
Tank capacity	300 Litre
Filter type	Paper (2-4 Pcs)
Resin chamber	5 Litre (Resin: Ion-exchange)
Filter cartridge	5-10 µm
Water electrical conductivity	Auto/Manual
Temperature control	Auto
Dimension of filtration system	1200×800×1000 mm

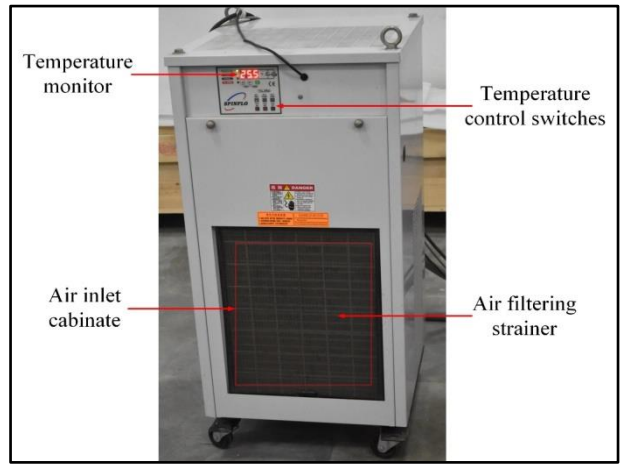

Figure 3.7 Chiller unit of EX-40 WEDM system

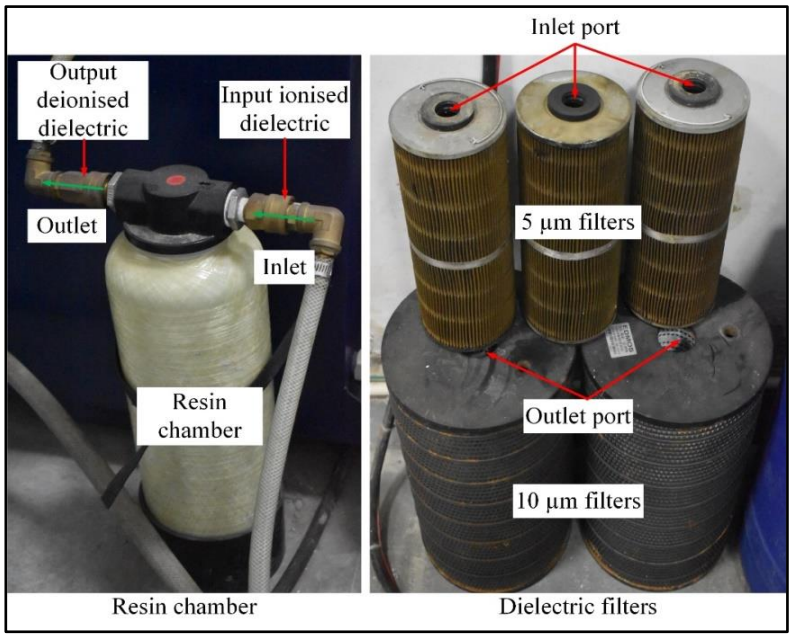

Figure 3.8 Resin chamber and filter cartridge used in the WEDM system

3.1.3 Power supply and control system used in EX-40 WEDM

The parts of the power supply system in WEDM comprise an electrical pulse generator, an axis motor driver for five axes, and a controller or MCU. A power supply to the machine is given by a three-phase AC servo controlled stabilizer (shown in Figure 3.9). The main function of a voltage stabilizer is to maintain a constant voltage. This constant supply voltage is used to generate an uninterrupted discharge pulse and smoothly run the chiller unit and dielectric pumps. The electrical pulse generator unit is used to generate the spark and convert alternating current (AC) into direct current (DC). The high frequency pulse is produced by the MOSFET. A pulse generator (electric) consists of electrical and electronic subsystems. In case of straight polarity, the positive terminal of the pulsed DC supply is connected with the worktable and the negative terminal is connected with the wire electrode at the upper and lower wire guide through a pair of current pick-ups. In other cases of reverse polarity, the positive terminal is connected with the wire electrode and the negative terminal is connected with the workpiece. Pulsed power is supplied to the workpiece and the wire electrode to generate a series of electrical pulses between the electrodes. The material removal takes place due to the electrical erosion caused by the pulse.

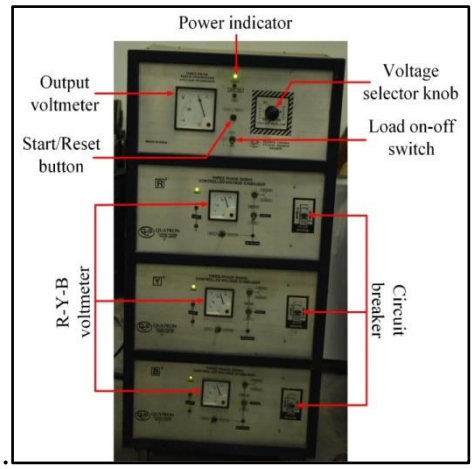

Figure 3.9 Stabilizer (3-phase AC)

The operation control unit of the machine controls the several machining factors such as pulse parameters and other machining condition. These setting formats are enlisted below:

i. Programme number: 000-999 (For operator) and 1000-9999 (Defined for factory)

ii. PM: Power mode; Range: 00-10 (Step variation of 1)

iii. OCV: Open circuit voltage; Range: 01-20 (Step variation of 1)

iv. T_{on}: Pulse on time; Range: 01-24 (Step variation of 1)

v. T_{off}: Pulse off time; Range: 04-50 (Step variation of 1)

vi. A_{on}: Arc on time; Range: 01-16 (Step variation of 1)

vii. A_{off}: Arc off time; Range: 04-50 (Step variation of 1)

viii. S_v: Servo voltage; Range: 10-90 (Step variation of 1)

ix. W_t: Wire tension; Range: 01-20 (Step variation of 1)

x. W_f: Wire feed rate; Range: 01-20 (Step variation of 1)

xi. W_a: Water pressure; Range: 01-08 (Step variation of 1)

xii. FR%: Percentage of feed rate; 001-500 %

xiii. F: Table feed; Range: 00-50 (Step variation of 1)

xiv. SM: Servo control mode; M90 (For auto feed), M91 (For constant feed)

xv. S_c: Servo sensitivity; 01-99 (Step variation of 1)

3.1.4 Software features in EX-40 WEDM

The machine control panel (MCP) in the machine control unit of the EX-40 WEDM system accomplishes the various controlling functions in programme control. MCP is a distinct component of MCU that resembles a cabinet. Different subunits in the panel, like display monitor, keyboard, mouse, functional key, number of manual control buttons, etc., appear in the MCP. Here, the machinist correlates with the machine via display monitor. An emergency stop, power on-off switch, power indicator, buzzer, and four different warning indicators are placed at the top of the control panel in a single row. The monitor is located below the emergency stop in the control panel. On the right side of the monitor, a total of 36 keys are placed in 12 different rows, which are known as control keys or sometimes called soft keys. Just below the display monitor is an ASCII computer keyboard. This computer keyboard is associated with F1 to F10 functional keys. Figure 3.10 demonstrates the MCP unit used in the EX-40 WEDM system.

Figure 3.10 Machine control panel of EX-40 WEDM system

The profile geometry is drawn by using master-CAM CNC programming software on the computer, and the wire movement path or cutting path is then defined along the profile in the drawing, in terms of various definition points, curves, lines, splines, and circles as tool route elements. The generated profile is initially stored in the computer. The wire compensation and taper gradient are given for each individual element discretely in the drawing. After completing the profile, the necessary programmes are directly generated by using the master-CAM software from the given geometry of the profile. After successful profile generation, the generated profile is saved on the hard disc of the computer by specifying a start and end point with the programme number. Then the developed programme and the CNC code are borrowed from a USB device to execute in the MCU for machining.

3.1.5 Part programing methodology

A part programming language is used to construct the required shapes. The path of that shape is generated for accurate movement of the electrode with respect to the starting point. The programming software itself generates a NC code when the cutting profile and the wire path movement are fed into the machine controller. There is so much high level programming software in WEDM to generate the contour profiles, which is evaluated automatically to minimize the total computational time. Different intricate shapes can be simply made by defining the up and down layers by connecting them in programming. The notable programming topology used in this study is enlisted below:

i. Complete geometry explanations for square, rectangle, point circle, lines, line segment, spline, etc.

ii. Simple demarcation of 2D and 3D wire path.

iii. For a complex profile, facility to connecting top and bottom layer edge or face.

iv. Conversions including several translations, various rotations, mirroring images about a line segment.

v. Sleek curve fitting for cam and gear profiles.

vi. Involute and cycloidal gears definitions with required corrections.

3.1.6 Descriptions of process parameters in EX-40 WEDM

Pulse on time (T_{ON}): The time interval of electron discharge (spark) that occurs between wire electrode and the workpiece once the break-down voltage of the dielectric is achieved. During this period of time, voltage is applied across the electrodes. This causes ionization of dielectric and then erosion of the workpiece material takes place. The discharge energy per pulse increases with the increase in pulse on time and resulting in a higher cutting rate.

Pulse off time (T_{OFF}): It is the time duration between two consecutive sparks. During this period of time, there is no current supply to the electrodes. At the same time, deionization of dielectric takes place and dielectric also flushes the machining debris (removed materials) from the inter electrode gap (IEG). Lower the pulse off value means more number of discharges in a given time, resulting in increase in sparking efficiency and cutting rate. Using a very low pulse off value, however, may cause wire breakage and an unstable discharge. As

and when a discharge condition becomes unstable, it is better to keep increasing the pulse off value. This will allow a lower pulse duty factor (defined as the ratio of T_{ON} and cycle time).

Arc on time (A_{ON}): Arc on time is auxiliary sparking current. The increase in arc on time value will increase the pulse discharge energy for a higher value of current and the gap condition will become unstable with improper combinations of T_{ON}, T_{OFF}, S_V etc. Reducing the arc on value helps turn an unstable discharge condition into a stable one.

Arc off time (A_{OFF}): Arc off time is control no sparking pulse time (i.e. T_{OFF}). When the value of A_{OFF} is increased, sparking off time (T_{OFF}) becomes longer. This improves the stability of cutting.

Open circuit voltage (V_{OC}): During initial cutting, open-circuit voltage is provided to stabilise the pulse generator circuit. When the circuit becomes stable, increase the V_{OC} to get faster cutting speed. This phenomenon can be explained by the relationship between maximum discharge energy per pulse and the capacitance of the generator as follows:

$$E_{max} = \left(\frac{1}{2} \times C \times V_{OC}^2\right) \quad (3.1)$$

Where, E_{max} represent the maximum discharge energy per pulse, C represents the charging capacitance and V_{OC} is voltage of open circuit. The discharge energy per pulse is only determined by V_{OC} and the capacitance. The effect of V_{OC} on the discharge energy is greater than that of capacitor. As the open circuit voltage increases, the energy of per pulse increases, so the amount of material erosion increases.

Servo voltage (S_V): This is a reference voltage for the actual gap voltage. The servo voltage decides the inter electrode gap that has to be maintained between the wire electrode and the workpiece throughout the machining process. This is expected to influence the concentration of discharge pulses in the machining zone. S_V prevent the gap short phenomenon when cutting speed is too fast.

Flushing pressure (W_p): In general, a high input pressure of dielectric is necessary for cutting with higher values of pulse power and, especially, while cutting the jobs of higher thickness. A low input pressure should be used for thin jobs and in trim cuts.

Wire feed rate (W_F): This is a feed rate at which the fresh thin wire is fed continuously to the machining zone during cutting. Obviously, for working with higher pulse power, higher values of wire feed rate are required.

Wire tension (W_t): This is a gram-equivalent load with which the wire being continuously fed to the system. The wire is kept under tension so that the same remains straight between the wire guides. The wire deflection is caused due to spark induced reactive forces and flow of water dielectric in the machining zone. The wire tension minimizes the undesirable wire deflection from its straight position between the wire guides.

Servo sensitivity (S_C): Servo sensitivity is the intensity with which the WEDM controller reacts in response to the change in error voltage between the desired gap voltage and the actual voltage. This parameter (S_C) is adjusted the servo voltage gain. With an increase in servo sensitivity for the same error voltage, machining speed tends to be higher to correct the error in gap voltage, which in turn reduces the gap voltage and consequently the inter-electrode gap (IEG).

3.2 Functional features of EX-40 WEDM system

As already exhibited in Figure3.2, the WEDM machine consists of a worktable, an auxiliary axis unit, and a wire driving system. Worktable and U-V tables move along longitudinal and transverse directions with a step variation of 0.1-10 μm, typically by means of AC stepper motors. Workpiece clamped tightly on the machining table before starting the machining operation. A precision dial gauge is used to ensure that the top face of the job surface is either accurately horizontal or not. If it is not horizontal, then the workpiece clamping must be adjusted by varying its position to make it horizontal. Cleaning is required before mounting the workpiece on the machining table to make it rust and oil free.

After switching on the machine, 5-axes referencing (X-Y-Z-U-V) is carried out. After completion of axis referencing, the upper nozzle guide is made exactly coaxial with the stationary lower guide by using the G0U0V0 command in manual data input mode. A wire threading operation is performed after making the wire vertical. In the NC program, quill position, or Z-axis height, is measured as the workpiece thickness and a small height, which is considered the clearance gap between the nozzle and workpiece. The height of the Z-axis is varied according to the thickness of the workpiece.

Wire is continuously fed from the wire spool through the workpiece and finally collects the used wire in a wire-collecting bin after machining. The wire electrode is supported by several rollers along the travelling path under a specific tension between two nozzle guides that are located above and below the mounted workpiece. The lower nozzle guide is known to be

fixed, but the upper nozzle guide, which is allocated in the U-V axis, can move along the U and V axes with respect to the lower guide. The upper nozzle guide can be manually positioned along the Z-axis by moving the quill. Predefined programmes are kept in the controller and the worktable transverses the job along the programmed path as the machining starts. A conventional cut (not the taper cut) with a predefined path is carried out by moving the work table along the predefined path while the auxiliary axis is kept immobile (also known as dry run machining).

3.2.1 Single pass cutting

Conventional cutting in WEDM is known as "rough" or "single pass cutting." In such conditions, the wire electrode moves and cuts the workpiece along the predefined programme path only once. In such circumstances, the prime objective is to increase the cutting rate where accuracy and surface finish are not so important. It is set to high power and a high process parameter setting for rough or single-pass cutting operations to improve cutting speed. Figure 3.11 shows the slot produced by a single-pass cutting operation.

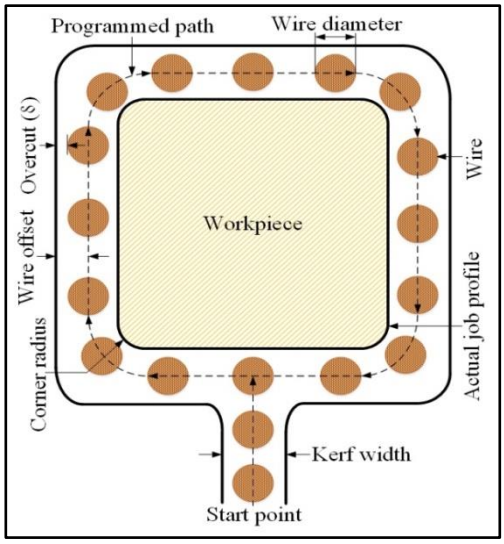

Figure 3.11 Slot produced by single pass cutting

3.2.2 Multipass cutting

In modern WEDM systems, multi-pass or trim cutting operations are provided to improve the accuracy and quality features of the product. The scheme of the trim cutting arrangement in the WEDM system is shown in Figure 3.12. The trim cutting operation is also known as the skim cutting operation at times. In this technique, the wire electrode traces back along the same path after the previous cut is completed. Generally, two to five skim cuts are carried out

over the rough cut surface, depending upon the needs. During the trim cutting operation, very low pulse power and dielectric flushing are applied to acquire a smaller amount of material removal. High power and flushing pressure are generally avoided in skim cutting operations to get precise accuracy and a better surface finish.

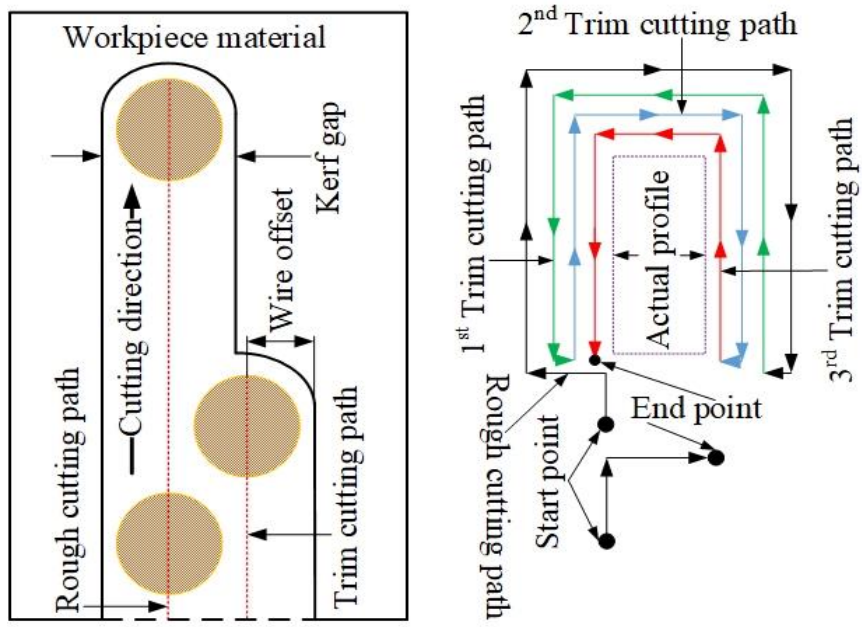

Figure 3.12 Wire path planning for rough and trim cutting operation

In WEDM, machined products are categorised as die and punch. During the trimming operation, the workpiece must be kept in a particular location. The punch piece is kept in position by a 3 mm uncut path length at the end of the profile. A single cut is made to remove the final 3 mm of uncut route length after completing the required number of trim cuts (2–5 skim cuts, as needed). When removing the uncut path length, a suitable wire offset value is given to maintain the job's proper dimensions. Trimming operations often require a small amount of material to be removed. The amount of material removed in the initial trim cutting operation is significantly lower than in the rough cutting operation. It's also evident that the amount of material that's removed in the second trim cutting operation differs greatly from what was removed in the first trim cutting operation as well. Machining parameter settings regulate this amount of material removal. Flushing pressure and current are kept as low as possible as the number of passes increases. In contrast, by choosing the right servo feed value, wire tension, servo sensitivity, and servo voltage can all be kept as high as possible without stopping the machine.

3.2.3 Taper cutting

Taper jobs are regularly required in the die-punch and mould-making industries. Apart from that, some other areas, like aviation, aerospace, and the automobile industries, needed complex taper shapes. During straight job cutting, the upper nozzle guide remains stationary (i.e., the U-V axes are kept in their home positions; U = 0 and V = 0) with respect to the lower guide. In reality, both nozzles remain stationary, although the worktable moves along a predetermined route. The bottom nozzle guide does not need to remain in the same position at all times. During straight cutting, the wire electrode should be aligned vertically to the X-Y and U-V axes.

During the taper cutting operation, the upper nozzle is moving along the U-V axes with respect to the worktable, whereas the lower nozzle remains in a stationary position. The wire electrode does not remain vertically straight, clasping the generation of motion in the U-V axes. Several points in the part programming can precisely control the angle of the taper with respect to the vertical axis. An auxiliary table (U-V axes) and worktable (X-Y axes) can be moved in sync along the programmed path to obtain the required taper angle.

In WEDM, taper cutting is done meticulously. Due to some difficulties, this operation is performed at a lower machining speed than a straight cutting operation. As much as possible, the upper and lower flushing valves are left open to ensure proper flushing. The smallest possible gap must be maintained between the flushing nozzle and the top of the work surface. Here is a list of things to look out for when cutting taper:

(a) It is difficult to make proper flushing in the machining zone, as the flushing nozzles are not in coaxial position; wire electrode is in tilting position whereas flushing is vertical. This results severe heating of wire electrode due to excessive thermal load during machining. For that reason, machining speed is limited in taper cutting.

(b) Excessive fluctuation of wire tension.

(c) A minor deformation of electrode becomes inescapable in exit area of upper nozzle and at the entrance of lower flushing nozzle increased the chances of wire rupture.

3.2.4 Electrode (wire) diameter compensation

Dimensional accuracy of the manufacturing product is controlled by wire compensation. The width of the slot produced by rough-cut is known as the kerf width. Wire vibration and pulse parameter setting influence the width of the kerf. Aggressive sparking and high discharge current are also responsible for increasing the kerf gap. The width of the kerf is always greater than the wire diameter. The width of the cut directly depends on the machining condition. Half of the kerf width dictates the wire offset value. This amount of wire offset or wire compensation has to be provided in part through programming during profile generation. Wire offset is evaluated as follows:

Wire offset or wire compensation = $\frac{1}{2} \times (Kerf\ width) = \frac{Wire\ diameter\ (d)}{2}$ + Overcut (δ) (3.1).

Chapter-4

Preliminary Investigation of Machining Parameters at Default Conductivity Setting

4.1 Statement of the problem

Wire electro discharge machining (WEDM) is a very complicated and useful machining technique where a wide number of control factors are involved. Therefore, the selection of an appropriate parametric combination is the critical task for machining materials, especially advanced alloys. The scenario becomes more complex when choosing the significant machining parameters for single-pass and multi-pass cutting. Levels of input process parameters are varied when the material to be machined is changed.

In the research study, experimental investigation has been carried out for the appropriate selection of process parameters in WEDM of Al 7075. Past WEDM researches have revealed the effect of input parameters on material removal rate (MRR) and surface characteristics (Borsellino et al. 1999, Gökler et al. 2000, Kim et al. 2001, Sarkar et al. 2005, Bobbili et al. 2013, Selvakumar et al. 2014, Gong et al. 2017, Nain et al. 2018, Singh et al. 2018). A few studies have been published on the wire lag phenomenon during rough cutting operations, which is an important and deciding factor in investigating corner accuracy (Hsue et al. 1999, Puri et al. 2003, Sarkar et al. 2011, Abyar et al. 2018). However, there is a scarcity of research on the effect of process parameters and optimization on dimensional accuracy (Lin et al. 2001, Han et al. 2007). Nevertheless, this response parameter is extremely important for achieving high precision jobs in WEDM. A few studies on WEDM of Al 7075-based MMCs have been published (Rao et al. 2014, Lal et al. 2015).

Furthermore, the effect of pulse on time (T_{ON}), arc on time (A_{ON}), pulse off time (T_{OFF}), arc off time (A_{OFF}), servo sensitivity (S_C), wire tension (W_t) and servo voltage (S_V) at default dielectric conductivity setting (i.e., conductivity while machining the steel or other conventional alloy) on machining speed (V_c), corner error (C_E) and surface roughness (R_a) has not been reported so far in the field of WEDM for this alloy. The main objective of the present research work is to carry out the experimental investigation of different input factors, T_{ON}, A_{ON}, T_{OFF}, A_{OFF}, S_C, S_V, & W_t on machining speed (V_c), corner error (C_E), and surface roughness (R_a) during single pass cutting operation at the default conductivity setting.

4.2 Experimentation

The experiments have been carried out on the EX-40 WEDM system using the Taguchi design technique. The L_{18} orthogonal array has been used to conduct eighteen experiments. Initially, a one factor at a time approach is used to select the appropriate range of process parameters. Al 7075 alloy of 25 mm thickness is taken as a workpiece material, and coated brass wire of 0.25 mm diameter is used as an electrode.

4.2.1 Selection of controllable process parameters

Based on a literature survey and an initial trial run, seven control factors have been selected as input process parameters. Input process parameters and their levels are illustrated in Table 4.1. During the trial run, it has been observed that the seven process parameters have a significant impact on machining speed, corner error, and surface roughness. Table 4.2 displays the experimental plan matrix and results. In this set of experiments, pulse off time and arc off time values are selected based on the pulse on time and arc on time, respectively, to ensure that the debris is flushed out of the gap and to prevent arcing from occurring in the same location. On the other hand, selection of pulse off time and arc off time values in WEDM is also determined by the material properties of the workpiece and the desired machining characteristics, such as corner error, surface finish and cutting speed.

Table 4.1 Input process parameters and their levels

Parameters	Notations	Units	Levels		
			1	2	3
Pulse on time	T_{ON}	µs	0.5	0.7	0.9
Pulse off time	T_{OFF}	µs	14	24	34
Arc on time	A_{ON}	µs	0.2	0.3	0.4
Arc off time	A_{OFF}	µs	10	30	-
Servo voltage	S_V	volt	10	15	20
Wire tension	W_t	kg	0.8	1.2	1.6
Servo sensitivity	S_C	-	1	2	3

Table 4.2 L_{18} experimental plan matrix and results

Sl. No.	Process parameters							Responses		
	T_{ON} (µs)	T_{OFF} (µs)	A_{ON} (µs)	A_{OFF} (µs)	S_V (volt)	W_t (Kg)	S_C (-)	V_c (mm/min)	C_E (µm)	R_a (µm)
1	0.5	14	0.2	10	10	0.8	1	1.25	81	2.998
2	0.5	24	0.3	10	15	1.2	2	3.24	80	3.053
3	0.5	34	0.4	10	20	1.6	3	2.78	51	3.001
4	0.7	14	0.2	10	15	1.2	3	4.61	97	3.179
5	0.7	24	0.3	10	20	1.6	1	0.93	68	3.125
6	0.7	34	0.4	10	10	0.8	2	3.00	101	2.987
7	0.9	14	0.3	10	10	1.6	2	3.80	69	3.242
8	0.9	24	0.4	10	15	0.8	3	4.42	118	3.180
9	0.9	34	0.2	10	20	1.2	1	0.91	62	3.217
10	0.5	14	0.4	30	20	1.2	2	2.28	75	2.961
11	0.5	24	0.2	30	10	1.6	3	3.19	85	2.953
12	0.5	34	0.3	30	15	0.8	1	0.92	79	2.882
13	0.7	14	0.3	30	20	0.8	3	3.53	114	3.022
14	0.7	24	0.4	30	10	1.2	1	1.22	70	3.005
15	0.7	34	0.2	30	15	1.6	2	2.32	63	2.987
16	0.9	14	0.4	30	15	1.6	1	1.14	58	3.191
17	0.9	24	0.2	30	20	0.8	2	2.32	95	3.188
18	0.9	34	0.3	30	10	1.2	3	4.31	91	3.084

In this context, it is pointed out that there are so many noise factors related with WEDM process as enlisted below:

a. Ambience of the laboratory where WEDM system is installed.

b. Small variation of wire geometry and nature of vibration.

c. Instantaneous change of dielectric conductivity.

d. Abrupt nature of sparking in a specific point.

e. Inhomogeneity of workpiece material.

f. Variation of controller performance.

g. Small variation of flushing pressure and flow rate etc.

4.2.2 Evaluation of response criteria

In Figure 4.1a, a schematic representation of the corner error measurement and the path produced by the wire electrode are shown. The corner error (C_E) of the machined surface along the cutting direction has been measured by the CV-3200 (Mitutoyo, Japan) high precision contour measuring instrument. Measurement of the corner profile has been taken along the bisector (45^0) of the actual corner angle (90^0). The surface roughness value is measured by the SJ-410 (Mitutoyo, Japan) contact type surface measuring instrument. The 3D surface topography of the machined surface is captured by a high-resolution CCI (Taylor & Hobson, UK) microscope. Raw data of machining speed is noted down from the monitor of the machine and an average value is calculated for analysis. The corner error and surface roughness measurements have been repeated five times to minimise the error, and an average value has been taken. The required measurements have been taken in a vibration-free and stable temperature ambience to avoid measurement error. Lastly, workpieces after machining is shown in Figure 4.1b.

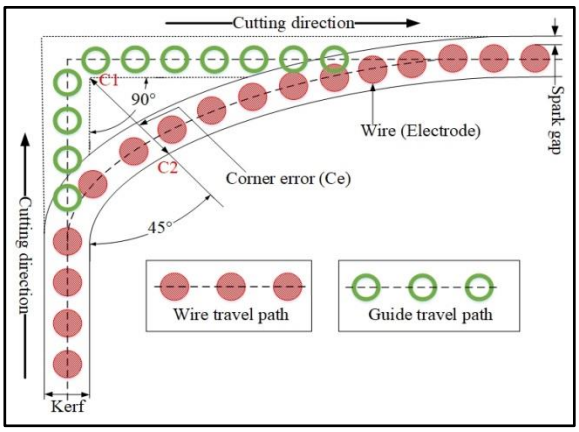

(a)

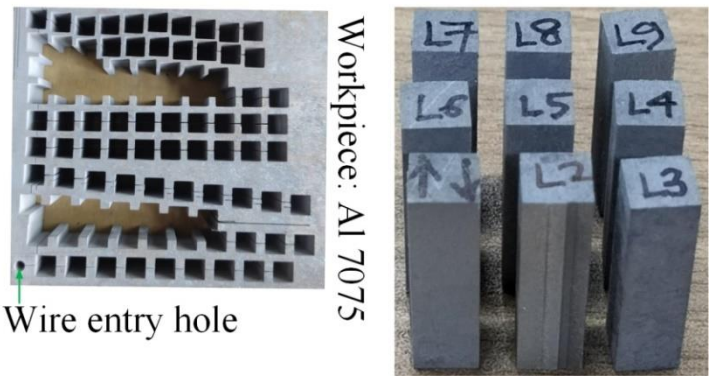

(b)

Figure 4.1 (a) Schematic representation of corner error (b) Machined workpieces

4.3 Mathematical modelling of the process parameters

The relations between process parameters and responses have been developed by using the non-linear regression technique. In the regression technique, the mathematical form of the correlation between output and input is as follows:

$$y = f(T_{ON}, T_{OFF}, A_{ON}, A_{OFF}, S_V, W_t, S_C) \quad (4.1)$$

Where y defined, the output and f represent the output function. In the process of analysis, estimate of y has been calculated by using above quadratic equation.

Mathematical model for machining speed, corner error and surface roughness are the function of WEDM input parameters, in terms of pulse on time, arc on time, pulse off time, arc off time, servo sensitivity, servo voltage and wire tension. The relation between input and output parameters are established based on the experimental results (Given in Table 4.2). Insignificant process parameters (P-value > 0.05) are eliminated from the model for better accuracy. The mathematical models for machining speed, corner error and surface roughness are shown in Eq. 4.2-4.4. The influence of the process parameters on output have been evaluated based on these mathematical models. Minitab-17 software package is used to develop the regression models and for the data analysis.

$$V_c = -8.71 + 3.28T_{ON} - 0.0281T_{OFF} + 20.30A_{ON} - 0.02061A_{OFF} + 0.3110S_V + 2.943S_C - 1.38T_{ON}^2 + 0.000175T_{OFF}^2 - 33.50A_{ON}^2 - 0.01260S_V^2 - 0.3925S_C^2 \quad (4.2)$$

$$C_E = 50.3 + 150.8T_{ON} + 1.35T_{OFF} + 66A_{ON} + 0.57S_V - 77.9W_t + 10.67S_C - 102.1T_{ON}^2 - 0.0333T_{OFF}^2 - 108A_{ON}^2 - 0.0333S_V^2 + 16.7W_t^2 + 0.67S_C^2 \quad (4.3)$$

$$R_a = 2.759 - 0.473T_{ON} + 0.00665T_{OFF} - 0.326A_{ON} + 0.0202S_V + 0.354W_t - 0.0012S_C + 0.711T_{ON}^2 - 0.000214T_{OFF}^2 + 0.27A_{ON}^2 - 0.000539S_V^2 \quad (4.4)$$

To verify the developed mathematical model, another set of confirmatory experiments have been carried out and results are given in Table 4.3. Percentage of prediction error shown in the Table 4.4 is defined as follows:

$$\%\ \text{prediction error} = \left\{\left|\frac{\text{Experimental value} - \text{Predicted value}}{\text{Experimental value}}\right|\right\} \times 100 \quad (4.5)$$

It has been observed that the predicted results are closed to the experimental values. This proves the fact that the devolved mathematical models for machining of Al 7075 are used for parametric analysis and optimization.

Table 4.3 Verification experiments for mathematical model

Control factors							Responses		
T_{ON}	T_{OFF}	A_{ON}	A_{OFF}	S_V	W_t	S_C	V_c	C_E	R_a
0.5	34	0.4	30	20	1.6	3	2.39	71	2.905
0.7	24	0.3	30	15	1.2	2	3.28	85	3.045
0.9	14	0.2	10	10	0.8	1	1.83	87	3.217
0.5	14	0.4	10	20	0.8	2	2.31	83	2.917
0.9	34	0.2	30	15	1.6	2	2.68	64	3.012

Table 4.4 Comparison between experimental results and model prediction values

Cutting speed (V_c)			Corner error (C_E)			Surface roughness (R_a)		
Experimental result	Predicted value	% error	Experimental result	Predicted value	% error	Experimental result	Predicted value	% error
2.39	2.43	1.67	71	73	2.82	2.905	2.924	0.65
3.28	3.19	2.74	85	88	3.53	3.045	3.098	1.74
1.83	1.89	3.28	87	84	3.45	3.217	3.258	1.27
2.31	2.42	4.76	79	82	3.79	2.917	3.016	3.41
2.68	2.55	4.45	64	61	4.68	3.012	3.145	4.42

4.4 Parametric analysis

Parametric analysis has been carried out to better understand the effect of individual factors on response criteria. In this case, developed mathematical models are used for parametric analysis. Initially, analysis of variance (ANOVA) is carried out to evaluate the level of significance of each parameter on the output. Predicted results based on models are then used to determine the influence of input factors on output responses.

4.4.1 ANOVA for machining speed, corner error and surface roughness

An analysis of variance (ANOVA) is a statistical approach for estimation of the relative influence of each variable on the overall measured response. In general, the relative importance of individual factors is often represented by the term F-value (Cochran & Cox, 1992). The F-value in the analysis of variance plays a significant role for input factors. Here, ANOVA has been employed to analyse the significance of seven input factors on machining speed, corner error, and surface roughness. ANOVA results for cutting speed, corner error, and surface roughness are given in Tables 4.5-4.7.

From the ANOVA tables, it has been observed that pulse parameters (i.e., T_{ON} & T_{OFF}) and arc on time (A_{ON}) are the most dominating factors (i.e., the larger the F-value) on machining speed (V_c), corner error (C_E), and surface roughness (R_a). Apart from the above parameters, servo sensitivity (S_C) plays a vital role in determining the machining speed (F-value = 120.23) and wire tension (W_t) plays a significant role in corner error (F-value = 114.21). Servo voltage (S_V) is another important factor that has a moderate influence on machining speed (F-value = 15.09), surface roughness (F-value = 15.34) and corner error (F-value = 62.05). In this work, analysis has been carried out at a 95% confidence level.

Table 4.5 ANOVA for cutting speed

Source	DOF	Adj SS	Adj MS	F-value	P-value
Regression	13	28.0241	2.15570	122.23	0.000
T_{ON}	1	0.848	0.8479	61.97	0.000
T_{OFF}	1	0.436	0.4356	47.77	0.000
A_{ON}	1	0.4537	0.45368	25.72	0.007
A_{OFF}	1	0.7647	0.76467	43.36	0.013
S_V	1	0.2662	0.26620	15.09	0.018
W_t	1	0.1046	0.10459	2.27	0.087*
S_C	1	2.1204	2.12040	120.23	0.000
T_{ON}^2	1	0.4212	0.42120	30.69	0.002
T_{OFF}^2	1	0.3211	0.32110	23.07	0.005
A_{ON}^2	1	0.4489	0.44890	25.45	0.007
S_V^2	1	0.3969	0.39690	22.50	0.009
W_t^2	1	0.0481	0.04810	1.04	0.223*
S_C^2	1	0.6162	0.61623	34.94	0.004
Error	4	0.0705	0.1764		
Total	17	28.0947			
Model summary					
S	R^2	R^2(adj)	R^2(pred)	*insignificant factors	
0.132801	99.75%	98.93%	92.82%	(P-value > 0.05)	

Table 4.6 ANOVA for corner error

Source	DOF	Adj SS	Adj MS	F-value	P-value
Regression	13	5204.50	400.346	20.41	0.000
T_{ON}	1	173.79	173.786	134.76	0.000
T_{OFFF}	1	131.19	131.189	71.36	0.000
A_{ON}	1	144.77	144.771	106.24	0.000
A_{OFF}	1	1.50	1.500	1.05	0.125*
S_V	1	73.88	73.884	62.05	0.012
W_t	1	214.94	214.939	114.21	0.000
S_C	1	27.86	27.864	14.12	0.032
T_{ON}^2	1	102.69	102.694	78.17	0.000
T_{OFF}^2	1	44.44	44.444	20.27	0.008
A_{ON}^2	1	82.69	82.694	64.14	0.000
S_V^2	1	11.21	11.212	16.89	0.032
W_t^2	1	76.12	76.124	47.84	0.000
S_C^2	1	10.21	10.219	7.15	0.048
Error	4	78.44	19.611		
Total	17	5282.94			
Model summary					
S	R^2	R^2(adj)	R^2(pred)	*insignificant factors	
0.151044	98.52%	94.69%	89.93%	(P-value > 0.05)	

Table 4.7 ANOVA for surface roughness

Source	DOF	Adj SS	Adj MS	F-value	P-value
Regression	13	0.195271	0.015021	19.08	0.000
T_{ON}	1	0.072601	0.072601	76.21	0.000
T_{OFF}	1	0.065727	0.065727	51.39	0.000
A_{ON}	1	0.050061	0.050061	34.75	0.005
A_{OFF}	1	0.001128	0.001128	1.43	0.098*
S_V	1	0.021719	0.021719	15.34	0.018
W_t	1	0.007361	0.007361	4.14	0.038
S_C	1	0.030209	0.030209	11.58	0.021
T_{ON}^2	1	0.041601	0.041601	32.11	0.011
T_{OFF}^2	1	0.033448	0.033448	23.17	0.034
A_{ON}^2	1	0.026200	0.026200	3.15	0.042
S_V^2	1	0.012687	0.012687	6.98	0.011
W_t^2	1	0.003200	0.003200	0.98	0.247*
S_C^2	1	0.000694	0.000694	0.12	0.085*
Error	4				
Total	17				
Model summary					
S	R^2	R^2(adj)	R^2(pred)	*insignificant factors	
0.028054	98.41%	92.26%	86.87%	(P-value > 0.05)	

4.4.2 Effects of process parameters on response criteria

Pulse on time (T_{ON}) and arc on time (A_{ON})

From Figure 4.2 and Figure 4.3, it is evident that the machining speed, corner error, and surface roughness are all increasing significantly with an increase in pulse on time and arc on time. With the increase of pulse on time and arc on time, energy per pulse increases, i.e., discharge energy increases, and as a result, more material is removed per pulse. This discharge energy is directly decided by pulse and arc parameter settings (i.e., pulse on time and arc on time). This results in increased machining speed and also increases the gap force (force induced due to spark). The generated spark force and wire vibrations are the main causes of wire lag (wire deflection). This wire lag is the deciding factor in determining the corner error. As the pulse on and arc on time increase, wire lag due to the gap force increases, this enhances the corner error. Material removal in each discharge increases as a result of the frequent sparking. This removed molten material partially flushed away by the high-pressure dielectric flushing and remaining materials stacked onto the machined surface. As a result, lumping of molten metal takes place, which forms different types of globules and makes bigger craters on the job surface. For that reason, the corner error and surface roughness are both increasing with the increase of pulse on time and arc on time.

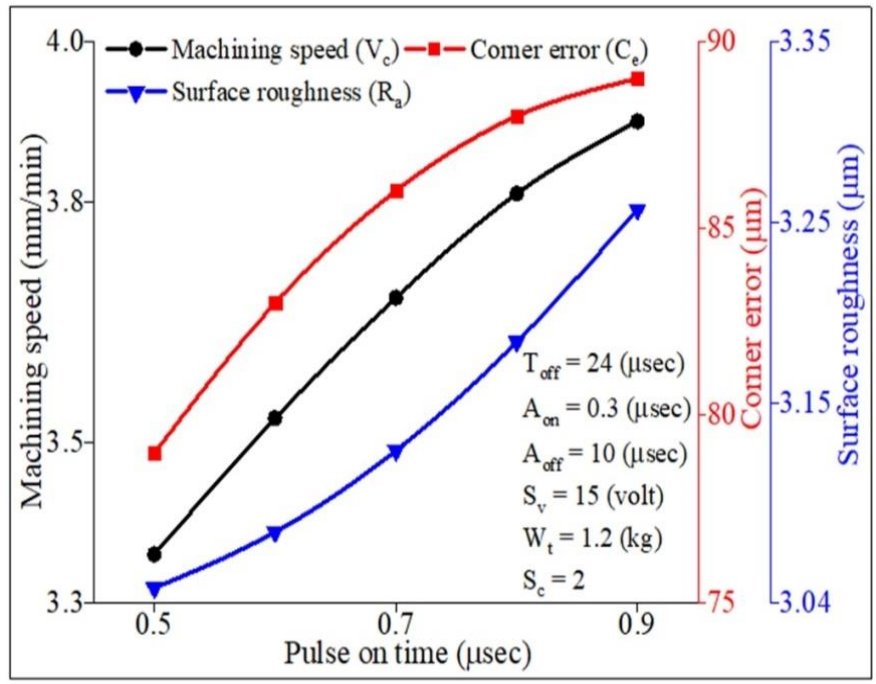

Figure 4.2 Effects of pulse on time on machining speed, corner error and surface roughness.

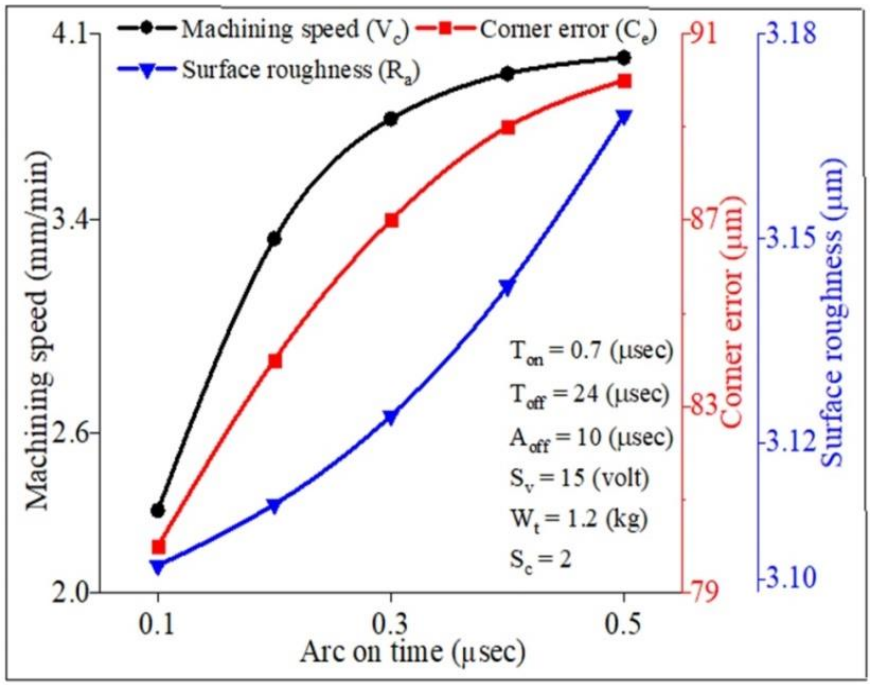

Figure 4.3 Effect of arc on time on machining speed, corner error and surface roughness.

Pulse off time (T_{OFF}) and arc off time (A_{OFF})

At the same time, from Figures 4.4-4.5, it is clearly observed that the machining speed, corner error and surface roughness all decrease with the increase in pulse off time and arc off time. An increase in pulse off and arc off time results in less aggressive pulse parameter settings and as such results in decreased machining speed and surface roughness. Due to less aggressive pulse parameter setting, the gap force as well as wire deflection are reduced, which in turn helps in reducing the corner error. Similarly, smaller craters are induced within the machining zone; as a result, surface roughness decreases. It is a good strategy to machine at a higher pulse off parameter (i.e., T_{OFF} & A_{OFF}) setting for better corner accuracy and surface finish, but it will frequently cause wire breakage and unstable machining. The maximum possible upper limits of pulse off time and arc off time for this material have been set to avoid these kinds of problems.

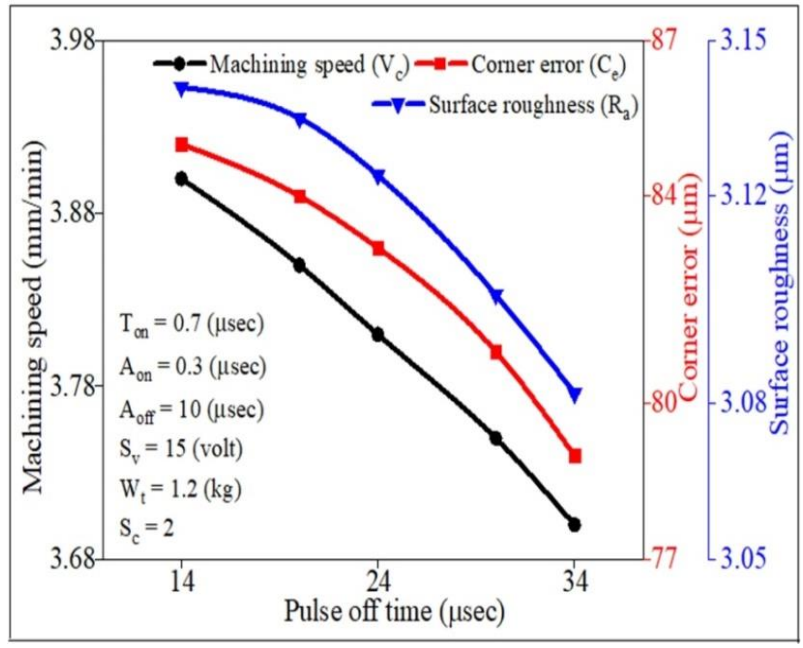

Figure 4.4 Effect of pulse off time on machining speed, corner error and surface roughness.

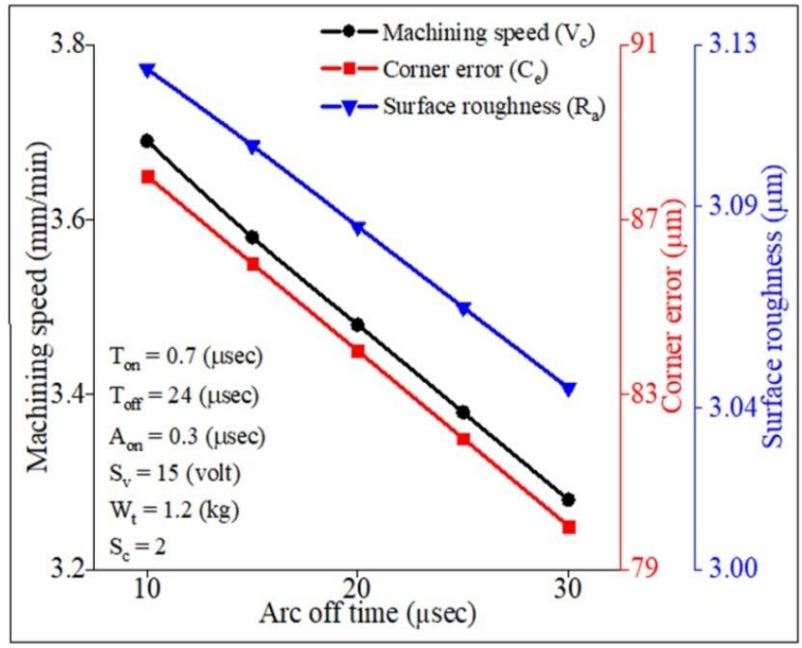

Figure 4.5 Effect of arc off time on machining speed, corner error and surface roughness.

Servo voltage (S_V)

It is observed from Figure 4.6 that with an increase in servo voltage, both machining speed and corner error decrease, but surface roughness increases. This can be explained by the fact that, with increasing servo voltage (i.e., desired gap voltage), the inter-electrode voltage also increases, which in turn increases the gap between two electrodes (wire and workpiece). Due

to this increased inter-electrode gap, the proportion of pulse energy absorbed by the dielectric also increases. This results in less efficient utilisation of pulse energy and, consequently, less machining speed. On the other hand, during sparking, the gap force generated between two electrodes is transferred to the workpiece, wire as well as dielectric. With increasing inter-electrode gaps, the amount of force transferred to the dielectric tends to be greater compared to that of wire. Due to this phenomenon, there will be less wire deflection and, consequently, less corner error due to increased servo voltage. As already mentioned, increased servo voltage results in increased gap voltage, which in turn promotes spark discharge at a higher voltage, which contains more energy. These again produce larger craters and consequently increase the surface roughness value.

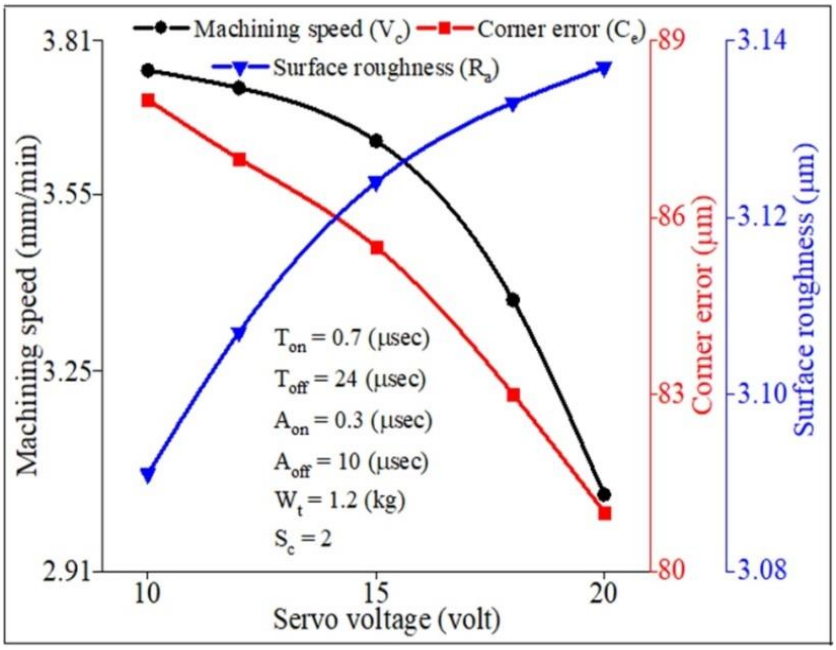

Figure 4.6 Effect of servo voltage on machining speed, corner error and surface roughness.

Wire tension (W_t)

From the Figure 4.7, it is observed that with increase in wire tension corner error reduces significantly, the wire deflection due to gap force reduces and as such, corner error reduces. However, no such significant effect has been observed on machining speed and surface roughness during machining of Al 7075 alloy. Nevertheless, it is required to give a limiting value of wire tension to avoid the wire breakage phenomenon under stable machining condition.

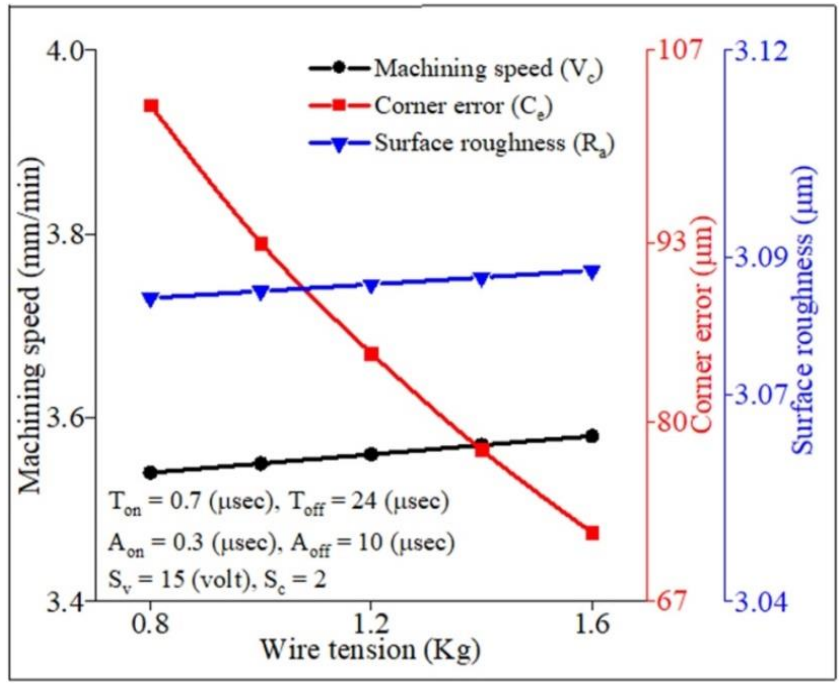

Figure 4.7 Effect of wire tension on machining speed, corner error and surface roughness.

Servo sensitivity (S_C)

It is observed from Figure 4.8 that with an increase in servo sensitivity, both machining speed and corner error increase, but surface roughness decreases. The servo sensitivity is the intensity with which the WEDM controller reacts (in respect of machining speed) in response to the change in error voltage between the desired gap voltage (servo voltage) and the actual voltage. Thus, with an increase in servo sensitivity for the same error voltage (i.e., for the same parameters setting), machining speed tends to be higher to correct the error in gap voltage, which in turn reduces the gap voltage and consequently the inter-electrode gap (IEG). Thus, the spark discharge takes place at a comparatively lower voltage, which will contain comparatively less energy and thus result in a smaller crater size. Hence, with an increase in servo sensitivity, there is a reduction in surface roughness value. Due to this decreased inter-electrode gap, the ratio of the gap force shared between the wire electrode and dielectric increases, thus the net force transferred to the wire electrode increases. Due to this increase in net gap force wire deflection as well as corner error increases with an increase in servo sensitivity.

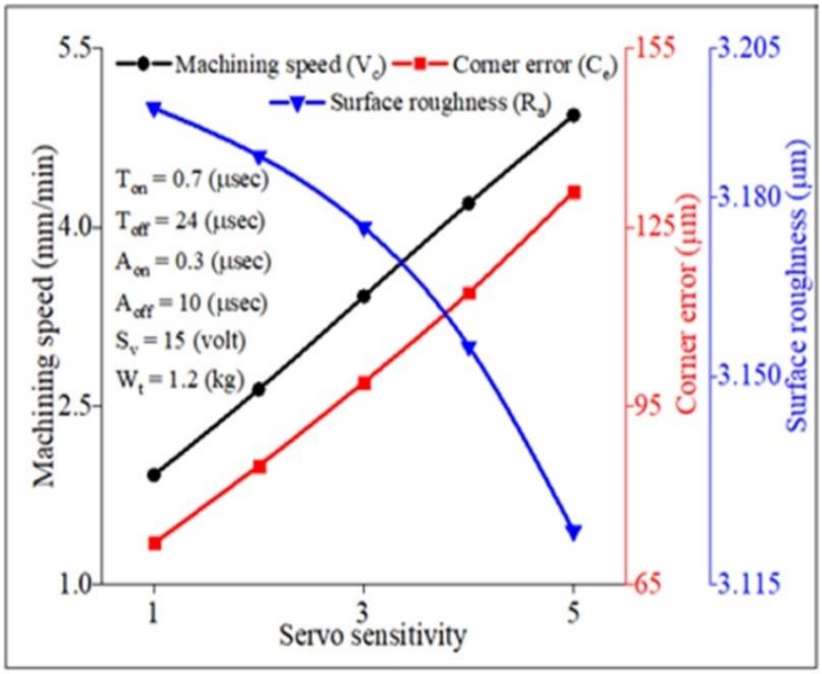

Figure 4.8 Effect of servo sensitivity on machining speed, corner error and surface roughness.

It is finally observed that all parameters except wire tension influence machining speed and corner error in a similar manner, i.e., the parameter that increases the corner error also increases the machining speed. From the present experimental investigation, it is obvious that a higher value of wire tension is always desirable for achieving better corner accuracy, but at the same time, it may be pointed out that there is an upper limit to this value to avoid wire breakage. A similar trend is observed for surface roughness values in respect of pulse on and arc on time, pulse off, and arc off time. It is evident that to get the desired outcome, an appropriate trade-off between all these response parameters is extremely essential.

4.5 Corner error and surface characteristics analysis

Figure 4.9a-b shows the corner profiles of the WEDM machined surface at two different parameter settings. From the figures, it is clear that the corner error of the machined profile largely depends on pulse parameter settings and gradually increases as the value of pulse parameters is increased. In a low pulse parameter setting, energy per pulse is on the lower side. The discharge energy produced in each spark becomes less and the result is that the main influencing factors, such as gap force, wire vibration, etc., also become low. As the pulse parameters are increased, discharge energy per pulse also increases, which promotes the wire lag value, as corner error significantly increases.

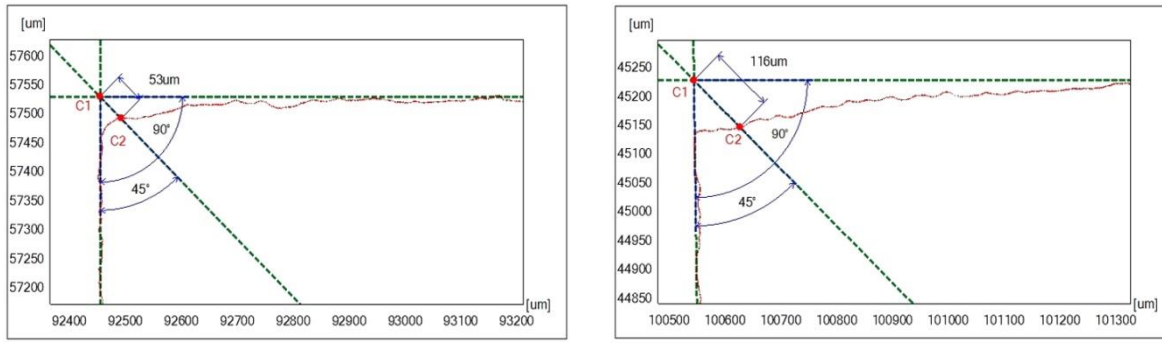

(a) (b)

Figure 4.9 Corner profile (a) T_{ON} = 0.5 µs & A_{ON} = 0.2 µs (b) T_{ON} = 0.9 µs & A_{ON} = 0.4.

Figure 4.10a-c exhibits the 3D topography of the Al 7075 machined surface. A high-resolution CCI microscope has been used to capture the 3D image of the surface. Full of scratches, wide and deep craters, high concentrations of molten metal (nuggets) and straits have been clearly visualised on the machined surface. The concentration of molten metal, the diameter and the depth of the craters depend on the energy per pulse, i.e., on the WEDM pulse parameter setting. It is clearly observed that as the pulse parameters increase, the dimensions of surface irregularities become larger (shown in Figure 4.10a-c). Corner error and surface roughness can both be controlled by adjusting the pulse parameter setting (i.e., either decreasing pulse on and arc on time or increasing pulse off and arc off time).

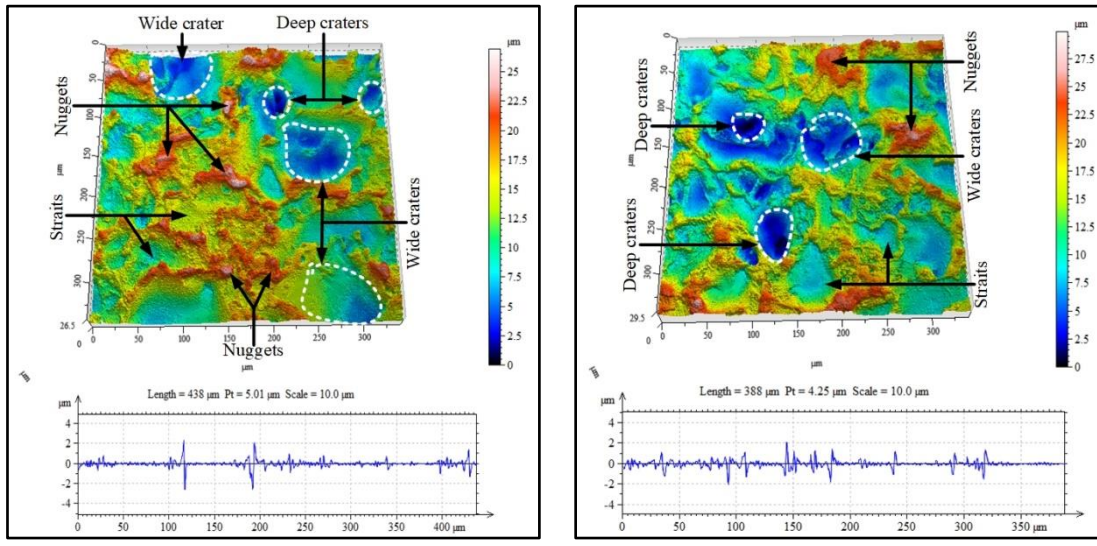

(a) (b)

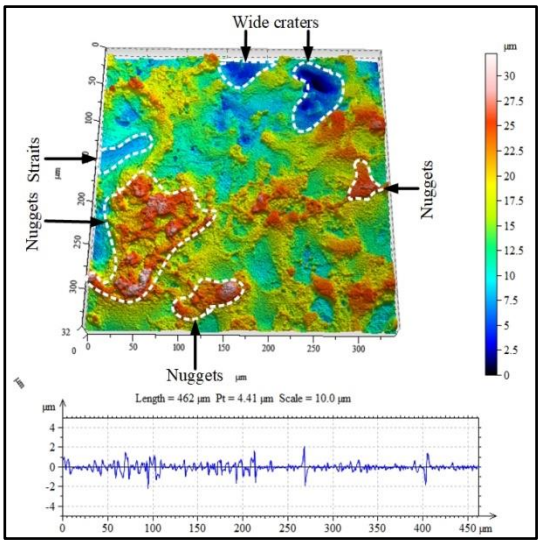

(c)

Figure 4.10 High resolution CCI image of the machined surface (a) T_{ON} = 0.5 µs & A_{ON} = 0.2 µs (b) T_{ON} = 0.7 µs & A_{ON} = 0.3 µs (c) T_{ON} = 0.9 µs & A_{ON} = 0.4 µs

4.6 Concluding remarks

A single-pass rough cutting operation in WEDM of Al 7075 has been carried out in this study. The influence of process parameters, e.g., pulse on time, arc on time, pulse off time, arc off time, servo voltage, wire tension and servo sensitivity on machining speed, corner error, and surface roughness has been investigated. The conclusions are summarised as follows:

- In the operating range of input factors, the main dominating factors on machining speed, corner error, and surface roughness are pulse on time, pulse off time, and arc on time. Wire tension plays a crucial role in corner errors. It is observed that corner error significantly decreases with the increase of wire tension. In the case of servo sensitivity, machining speed and corner error are increased and surface roughness decreases when sensitivity is increased.

- From the experimental investigation it is observed that in order to get the best corner accuracy, the parameters setting should be T_{ON} = 0.5 µsec, T_{OFF} = 34 µsec, A_{ON} = 0.1 µsec, A_{OFF} = 30 µsec, S_V = 20 volt, W_t = 1.6 kg, S_C = 1. To achieve the maximum possible machining speed, parameters value should be T_{ON} = 0.9 µsec, T_{OFF} = 14 µsec, A_{ON} = 0.5 µsec, A_{OFF} = 10 µsec, S_V = 10 volt, W_t = 1.6 kg, S_C = 5 and for

minimum surface roughness value, parameter setting should be T_{ON} = 0.5 µsec, T_{OFF} = 34 µsec, A_{ON} = 0.1 µsec, A_{OFF} = 30 µsec, S_V = 10 volt, W_t = 0.8 kg, S_C = 5.

- It is impossible to achieve simultaneously the best corner accuracy and surface roughness along with the maximum machining speed. Thus, a systematic trade-off between the response parameters is extremely essential.
- Majority of the input parameters influences the response parameters in a similar manner i.e. the change in input parameters that tends to improve the machining speed also deteriorates the corner accuracy and surface roughness.

Chapter-5

Influence of Dielectric Conductivity on Corner Accuracy and Surface Roughness in WEDM

5.1 Objective of the work

The electrical conductivity of the dielectric plays a vital role while machining the materials in WEDM. Comprehensive research has been carried out to investigate the effect of electrical conductivity of the dielectric along with other process parameters in wire electrical discharge machining (WEDM) of Al 7075 alloy. The effects of open circuit voltage (V_{OC}), pulse on time (T_{ON}), pulse frequency (f_P) and servo sensitivity (S_C) on corner accuracy, including different other response criteria, have been studied in this work.

From the review of past literature, it is observed that most of the research focused on machining efficiency and surface evaluation of the WEDM process (Tosun et al. 2004, Aspinwall et al. 2008, Mouralova et al. 2018). Some researchers have also explored dimensional and corner accuracy features in WEDM (Puri et al. 2003, Sarkar et al. 2011, Maher et al. 2015). The effects of dielectric conductivity on corner accuracy in WEDM of Al 7075 alloy have not been reported in any research journal till now. The dielectric conductivity that is suitable for wire machining of steel and other common alloys may not be suitable for the machining of this highly conductive new generation metal. Generally, 20 µS/cm dielectric conductivity is used during WEDM machining, and this amount of conductivity is not optimal for all the response parameters. The influence of dielectric conductivity during machining of Al 7075 has never been considered in any research study. It is therefore extremely essential to explore the influence of dielectric conductivity apart from other conventional WEDM process parameters. So, in the present research work, the effects of dielectric conductivity on wire electrical discharge machining of Al 7075 have been explored.

The experimental result shows that dielectric conductivity plays a significant role with respect to corner accuracy and surface finish in a single pass cutting operation. Surface topography and elemental analysis of the machined surface have been carried out for a deeper understanding of the influence of dielectric conductivity in WEDM. Experimental investigation and subsequent analysis of results showed that for a broad range of response variables (e.g., corner accuracy and surface finish), a 12 µS/cm conductivity setting gives the

optimum result. However, to attain corner error (C_E) and surface roughness (R_a) below a certain critical limit (i.e., C_E = 0.101 mm & R_a = 2.671 µm), a 4 µS/cm conductivity setting is found to be the best setting for this alloy.

5.2 Experimentation

Al 7075 alloy conforming to ASTM has been used in this study. X-ray diffraction pattern (XRD) of the alloy has been carried out at room temperature (Shown in Figure 5.1) and the different phases existed in the alloy are exhibited in the Figure 5.1.

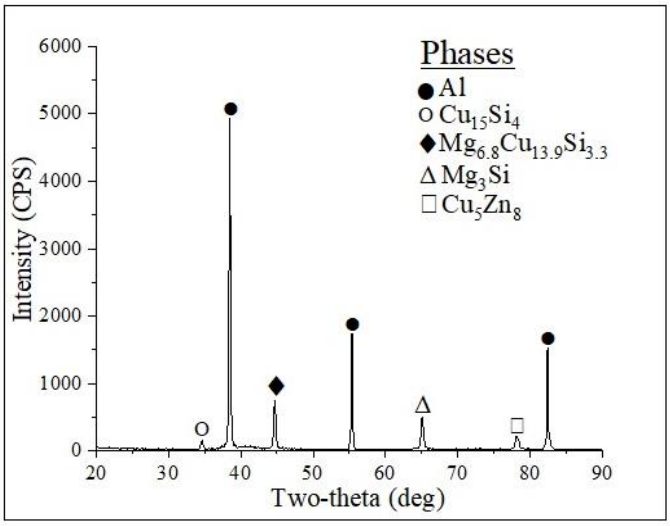

Figure 5.1 XRD pattern of the Al 7075 alloy

5.2.1 Setup and plan of the experimentation

Experimentations have been carried out on 5-axis EX 40 (Exetec S & T Pvt. Ltd., Taiwan) wire cut machine. The experimental setup was presented in Figure 5.2a. To exploit the process capabilities to its full extent, the maximum possible range of input parameters are kept different for three different levels of conductivities. For this reason and to avoid possible interactions among the process parameters, three different sets of experiments were carried out for three different levels of conductivities. Based on fundamental understanding and some trial run, open circuit voltage (V_{OC}), pulse on time (T_{ON}), pulse frequency (f_P) and servo sensitivity (S_C) have been considered as four independent input process parameters. The conductivity of the dielectric liquid (Deionised water) have been increased by adding sodium chloride (NaCl) salt and ion exchange resin have been used to decrease the conductivity level as per requirement. Initially, fresh deionised water is poured in the dielectric tank. The conductivity level has been manually set to the dielectric conductivity meter as per the required value and then gradually NaCl salt have been added into the deionised water until it

reaches the required level of conductivity. Machining has been carried out when the conductivity of the dielectric reached the prescribed limit. If conductivity exceeds the required limit (i.e. more NaCl added into the deionised water), the resin pump will automatically start and ion exchange resin reduces the conductivity or some amount fresh deionised water is added to reduce the conductivity for maintaining an appropriate amount of conductivity level of the deionised water. Thus, the conductivity is changed to different required levels.

Moreover, from the preliminary experiment, it is observed that the above four parameters are highly significant and independent of each other during machining of Al 7075 alloy. To achieve better additivity instead of pulse off time (T_{OFF}), pulse frequency (f_P) has been selected as an input parameter. Pulse off time (T_{OFF}) was adjusted to achieve the desired level of pulse frequency (f_P) in each case by adopting a sliding parameter setting in accordance with the following equation:

$$\text{Pulse frequency } (f_P) = \left\{\frac{1}{\text{Pulse on time} + \text{Pulse off time}}\right\} \text{MHz} \qquad (5.1)$$

The controllable parameter settings and their levels are shown in Table 5.1. The maximum possible ranges of input parameters were selected on the basis of the initial trial run. During the trial run, the emphasis has been given to achieve a stable machining condition without any wire breakage. The wire electrode is zinc coated brass wire and the diameter is 0.250 mm.

The impact of control factors on cutting speed (C_S), corner error (C_E), overcut (O_C), surface roughness (R_a), and surface topography of Al 7075 alloy have been studied. L_9 orthogonal experimental design has been selected for three separate levels of conductivities. The results are exhibited in Table 2. Cutting speed is noted down from the monitor of the machine. The corner error value of the machined profile has been measured using a Mitutoyo CV 3200 high precision contour measuring instrument. To get precise corner error measurement, bisector (45°) of the interior angle (90°) has been drawn as shown in Figure 5.2b. The distance between the theoretical corner point and actual point on the profile (along the bisector) have been considered as a measurement of the corner error. Overcut is measured by Mitutoyo (ABSOLUTE) high accuracy digimatic micrometre with 0.1 µm resolution. Surface roughness measurement have been carried out by Mitutoyo SJ 410 roughness tester and a scanning electron microscope (SEM) is employed to observe the surface topography of the machined surface. Non-contact type Taylor-Hobson CCI also has been used to observe the

3D stereogram of the machined surface. Figure 5.2c shows the workpiece material and slot produced after machining.

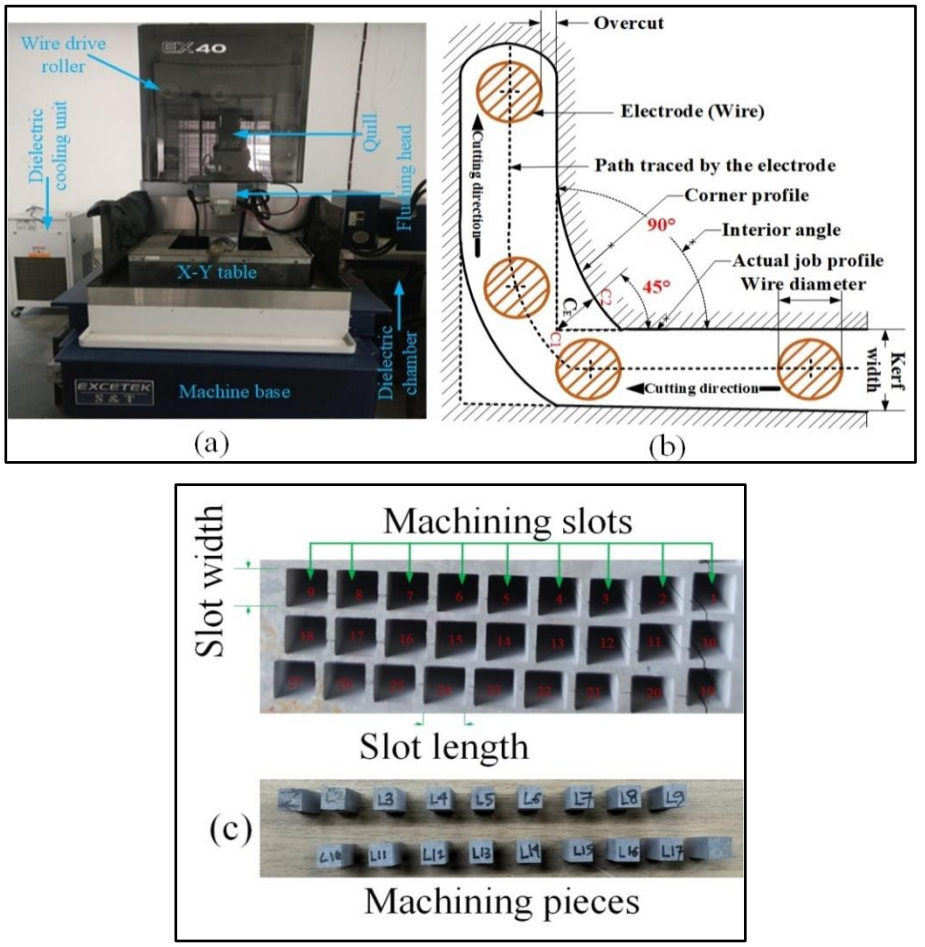

Figure 5.2 (a) Experimental setup and (b) Profile produced by WEDM (c) Workpiece and slot produced after WEDM

Table 5.1 Machining parameters and levels

Factors	Levels and values								
Conductivity: κ (µS/cm)	4			12			22		
Levels	1	2	3	1	2	3	1	2	3
Open circuit voltage: V_{OC} (volt)	74	97	120	64	97	129	64	92	120
Pulse on time: T_{ON} (µsec)	0.05	0.40	0.75	0.05	0.50	0.95	0.05	0.40	0.75
Pulse frequency: f_P (MHz)	0.036	0.028	0.024	0.034	0.029	0.024	0.033	0.029	0.025
Servo sensitivity: S_C	10	13	16	12	15	18	2	6	10

5.2.2 Design of experiments via Taguchi method

The quality of the product machined by WEDM is affected by the machining parameters. Genichi Taguchi had developed a three-stage design methodology, to understand the importance of design of experiment (Phadke: 1989). The full factorial design for four factors with three levels is L_{18} (3^4) orthogonal array (OA). However, in this case L_9 OA fractional factorial design has been used for each set of experiments. The design matrix (L_9 orthogonal array) as shown in Table 5.2 has been employed to verify the influence of WEDM process parameters on cutting speed, corner error, overcut, and surface roughness. The Signal to Noise (S/N) ratio is used in the Taguchi method to determine the performance characteristics of the variables. In this work, two different categories of performance variability are used, namely 'higher the better' and 'smaller the better' (Shown in Eq. 5.2-5.3). Higher cutting speed is always looked-for superior productivity in any machining process. So, cutting speed has been classified as larger the better kind of problem. For any production process corner error, overcut and surface roughness value should be on the lower side. Therefore, corner error, surface roughness, and overcut have been chosen as smaller the better kind of response variables.

Higher the better: S/N ratio $-10log\left\{\frac{1}{n}\sum_{i=1}^{n}\left(\frac{1}{y_i^2}\right)\right\}$ (5.2)

Smaller the better: S/N ratio $-10log\left\{\frac{1}{n}\sum_{i=1}^{n}(y_i^2)\right\}$ (5.3)

where y_i is the experiential response and n is the number of runs.

Table 5.2 Experimental design matrix

Input process parameters					Response parameters				S/N ratio (η)			
Conductivity (κ: μS/cm)	Open circuit voltage (V_{OC}: volt)	Pulse on time (T_{ON}: μsec)	Pulse frequency (f_P: MHz)	Servo sensitivity (S_C)	Cutting speed (C_S: mm/min)	Corner error (C_E: mm)	Surface roughness (R_a: μm)	Overcut (O_c: μm)	η (Cutting speed)	η (Corner error)	η (Surface roughness)	η (Overcut)
	74	0.05	0.036	10	2.55	0.110	2.568	65	8.13	19.14	-8.19	-36.26
	74	0.4	0.028	13	3.32	0.143	2.892	64	10.42	16.92	-9.22	-36.12
	74	0.75	0.024	16	4.57	0.148	3.051	66	13.20	16.62	-9.69	-36.39
	97	0.05	0.028	16	3.12	0.122	2.789	58	9.88	18.27	-8.91	-35.27
4	97	0.4	0.024	10	2.64	0.125	2.643	61	8.43	18.08	-8.44	-35.71
	97	0.75	0.036	13	5.62	0.168	3.173	78	14.99	15.48	-10.03	-37.84
	120	0.05	0.024	13	2.42	0.102	2.689	55	7.68	19.85	-8.59	-34.81
	120	0.4	0.036	16	3.85	0.168	2.988	67	11.71	15.50	-9.51	-36.52
	120	0.75	0.028	10	3.95	0.153	2.812	76	11.93	16.31	-8.98	-37.62
	64	0.05	0.034	12	3.89	0.090	3.085	76	11.80	17.85	-9.79	-37.62
	64	0.5	0.029	15	5.3	0.155	3.593	73	14.49	16.19	-11.11	-37.27
	64	0.95	0.024	18	7.48	0.182	3.998	75	17.48	14.81	-12.04	-37.50
	97	0.05	0.029	18	4.58	0.145	3.381	68	13.22	16.78	-10.58	-36.65
12	97	0.5	0.024	12	4.18	0.136	3.108	71	12.42	17.30	-9.85	-37.03
	97	0.95	0.034	15	9.01	0.194	4.112	86	19.09	14.27	-12.28	-38.69
	129	0.05	0.024	15	3.73	0.134	3.179	65	11.43	17.46	-10.05	-36.26
	129	0.5	0.034	18	6.45	0.183	3.938	77	16.19	14.75	-11.91	-37.73
	129	0.95	0.029	12	7.01	0.171	3.543	84	16.91	15.34	-10.99	-38.49
	64	0.05	0.033	2	1.64	0.128	3.089	78	4.30	20.92	-9.80	-37.84
	64	0.4	0.029	6	5.12	0.173	3.998	77	14.19	15.26	-12.04	-37.73
	64	0.75	0.025	10	9.47	0.171	4.984	79	19.53	15.34	-13.95	-37.95
	92	0.05	0.029	10	6.35	0.196	4.049	70	16.06	14.16	-12.15	-36.90
22	92	0.4	0.025	2	1.98	0.110	3.608	75	5.93	19.19	-11.15	-37.50
	92	0.75	0.033	6	7.22	0.178	5.454	91	17.17	14.99	-14.73	-39.18
	120	0.05	0.025	6	4.25	0.147	3.486	66	12.57	16.68	-10.85	-36.39
	120	0.4	0.033	10	8.5	0.185	4.828	81	18.59	14.66	-13.68	-38.17
	120	0.75	0.029	2	3.48	0.107	4.718	86	10.83	19.41	-13.48	-38.69

5.2.3 Parametric analysis

Figure 5.3-5.6 shows the effect of individual input factor on cutting speed (C_S), corner error (C_E), surface roughness (R_a), and overcut (O_c) at different levels of dielectric conductivities. It is found that each three response parameter increases with the increase of pulse on time (T_{ON}), pulse frequency (f_P), and servo sensitivity (S_C) for all the three level of different dielectric conductivities. From the graph, it is observed that the open circuit voltage (V_{OC}) is the least significant process parameter. The energy contained and frequency in each pulse during machining is the deciding factor on material removal rate (MRR) or cutting speed (C_S). Hence, with an increase in pulse on time and decreasing frequency, there has been an increasing trend observed in cutting speed. At the same time, material removal i.e. crater volume per unit spark also increases with an increase in the energy contained in each spark. Therefore, the surface roughness also increases with an increase in pulse on time. With an increase in pulse frequency, the energy is distributed per unit time into the more number of sparks. The supplied energy per unit time remains constant for a constant voltage and current. Therefore, there is a reduction in the energy supplied per spark. As a result, it creates a shallow crater resulted in a better surface finish. From the graph, it is observed that there is also an increase in corner error with an increase in pulse on time and pulse frequency. With an increase in pulse parameters e.g. an increase in pulse on time and pulse frequency, there will be an increase in gap force and consequently the wire lag value. This increased wire lag value is again responsible for an increase in the corner error. It is further expected that with an increase in servo sensitivity there will be enhanced response from the controller which in turn will reduce the gap distance. Due to this reduced gap, the loss of spark energy in dielectric reduces. Thus, there will be more efficient utilization of spark energy with an increase in servo sensitivity, which is equivalent to an increase in pulse parameter. For this reason, with an increase in servo sensitivity, there has been an increasing trend in cutting speed, surface roughness, and corner error values.

It is observed from Figure 5.5 that except open circuit voltage other parameters are having a significant influence on overcut. It is clearly observed with an aggressive parameter setting i.e. with the increase in pulse on time and pulse frequency there is an increase in overcut. At high pulse parameters setting, the rate of discharge energy increases and enhances the material removal rate (MRR) as well as the kerf width. Kerf width is the summation of wire diameter and overcut. Hereafter, the overcut increases with the increase in MRR or vice

versa. Again, with an increase in servo sensitivity, there is a dropping in gap voltage as well as a reduced spark gap i.e. overcut. Hence, it is observed that there is a reduction in overcut with an increase in servo sensitivity.

As already anticipated, some significant interactions are observed for some input parameters. From Figure 5.3 it is clearly observed that due to the change in conductivity level, a significant amount of interaction is noted in cutting speed in respect of the servo sensitivity input parameter. Similarly, due to a change in conductivity level, moderate to high interactions are also observed (Figure 5.4 and 5.6) for other response parameters as well.

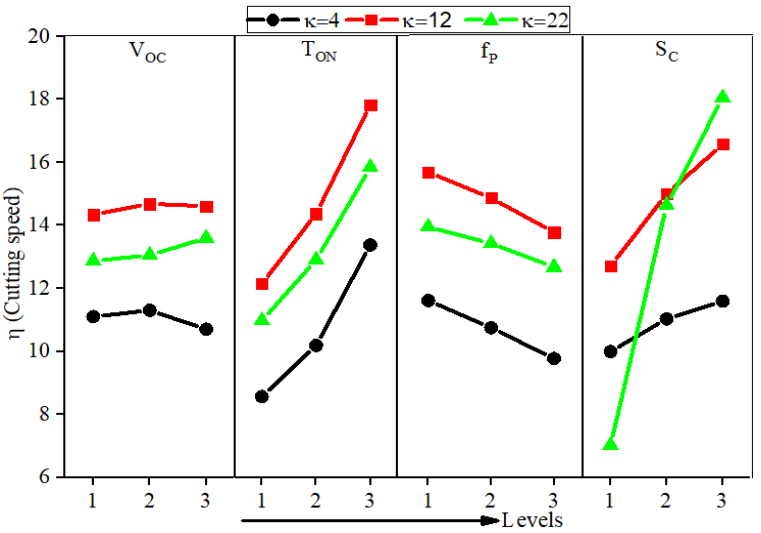

Figure 5.3 Effect of machining parameters on cutting speed at different levels of conductivities

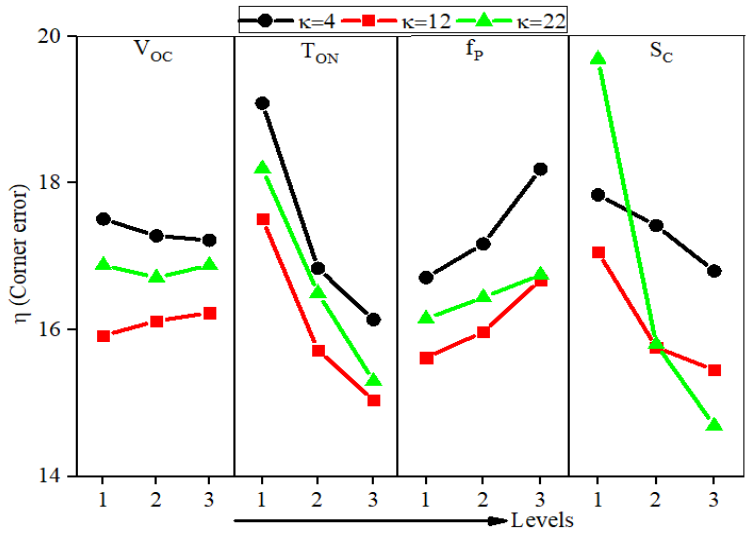

Figure 5.4 Effect of machining parameters on corner error at different levels of conductivities

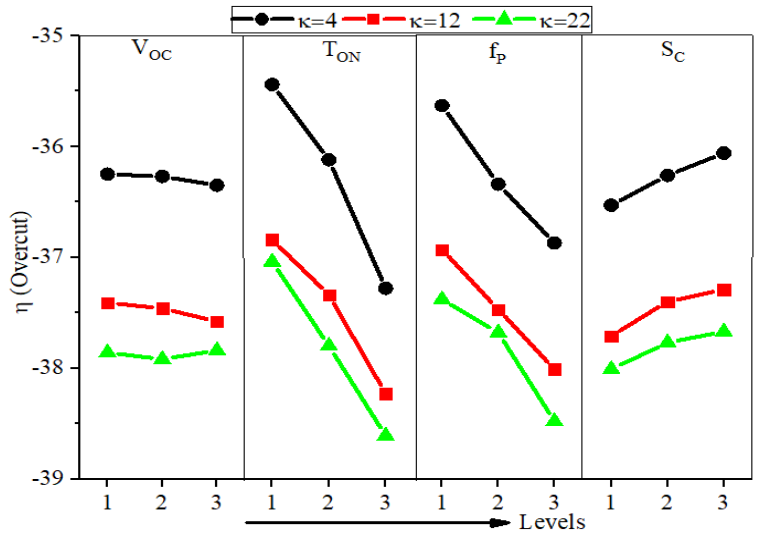

Figure 5.5 Effect of machining parameters on overcut at different levels of conductivities

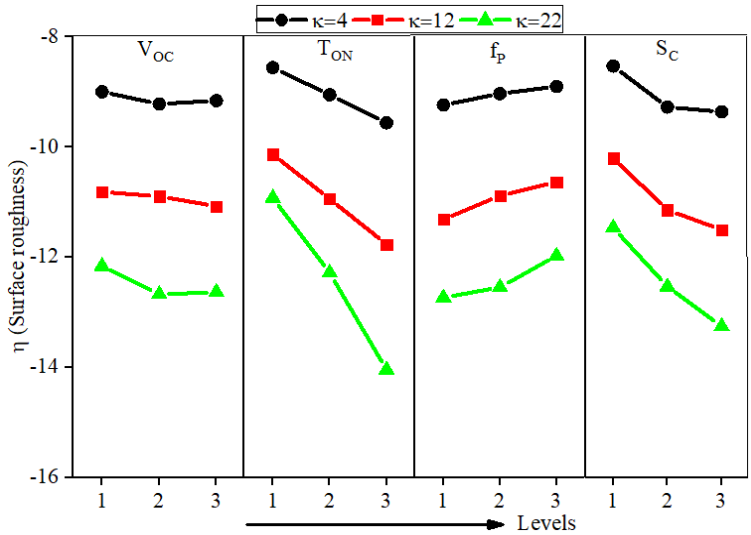

Figure 5.6 Effect of machining parameters on surface roughness at different levels of conductivities

5.3 Mathematical modelling of WEDM process by nonlinear regression method

The experimental value from Table 5.2 has been used to mathematical modelled (regression) the WEDM process. The mathematical model (regression), which has been found out from the experimental results are shown in Table 5.3. Output responses are predicted with this model by choosing any random level of input parameters. Verification experimentation has been performed to verify the proposed mathematical model. The verified results are enlisted in Table 5.4. It has been observed from Table 5.5 that the predicted value from the

mathematical model is very close to the experimental results. The percentage of prediction error has been given in Table 5.5 and calculated as follows:

$$\% \text{ prediction error} = \left\{\left|\frac{\text{Experimental value} - \text{Predicted value}}{\text{Experimental value}}\right|\right\} \times 100 \qquad (5.4)$$

Table 5.3 Regression equations in different conductivity settings

Conductivity (κ)	Regression equations
4	$C_S = -12.66 + 0.1268\ V_{OC} + 0.04014\ T_{ON} + 43.47\ f_P + 1.018\ S_C - 0.000662\ V_{OC}^2 + 3.551\ T_{ON}^2 + 381.9\ f_P^2 - 0.03778\ S_C^2$
	$C_E = -0.2009 + 0.000589 V_{OC} + 0.1373\ T_{ON} + 14.20\ f_P + 0.002159\ S_C - 0.000002\ V_{OC}^2 - 0.09156\ T_{ON}^2 - 203.1\ f_P^2 + 0.000015\ S_C^2$
	$R_a = -0.7214 + 0.01268\ V_{OC} + 0.4322\ T_{ON} + 6.278\ f_P + 0.3611\ S_C - 0.000066\ V_{OC}^2 + 0.04898\ T_{ON}^2 + 55.56\ f_P^2 - 0.01217\ S_C^2$
	$O_C = -24.54 + 0.08286\ V_{OC} + 4.762\ T_{ON} + 4944\ f_P - 0.1296\ S_C - 0.000315\ V_{OC}^2 + 19.05\ T_{ON}^2 - 69444\ f_P^2 - 0.01852\ S_C^2$
12	$C_S = -10.03 + 0.05360\ V_{OC} + 1.025\ T_{ON} - 239.2\ f_P + 1.774\ S_C - 0.000264\ V_{OC}^2 + 3.160\ T_{ON}^2 + 6400\ f_P^2 - 0.04611\ S_C^2$
	$C_E = -0.2751 - 0.000213\ V_{OC} + 0.09655\ T_{ON} + 4.722\ f_P + 0.03896\ S_C + 0.000001\ V_{OC}^2 - 0.04733\ T_{ON}^2 - 47.33\ f_P^2 - 0.001137\ S_C^2$
	$R_a = 0.4506 - 0.004156\ V_{OC} + 0.7272\ T_{ON} - 120.9\ f_P + 0.5151\ S_C + 0.000021\ V_{OC}^2 + 0.01646\ T_{ON}^2 + 2573\ f_P^2 - 0.01324\ S_C^2$
	$O_C = 62.79 + 0.009319\ V_{OC} + 3.457\ T_{ON} + 933.3\ f_P - 2.278\ S_C + 0.000005\ V_{OC}^2 + 9.877\ T_{ON}^2 - 0.000000\ f_P^2 + 0.05556\ S_C^2$
22	$C_S = 26.81 - 0.05320\ V_{OC} + 2.459\ T_{ON} - 1840\ f_P + 0.7415\ S_C + 0.000289\ O_V^2 + 1.646\ T_{ON}^2 + 32917\ f_P^2 - 0.01833\ S_C^2$
	$C_E = -0.7715 + 0.002495\ V_{OC} + 0.01192\ T_{ON} + 51.70\ f_P + 0.02368\ S_C - 0.000014\ V_{OC}^2 + 0.008435\ T_{ON}^2 - 907.3\ f_P^2 - 0.001132\ S_C^2$
	$R_a = -1.968 + 0.04949\ V_{OC} + 1.165\ T_{ON} + 102.8\ f_P + 0.1769\ S_C - 0.000238\ V_{OC}^2 + 1.241\ T_{ON}^2 - 843.8\ f_P^2 - 0.006250\ S_C^2$
	$O_C = 63.51 + 0.1896\ V_{OC} + 15.65\ T_{ON} - 1167\ f_P - 0.5000\ S_C - 0.001063\ V_{OC}^2 + 5.442\ T_{ON}^2 + 41667\ f_P^2 + 0.01042\ S_C^2$

Table 5.4 Verification experiments for the proposed model

	Process parameters				Responses		
κ	V_{OC}	T_{ON}	f_P	S_C	C_S	C_E	R_a
	74	0.05	0.024	10	1.82	0.089	2.394
4	97	0.4	0.028	13	3.47	0.146	3.008
	120	0.75	0.036	10	4.49	0.163	2.891
	64	0.05	0.029	18	4.21	0.148	3.406
12	97	0.5	0.029	15	5.92	0.177	3.461
	129	0.95	0.034	18	8.89	0.197	4.196
	64	0.05	0.025	2	1.12	0.098	2.538
22	92	0.4	0.029	6	5.22	0.181	4.464
	120	0.75	0.033	6	7.45	0.152	5.428

Table 5.5 Prediction results and percentage (%) error

κ	Experimental value			Predicted value			% error		
	C_S	C_E	R_a	C_S	C_E	R_a	C_S	C_E	R_a
	1.82	0.089	2.394	1.75	0.087	2.454	3.61	1.94	2.50
4	3.47	0.146	3.008	3.63	0.149	2.925	4.75	2.23	2.75
	4.49	0.163	2.891	4.48	0.166	2.894	0.02	1.78	0.10
	4.21	0.148	3.406	4.22	0.150	3.407	0.07	1.10	0.03
12	5.92	0.177	3.461	5.67	0.176	3.568	4.25	0.68	3.09
	8.89	0.197	4.196	8.97	0.202	4.275	0.95	2.44	1.89
	1.12	0.098	2.538	1.09	0.100	2.657	2.61	1.76	4.70
22	5.22	0.181	4.464	4.9	0.183	4.343	6.19	1.24	2.71
	7.45	0.152	5.428	7.44	0.159	5.425	0.04	4.64	0.04

5.4 Influence of dielectric conductivity on performance measured

The role of conductivity while machining Al 7075 alloy is separately analysed using the developed non-linear regression model (Given in Table 5.3). Figure 5.7-5.9 represents the effects of dielectric conductivity on response factors (i.e. C_s, C_E & R_a). Plotted results shown in Figure 5.7-5.9, are obtained from the developed mathematical models. Other variable factors i.e. open circuit voltage (97 volt), pulse on time (0.5 µs), pulse frequency (0.029 MHz) and servo sensitivity (13) are kept constant during analysis. Cutting speed is an important factor in WEDM because of its significant consequence on productivity, surface quality, and geometrical features. Figure 5.7 shows the influence of dielectric conductivity on cutting speed. In case of cutting speed, it gradually increases first and then decreases as the conductivity increases. This can be explained by the fact that with increasing conductivity the dielectric is getting ionized readily (i.e. spark delay time is likely to be less) and thereby energy contained per spark also increases and this promotes higher cutting speed. But at the same time, the spark gap increases with increasing conductivity. Due to this increased gap, the fraction of spark energy utilized for the melting of the workpiece material is also getting reduced and thereby resulting in reduced cutting speed. It is clearly observed in Figure 5.8, that corner error increases with an increase in conductivity. As already mentioned that energy per spark increases with an increase in conductivity, results in increases in the gap force. It is established that the reason for this gap force is owing to the explosive force of the gas bubbles. Though there are other contributing factors i.e. hydraulic forces, electromagnetic force, electrostatic force, etc. This enhanced gap force also increases the wire deflection which in turn again increases the corner error. From Figure 5.9, it is also observed that the surface roughness is almost directly proportional to the conductivity. As already pointed out that with increasing conductivity, the energy contained in each pulse increases, and eventually this spark will remove more material and create bigger craters on the workpiece surface. This in turn will produce higher surface roughness with increasing conductivity.

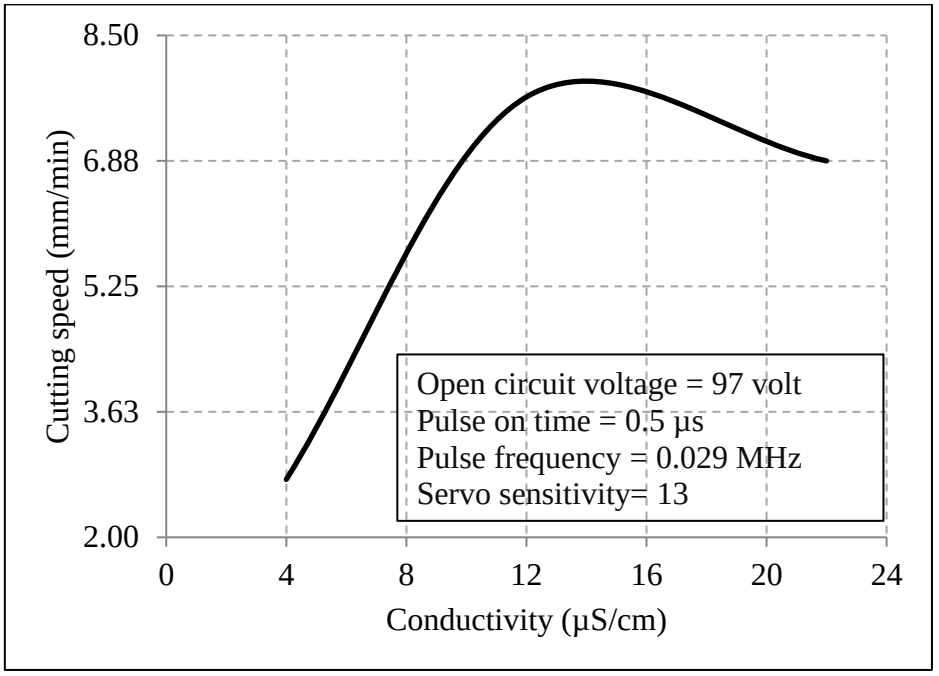

Figure 5.7 Graphical representation of conductivity vs. cutting speed

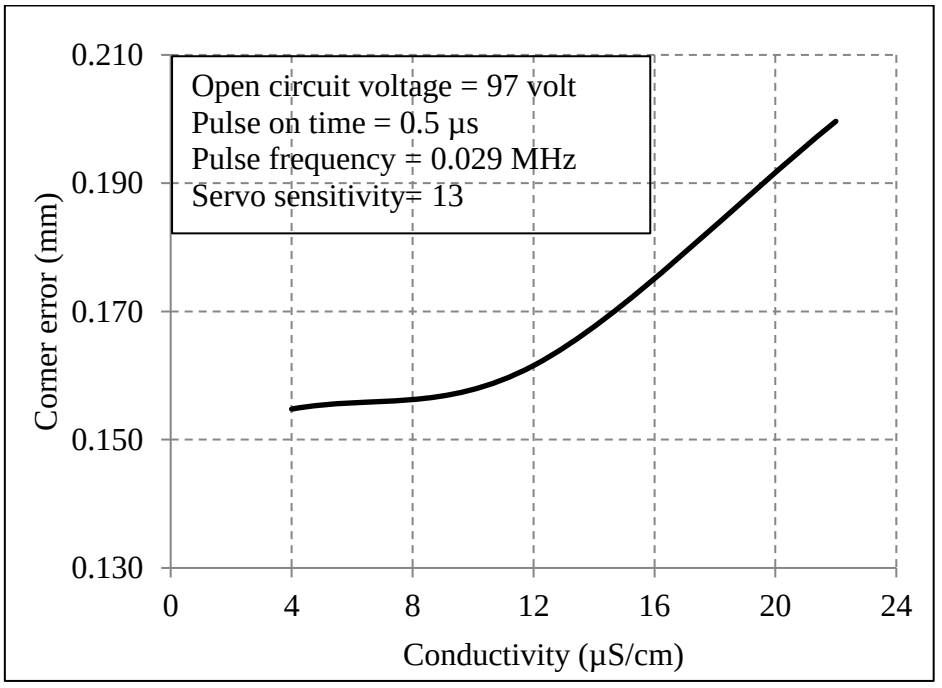

Figure 5.8 Graphical representation of conductivity vs. corner error

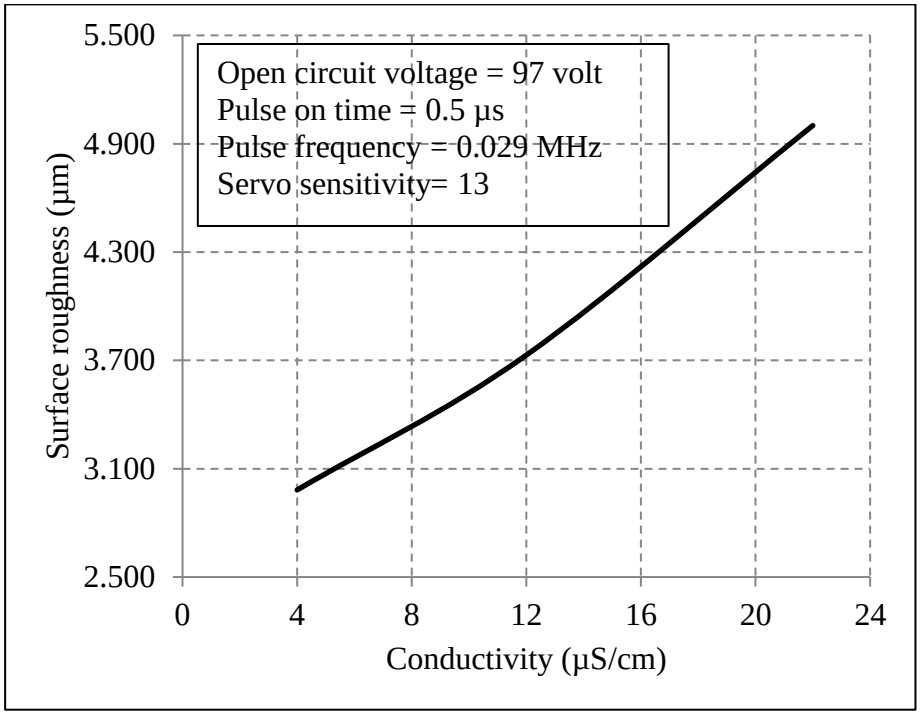

Figure 5.9 Graphical representation of conductivity vs. surface roughness

5.5 Parametric optimization using constrained Pareto algorithm

It is evident from Figure 5.3-5.4 and Figure 5.6 that parameter setting that will promote higher cutting speed will also increase the undesirable response parameters like surface roughness and corner error. Thus, both the corner error as well as surface finish are conflicting in nature with the cutting speed and as such there cannot be any single suitable optimal solution which will promote the best result i.e. simultaneously the maximum cutting speed with the minimum values of surface roughness and corner error. So a multi-objective optimization technique is adopted to prepare a Pareto-optimal chart so that one shop floor operator can set the process parameter without any trial and error approach to achieving the optimum machining condition for Al 7075 alloy.

The Pareto-optimality approach can find multiple optimum solutions within the specified solution space. Here the objective is to maximize the cutting speed and minimize surface roughness and corner error. Here two pairs of conflicting nature of output parameters were chosen for optimization e.g. $1/C_E$ vs. C_S and $1/R_a$ vs. C_S. A MATLAB program has been implemented to search out the optimum point from the set of all experimental responses. Using this Pareto optimization, two sets of solutions were generated for the two pairs of output parameters as shown in Figure 5.10 and Figure 5.11 at different levels of conductivity.

The variation of $1/C_E$ and $1/R_a$ vs. C_S has been considered along the vertical (Y) axis and horizontal (X) axis respectively. The Pareto optimal results have been found out with respect to individual conductivity settings. Here, the optimum Pareto result implies that it is better than any other response at least with respect to at least one process criterion i.e. $1/C_E$, $1/R_a$ or C_S. If one parameter combination results in higher in both the process criterion or if it is higher with respect to at least one process criterion and is equal with respect to other process criteria to a second, then the second parametric combination should never be selected in preference to the first (Sarkar et al. 2005). Differently, a point may not be graphically optimum if nearby some other point, which would be either above or right to the respective point. These all non-dominated points within the solution space for corner error and surface roughness against cutting speed are shown in Figure 5.10 and Figure 5.11.

It is observed from Figure 5.10 that better corner accuracy can be achieved at lower cutting speed using 4 µS/cm conductivity levels. From the Pareto optimal data, it is evident that if the required corner error is below 0.101 mm (i.e. $1/C_E = 9.91$) then 4 µS/cm conductivity setting is the only solution but this is not the usual case in the rough cutting operation. In rough cutting operation, generally higher cutting speed is more important. From the Pareto optimal chart of corner error (Figure 5.10) for all three levels of conductivities, it is evident that 12 µS/cm is the best option because for a specified value of corner error (above 0.101 mm) it always gives better cutting speed compared to other two levels of conductivity settings. Again, from the Pareto optimal chart (Figure 5.11) of surface roughness for all three levels of conductivities, it is observed that a better surface finish can be achieved by using 4 µS/cm conductivity levels. As long as the surface roughness value is less than or equal to 2.671 µm (i.e. $1/R_a = 0.371$) 4 µS/cm conductivity gives better cutting speed. However, if the required surface roughness value is above 2.671 µm then 12 µS/cm conductivity setting will give higher cutting speed.

Thus, it is concluded that a 4 µS/cm conductivity setting will be used if either the required corner error is less than or equal to 0.101 mm or the required surface roughness value is less than or equal to 2.671 µm. In all other cases, 12 µS/cm conductivity should be used.

In this connection, it may be pointed out that unlike other process parameters conductivity cannot be changed now and then for each and every machining operation. On the other hand, most of the time, cutting speed is the most crucial parameter in rough cutting operation and under such circumstances, 12 µS/cm conductivity is, obviously, a natural choice. Particularly

when rough cutting is followed by a trim cutting operation. Thus it is clearly seen that the conventional value of conductivity (i.e. around 20 µS/cm) that are being used for cutting steel and other similar materials is not suitable for cutting Al 7075. Based upon the outcome of this experimental study it is recommended that in general 12 µS/cm conductivity should be used for rough cutting operation if allowable corner error and surface roughness values are above 0.101 mm and 2.671 µm respectively.

Finally, the process has been optimized using multi constrained optimization algorithm. For example, if the desire values of corner error and surface roughness is less than or equal to 0.160 mm (i.e. $1/C_E = 6.25$) and 3.600 µm (i.e. $1/R_a = 0.28$) respectively, then 12 µS/cm conductivity should be used as these values are greater than the critical C_E (0.101 mm) and R_a (2.671 µm) values as mentioned above. Now the problem may be formulated as follows;

Maximize cutting speed (C_S) = f (V_{OC}, T_{ON}, f_P, S_C)

Subjected to $C_E \leq 0.160$ mm and $R_a \leq 3.600$

$4 \leq \kappa \leq 22$ (µS/cm) $64 \leq V_{OC} \leq 129$ (volt) $0.05 \leq T_{ON} \leq 0.95$ (µs)

$0.024 \leq f_P \leq 0.034$ (MHz) $12 \leq S_C \leq 18$

By using the constrained optimization technique the optimum machining condition can be evaluated as follows:

$\kappa = 12$ µS/cm $V_{OC} = 64$ volt $T_{ON} = 0.5$ µs $f_P = 0.034$ MHz $S_C = 12$

The optimized cutting speed will be 5.35 mm/min and the corresponding corner error and surface roughness are 0.159 mm and 3.524 µm respectively. The overcut value under this machining condition is 80 µm and thus the wire offset setting for this case is 0.205 mm.

Any other parameter setting other than specified above will result in lower cutting speed or may either exceed the specified corner error or surface roughness value. Table 5.6 shows the Pareto optimal chart for Al 7075 alloy which can be used as guidelines for the industry. The experimental study and subsequent outcome are extremely useful for optimum machining of Al 7075 in modern manufacturing industries.

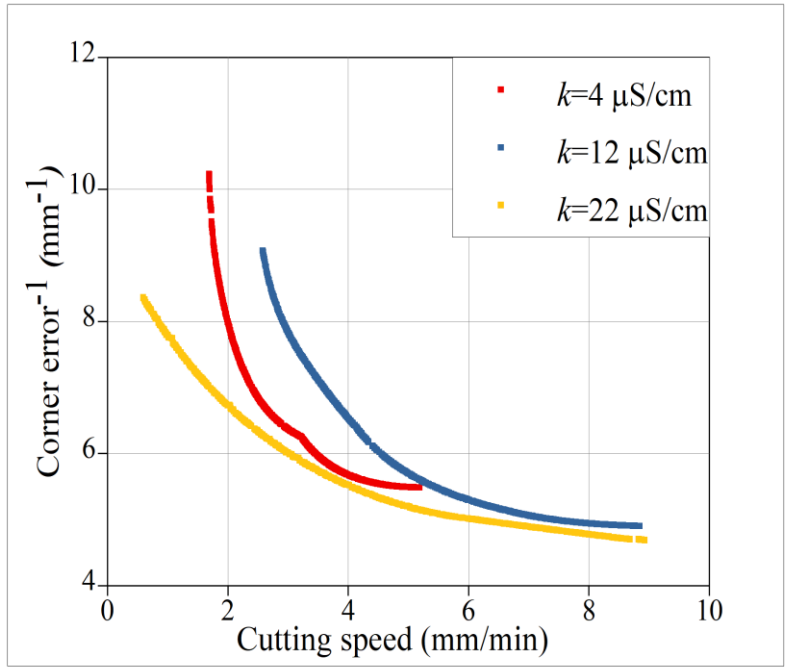

Figure 5.10 Pareto optimal solution plot for cutting speed vs. corner error

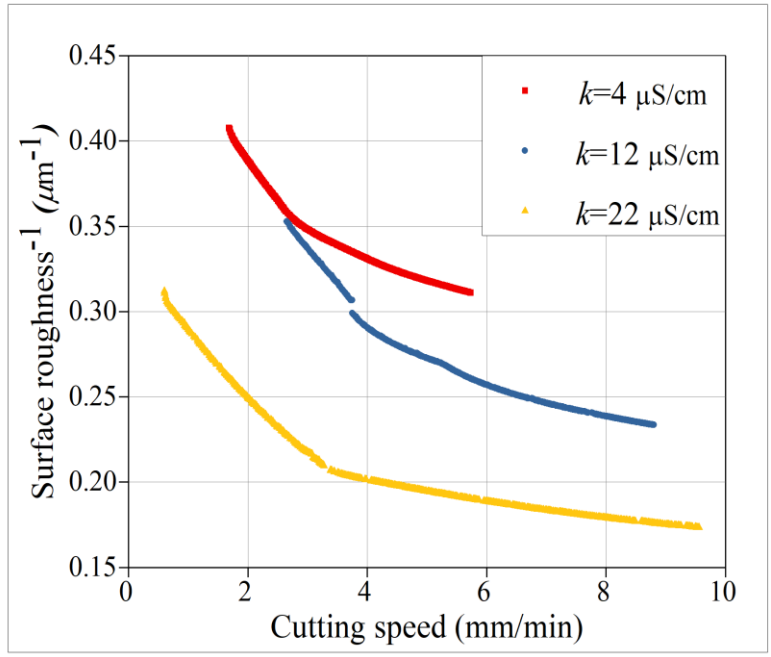

Figure 5.11 Pareto optimal solution plot for cutting speed vs. surface roughness

Table 5.6 Pareto optimal chart for Al 7075 alloy

	Input factors				Responses		
κ	V_{OC}	T_{ON}	f_P	S_C	C_S	C_E	R_a
	120	0.05	0.024	10	1.85	0.096	2.445
	74	0.05	0.028	10	2.01	0.101	2.484
	120	0.4	0.028	10	2.21	0.110	2.556
	120	0.05	0.028	13	2.44	0.116	2.671
	97	0.05	0.036	10	2.63	0.123	2.728
	74	0.4	0.024	13	3.04	0.132	2.775
	120	0.05	0.036	16	3.28	0.136	2.819
4	97	0.05	0.036	13	3.60	0.144	2.873
	74	0.75	0.024	10	3.77	0.149	2.898
	97	0.75	0.024	10	4.11	0.152	2.929
	120	0.75	0.024	16	4.50	0.164	3.019
	74	0.75	0.028	13	4.76	0.169	3.058
	97	0.75	0.028	13	5.08	0.171	3.094
	120	0.75	0.036	16	5.29	0.175	3.142
	97	0.75	0.036	16	5.68	0.176	3.198
	64	0.05	0.024	12	2.78	0.102	2.777
	64	0.05	0.029	12	3.07	0.114	2.854
	64	0.05	0.024	15	3.56	0.122	3.060
	64	0.05	0.029	15	4.06	0.134	3.185
	97	0.5	0.029	12	4.68	0.147	3.401
	129	0.5	0.024	18	4.95	0.153	3.466
	64	0.5	0.034	12	5.35	0.159	3.524
12	129	0.5	0.029	18	5.63	0.168	3.607
	64	0.5	0.034	15	6.12	0.175	3.655
	97	0.5	0.034	18	6.64	0.177	3.749
	97	0.95	0.029	12	7.20	0.179	3.794
	97	0.95	0.024	15	7.69	0.181	3.906
	97	0.95	0.029	15	8.19	0.184	4.070
	64	0.95	0.034	18	8.80	0.187	4.197
	97	0.95	0.034	18	9.17	0.188	4.281
	92	0.05	0.029	2	0.57	0.113	3.112
	120	0.05	0.033	2	1.64	0.129	3.687
	64	0.4	0.025	6	2.21	0.138	3.890
	120	0.4	0.033	2	2.55	0.147	3.987
	64	0.75	0.025	2	2.97	0.154	4.121
	64	0.05	0.025	6	4.25	0.169	4.652
	120	0.05	0.033	6	4.80	0.178	4.758
22	120	0.4	0.025	6	5.37	0.181	4.997
	120	0.4	0.033	6	5.92	0.185	5.226
	64	0.05	0.029	10	6.58	0.189	5.312
	92	0.05	0.033	10	7.15	0.190	5.431
	120	0.4	0.029	10	7.70	0.194	5.521
	92	0.4	0.033	10	8.27	0.196	5.635
	92	0.75	0.029	10	8.99	0.197	5.698
	120	0.75	0.033	10	9.52	0.201	5.762

5.6 Corner error and surface characteristics analysis

The corner profile traced by CV 3200 in three different conductivity settings is shown in Figure 5.12a-c. It has been observed that the corner error (C_E) significantly increases as the conductivity increased. This is happening due to the high energy contained in each pulse. As the energy concentration increases in the machining zone due to conductivity increase, wire-lag and vibration also increases and as a result, corner accuracy suggestively deteriorates.

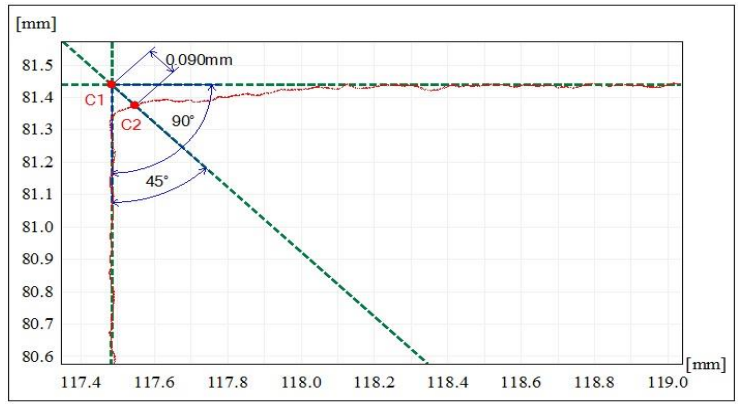

(a)

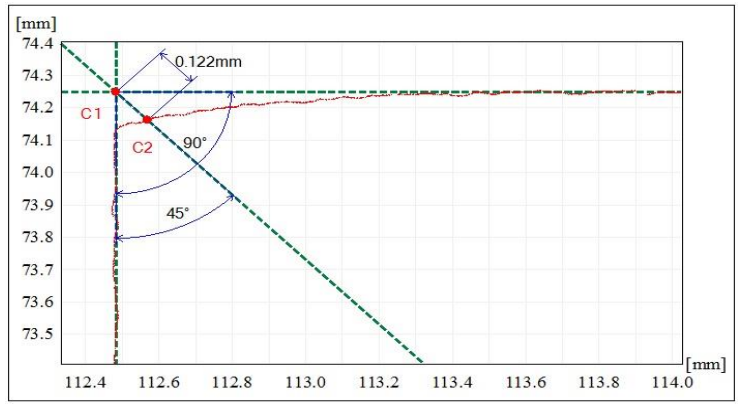

(b)

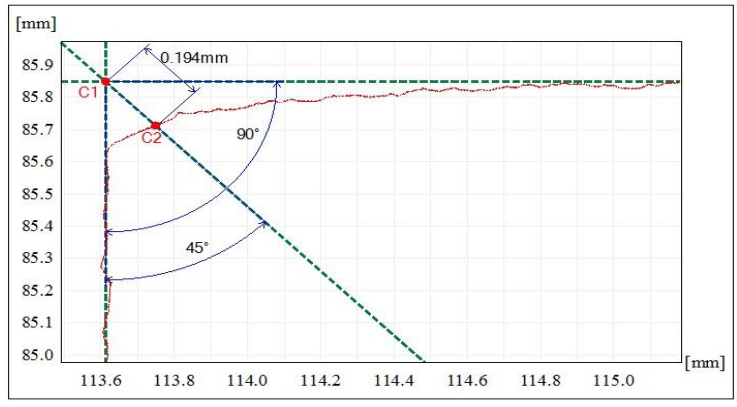

(c)

Figure 5.12 Corner error measurement by CV 3200 in different conductivity settings (a) κ = 4 µS/cm (b) κ = 12 µS/cm (c) κ = 22 µS/cm.

Figure 5.13a-b represents the 3D surface topography using CCI (Taylor & Hobson) and 2D surface evaluation profile of the machined surface using SJ 410 (Mitutoyo). From the figures, it is observed that due to the higher conductivity and pulse on time, the crater produced in the second case (Figure 5.13b) is deeper, and it also promotes higher surface roughness value. From the 2D surface evaluation profile, the same trend is also evident.

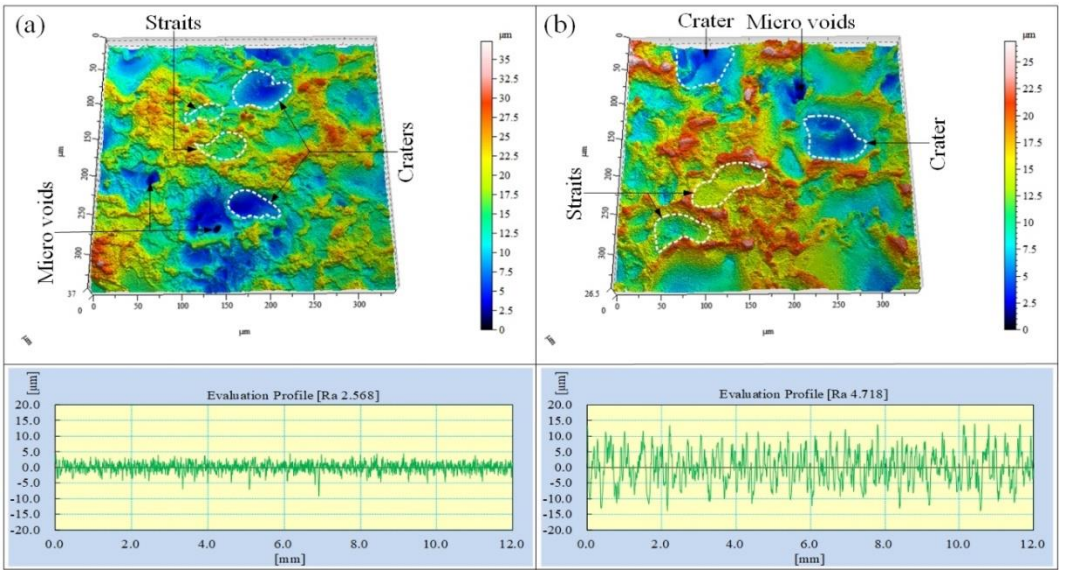

Figure 5.13 3D surface stereogram and 2D evaluation profile of the machined surface (a) κ = 4 µS/cm, V_{OC} = 74 volt, T_{ON} = 0.05 µs, f_P = 0.036 MHz & S_C = 10 (b) κ = 22 µS/cm, V_{OC} = 120 volt, T_{ON} = 0.75 µs, f_P = 0.029 MHz & S_C = 2.

The SEM image of the WEDM surfaces is shown in Figure 5.14a-b, which are characterised by micro voids and recast materials in the machining area. It has been clearly observed that the increase of dielectric conductivity induces a large volume of material removal. It has been already mentioned that with an increase in conductivity dielectric media readily ionize and as such it promotes bigger spark and as a result, larger crater is produced and recast and re-solidified materials increases. It is further observed that number of micro voids also regularly visualised at lower conductivity level but it decreased as the conductivity increased.

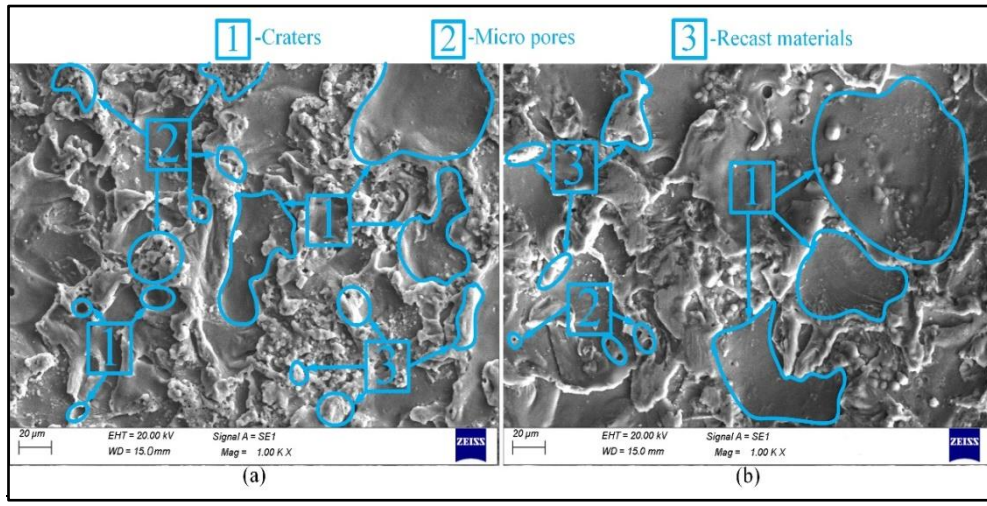

Figure 5.14 SEM image of Al 7075 surface under various conductivity setting (a) κ = 12 µS/cm (b) κ = 22 µS/cm.

The energy-dispersive X-ray spectroscopy (EDS) after machining of Al 7075 surface at 12 µS/cm and 22 µS/cm dielectric conductivity has been illustrated in Figure 5.15a-b. The surfaces after machining include several metallic compounds such as copper (Cu), zinc (Zn), aluminum (Al), magnesium (Mg), silicon (Si) and manganese (Mn) have been recognized over the analysis of EDS peaks. It also has been observed that a high percentage of overseas components (carbon: C, oxygen: O and sodium: Na) is placed on the surface at higher conductivity as compared to lower conductivity. At high conductivity, more sodium chloride (NaCl) is dissolved in the dielectric fluid. For that reason, more discharge energy can be transferred to the machining zone and enhance the rate of molten metal. Larger globules have been formed due to the re-solidification of molten metal entire the work surface. Due to this rapid ionization (i.e. at high discharge energy) of dielectric NaCl reacts with water at high temperature and induced plentiful amounts of oxygen in the machining zone. As the amount of salt increases in the dielectric, the amount of oxygen present in the plasma channel is also increased and as a result, the deposition of oxygen in the machined surface becomes more. Since EDS is a very surface sensitive technique, the detection of oxygen and Carbon suggests various sources of surface contamination. The sample is exposed to the atmospheric air before the introduction into the SEM chamber during measurement (Figure 5.15) corresponds to contamination.

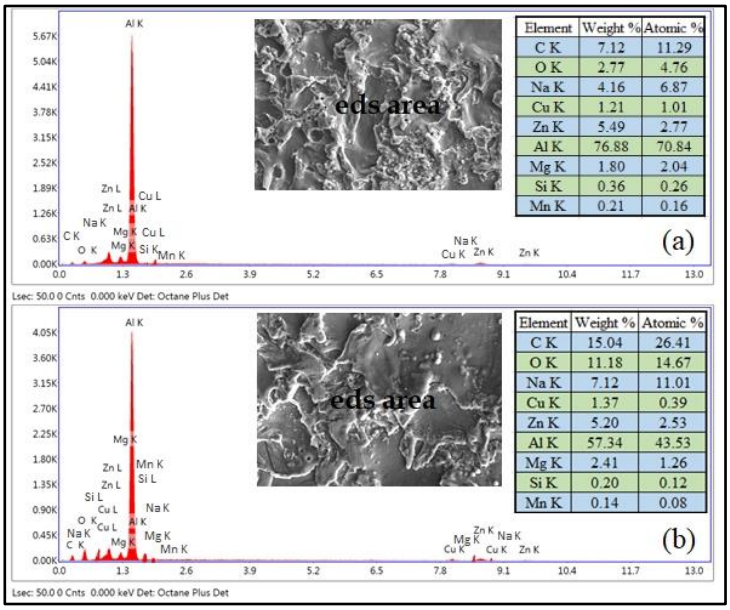

Figure 5.15 EDS pattern and elemental composition of Al 7075 in different conductivity settings (a) 12 µS/cm and (b) 22 µS/cm.

5.7 Conclusions arrived from modular experiments

An extensive experimental investigation in WEDM of Al 7075 alloy has been performed. In view of dielectric conductivity, special emphasis has been given to find out the best conductivity setting for Al 7075 alloy. The influence of conductivity has been investigated and it is observed that there is an optimum level of conductivity for which cutting speed is the maximum. It is also observed that the corner error and surface roughness increases with an increase in conductivity. From the experimental investigation, it is clearly perceived that corner error and cutting speed are strongly influenced by pulse on time, pulse frequency and servo sensitivity. Both of them increase with an increase in pulse on time and servo sensitivity but decreases with an increase in pulse frequency. This clearly indicates that it is impossible to maximize both cutting speed and corner accuracy simultaneously. A similar trend is also observed in respect of cutting speed and surface roughness. To tackle this problem Pareto optimization technique has been implemented for all three levels of conductivities separately. After analysing the results, it is observed that if the required surface roughness and corner error are lower than the critical values (e.g. C_E = 0.101 mm and R_a = 2.671 µm) then 4 µS/cm conductivity is the best choice. Generally, in the rough cutting operation, cutting speed is a prime importance and it is clearly found that higher conductivity (12 µS/cm in this case) yields the best cutting speed. Particularly when rough cutting is followed by a trim cutting operation. Additionally, from 2D as well as 3D surface topography it is observed that higher conductivity promotes a bigger crater, micro voids and recast globules.

Chapter-6
Multipass Cutting Strategy for Enhanced Corner Accuracy and Surface Finish

6.1 Problem statement

It is impossible to make a precision job with a single pass cutting in WEDM. Generally, multipass cutting is carried out to improve the accuracy (i.e., maximum elimination of corner and dimensional errors) and surface finish of the WEDM product. In the previous work, it has been demonstrated that modifying process parameters during rough cutting is not an effective strategy for producing high precision jobs. For that reason, multiple trim cutting operations are carried out on rough cut surface to enhance the accuracy and surface quality of the product.

The present experimental study is carried out to explore the influence of process parameters on different performance characteristics like corner error, surface finish and effective cutting speed in multipass (i.e. multiple trim cut followed by rough cut) cutting operations. In this study, three successive trim cuts followed by rough cuts are accomplished to improve the corner accuracy and surface finish of the final product. Effects of process parameters on responses are studied through Taguchi methodology. Finally, the improvement in corner accuracy and surface finish achieved by the respective trim cut is compared with the result of rough cut.

6.2 Basics of multipass cutting operation

In WEDM, trim cutting is carried out after rough cutting to eliminate the rough layer deposited on the machined surface due to re-solidification of the molten metal and also improve the dimensional accuracy of the workpiece. In a trim cutting operation, the moving wire electrode follows back in the same path with some amount of wire offset where the rough cut operation was carried out. High offset value (hard) and low offset value (soft) trimming operations have been performed on the rough cut surface based upon the inaccuracy and undulations present on the job surface. Generally, the number of finish cuts followed by rough cuts varied from one to five, depending on the amount of wire offset values used. This combined operation (i.e., trim cuts followed by rough cut) is known as "multipass cutting" in WEDM. Sometimes it is also known as a "trim" or "finish" cutting operation. Rough cutting (i.e., first cut) is performed at a high pulse parameter setting and high flushing condition with an optimal level of conductivity to enhance the cutting speed and material removal rate

(MRR). In the semi finish cutting stage, power and flushing conditions are kept on the lower side to improve the accuracy and surface finish. The final trim cut is performed with a very low pulse parameter setting, gentle flow of dielectric liquid and of course the highest wire tension value possible. The aim of the trim cutting operation is given as follows:

i. Improve the accuracy and surface finish of the workpiece.

ii. Eliminate minor deformations present in the workpiece due to residual stress.

iii. Remove recast layer from the machined surface and improved the cycle life of the product by eliminating thermal layer formed due to aggressive cutting.

iv. Curtail the bow effect present in the rough-cut surface due to adverse cutting condition.

The slot produced by the wire electrode, machining workpiece and the schematic representation of the trim cutting operation are shown in Figure 6.1a-b and Figure 6.2. In multi-pass cutting, the term "dimensional shift (D_S)" is defined as the perpendicular distance between the actual machined profile and the pre-defined programed path during rough cutting without any wire offset (i.e., zero wire offset). Another important term used in multipass cutting operations is "effective wire offset (WO_E)." It is the perpendicular distance between the rough and the trim cutting programed path. The details of wire path planning, dimensional shift, and effective wire offset are presented in Figure 6.2. In the first cut, the wire offset value is kept constant at zero. To achieve the actual dimensional accuracy during machining, the following wire offset setting must be incorporated into multi-pass cutting.

Wire offset for first cut (WO_R) = D_S

Wire offset value for trim cut (WO_T) = D_S - E_{WO}

Effective wire offset value for trim cut (WO_E) = WO_R - WO_T

It is to be noted that the wire offset in trim (WO_T) and the effective wire offset in trim (WO_E) are not the same thing. The term "dimensional shift" (D_S) is generally used to figure out the actual wire offset value during rough and trim cutting. Dimensional shift is considered an output, but actually it is an input parameter setting and termed as "wire offset" (WO_R) in rough cutting operations.

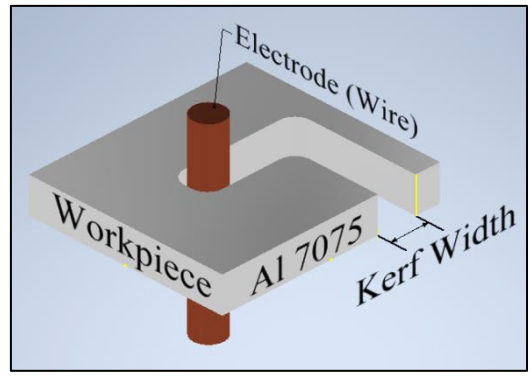

(a)

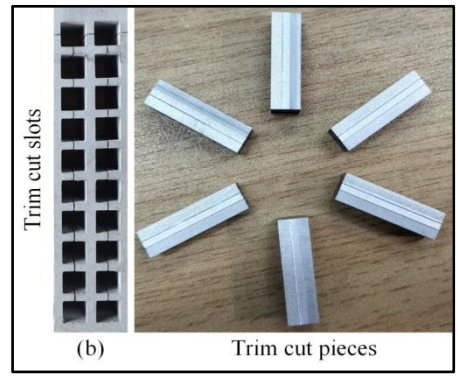

(b)

Figure 6.1 (a) Slot produced by WEDM (b) Workpiece after trim cutting operation

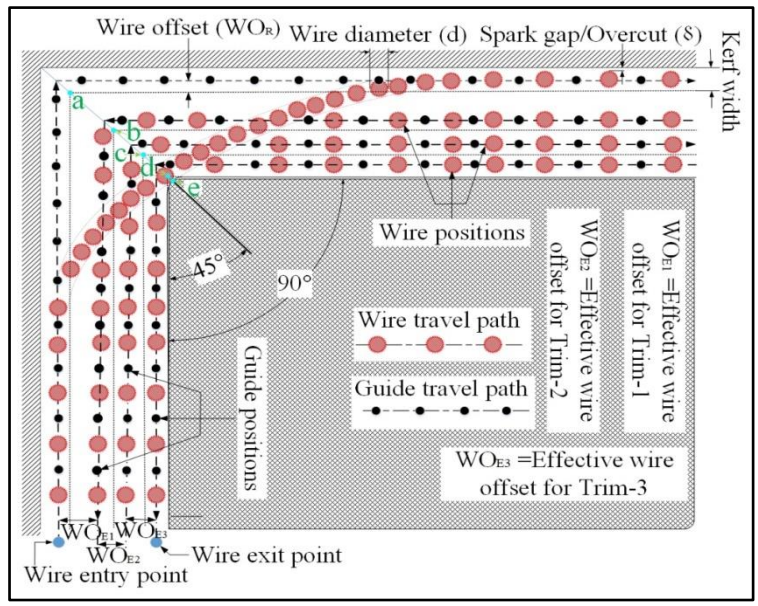

Figure 6.2 Schematic diagram of trim cutting operation in WEDM

6.3 Experimentation

The layer of material removed from the workpiece during trim cutting is shown in Figure 6.2. It is apparent that the maximum dimensional inaccuracy and surface irregularities induced by

the rough cut are eliminated by trim cut. As the number of trim cuts increases, accuracy and surface finish both increases. Generally, one or two trim cuts are performed on rough cut surface to improve the accuracy and quality. Sometimes, desired accuracy and finish may not be achieved by a single or dual trimming operation when the hard to machine material is highly conductive. In such circumstances, three successive finish cuts are a better choice to obtain the desired accuracy and surface finish. It is anticipated that the parameter setting in rough cut has an impact on the first trim cut. Similarly, parameter settings in the first trim cut have an impact on the second trim cut, and likewise, second trim cut parameters have an impact on the third cut. The main objective of the rough cutting operation is to maximize the cutting speed, or MRR. Whereas, the prime objective of the trim cutting operation is to minimize the dimensional error and maximize the surface quality without sacrificing the cutting speed. In trim cutting operations, very low pulse power and flushing pressure are generally employed to improve the surface quality and eliminate the oxide layers from the job surface. Apart from this, higher wire tension and lower servo sensitivity are always preferable in finish cutting operations to obtain better dimensional accuracy.

Considering the above criteria, it has been decided to choose the particular process factor combination that can maximize the cutting speed in rough cutting irrespective of the surface roughness. Pulse on time (T_{ON}) and servo sensitivity (S_C) have been considered as input factors to maximize the cutting speed in first cutting. Improvement of corner accuracy and surface finish are prime concerns in the trim cutting operation. For that reason, three successive trim cuts have been carried out to obtained better accuracy and surface finish for this material. Based on rough cutting experiments (from the Chapter 6), two major influencing factors, pulse on time (T_{ON}) and wire offset (WO), were considered as input parameters for three subsequent trim cutting operation. Cutting speed, corner error, and surface roughness are considered as response criteria in three respective trim cuts. Rough and trim cutting process parameters and their levels are given in Table 6.1–Table 6.4.

Some other machining parameters that may have an influence on the response measure are kept constant. The constant parameters are electrical conductivity of the dielectric (12 µS/cm), temperature of the dielectric (24°C), coated brass wire electrode with a diameter of 250 µm, wire feed rate (16 m/min), pulse off time (20 µs), open circuit voltage (102 volts), servo voltage (45 volts), servo sensitivity (18), wire tension (1.5 kg), flushing pressure (5 kg/cm^2), and workpiece thickness (25 mm).

Taguchi orthogonal array technique has been employed to design the experiments for the rough and respective trim cuts. An intricate design concept has been used to carry out the 1st, 2nd and 3rd trimming operations. L_9 orthogonal array is employed to design the rough cut and the first trim cut process. Likewise, L_{18} orthogonal array is used for the 2nd trim cut and L_{27}

for 3rd cut process. Sixty-three numbers of experiments are performed for rough and trim cutting operations.

Table 6.1 Process parameters and levels for rough cut

Parameters	Units	Levels		
		1	2	3
Pulse on time (T_{ON})	µs	0.5	0.7	0.9
Servo sensitivity (S_C)	-	8	12	16

Table 6.2 Process parameters and levels for 1st trim cut

Parameters	Units	Levels		
		1	2	3
Pulse on time (T_{ON})	µs	0.5	0.7	0.9
Servo sensitivity (S_C)	-	8	12	16
Pulse on time for 1st trim cut $(T_{ON})_1$	µs	0.35	0.4	0.45
Effective wire offset for 1st trim cut $(WO)_{E1}$	µm	140	150	160

Table 6.3 Process parameters and levels for 2nd trim cut

Parameters	Units	Levels		
		1	2	3
Pulse on time (T_{ON})	µs	0.5	0.7	0.9
Servo sensitivity (S_C)	-	8	12	16
Pulse on time for 1st trim cut $(T_{ON})_1$	µs	0.35	0.4	0.45
Effective wire offset for 1st trim cut $(WO)_{E1}$	µm	140	150	160
Pulse on time for 2nd trim cut $(T_{ON})_2$	µs	0.2	0.25	0.3
Effective wire offset for 2nd trim cut $(WO)_{E2}$	µm	30	45	60

Table 6.4 Process parameters and levels for 3rd trim cut

Parameters	Units	Levels		
		1	2	3
Pulse on time (T_{ON})	µs	0.5	0.7	0.9
Servo sensitivity (S_C)	-	8	12	16
Pulse on time for 1st trim cut $(T_{ON})_1$	µs	0.35	0.4	0.45
Effective wire offset for 1st trim cut $(WO)_{E1}$	µm	140	150	160
Pulse on time for 2nd trim cut $(T_{ON})_2$	µs	0.2	0.25	0.3
Effective wire offset for 2nd trim cut $(WO)_{E2}$	µm	30	45	60
Pulse on time for 3rd trim cut $(T_{ON})_3$	µs	0.05	0.10	0.15
Effective wire offset for 3rd trim cut $(WO)_{E3}$	µm	5	10	15

6.3.1 Machining strategy for rough and trim cutting operation

Different researchers have carried out multipass cutting operations in WEDM of different alloys and then optimized the process criteria. So far, for a given corner accuracy and surface finish which machining strategy (i.e., rough or trim cutting) is more suitable, the problem has

not been fully solved. The choice of a suitable machining strategy plays a vital role in determining the overall efficiency and economic solution for the entire machining operation. This section is focused on how to choose the appropriate machining strategy to improve the accuracy and efficiency keeping in view the economic implications (Sarkar et al. 2010).

In case of multiple cutting operations, the average cutting speed can be expressed as follows:

$$V_{avg} = \frac{2V_R V_T}{V_R + V_T} \tag{6.1}$$

Where, V_{avg} is the average cutting speed, V_R is the rough cutting speed, and V_T is the trim cutting speed.

To integrate the rough and trim cutting operations, the term "effective cutting speeds" (V_E) has been presented. It is defined as the length of the machining per unit time. It can be noted that for multipass cutting operations, the wire electrode repetitively travels along a predefined path to be cut. In the case of a single trim cut followed by a rough cut, the electrode travels the same path twice. Similarly, for the second and third trimming operations, the wire electrode travels in the same path three and four times. Therefore, the effective cutting speed for three different trim cuts can be expressed as follows:

For first trim cutting: $V_E = \frac{V_{avg}}{2} \Rightarrow V_e = \frac{V_R V_{T1}}{V_R + V_{T1}}$ (6.2)

For second trim cutting: $V_E = \frac{V_{avg}}{3} \Rightarrow V_e = \frac{V_R V_{T1} V_{T2}}{V_R + V_{T1} + V_{T2}}$ (6.3)

For third trim cutting: $V_E = \frac{V_{avg}}{4} \Rightarrow V_e = \frac{V_R V_{T1} V_{T2} V_{T3}}{V_R + V_{T1} + V_{T2} + V_{T3}}$ (6.4)

Where, V_{T1} is the 1st trim cutting speed, V_{T2} is the 2nd trim cutting speed, V_{T3} is the 3rd trim cutting speed.

For single pass cutting operations, the effective cutting speed is equal to the rough cutting speed (wire passes only once in the predefined programed path). Therefore, for a single pass or rough cutting operation, effective cutting speed is-

$$V_E = V_R \tag{6.5}$$

In first trim cutting operation, rough cutting process parameters i.e., pulse on time and servo sensitivity, and trim cutting parameters, e.g., pulse on time $(T_{on})_1$ and wire offset $(WO)_{E1}$ are considered as input factors. Similarly, rough cut and 1st trim cut parameters are considered and included into second trim cutting $\{(T_{on})_2$ and $(WO)_{E2}\}$ operation. Finally, rough cutting,

first trim cutting, and second trim cutting parameters are used in the final finish cutting {$(T_{on})_3$ and $(WO)_{E3}$} operation. Experimental results for rough and trim cutting operations are given in Table 6.5–6.8.

Table 6.5 Experimental results for rough cutting operation

	Inputs		Responses		
Sl. No.	Pulse on time (T_{ON}: µs)	Servo sensitivity (S_C)	Effective cutting speed (CS_E: mm/min)	Corner error (C_E: µm)	Surface roughness (R_a: µm)
1	0.5	8	4.52	143.93	3.321
2	0.5	12	6.05	147.83	3.209
3	0.5	16	7.15	155.13	3.170
4	0.7	8	5.08	164.75	3.835
5	0.7	12	6.75	165.31	3.576
6	0.7	16	8.05	175.40	3.496
7	0.9	8	5.46	164.08	4.112
8	0.9	12	7.25	169.46	3.944
9	0.9	16	8.71	176.84	3.821

Table 6.6 Experimental results for first trim cutting operation

	Inputs			Responses			
Sl. No.	Pulse on time (T_{ON}: µs)	Servo sensitivity (S_C)	Pulse on time for 1st trim cut {$(T_{ON})_1$: µs}	Wire offset for 1st trim cut {$(WO)_{E1}$: µm}	Effective cutting speed (CS_E: mm/min)	Corner error (C_E: µm)	Surface roughness (R_a: µm)
1	0.5	8	0.35	140	2.72	100.89	2.182
2	0.5	12	0.40	150	3.42	90.65	2.534
3	0.5	16	0.45	160	3.86	81.54	2.895
4	0.7	8	0.40	160	2.97	85.81	2.615
5	0.7	12	0.45	140	3.81	91.36	3.176
6	0.7	16	0.35	150	3.67	89.10	2.157
7	0.9	8	0.45	150	3.29	86.24	3.209
8	0.9	12	0.35	160	3.40	84.82	2.238
9	0.9	16	0.40	140	4.21	89.90	2.710

Table 6.7 Experimental results for second trim cutting operation

	Inputs						Responses		
Sl. No.	Pulse on time (T_{ON}: µs)	Servo sensitivity (S_C)	Pulse on time for 1st trim cut {$(T_{ON})_1$: us}	Wire offset for 1st trim cut {$(WO)_{E1}$: µm}	Pulse on time for 2nd trim cut {$(T_{ON})_2$: µs}	Wire offset for 2nd trim cut {$(WO)_{E2}$: µm}	Effective cutting speed (CS_E: mm/min)	Corner error (C_E: µm)	Surface roughness (R_a: µm)
1	0.5	8	0.35	140	0.20	30	2.23	77.08	1.037
2	0.5	12	0.40	150	0.25	45	2.68	63.55	1.166
3	0.5	16	0.45	160	0.30	60	3.01	55.23	1.618
4	0.7	8	0.35	150	0.25	60	2.36	54.83	1.251
5	0.7	12	0.40	160	0.30	30	2.79	69.76	1.615
6	0.7	16	0.45	140	0.20	45	3.12	66.86	1.015
7	0.9	8	0.40	140	0.30	45	2.64	59.60	1.669
8	0.9	12	0.45	150	0.20	60	2.90	58.27	1.065
9	0.9	16	0.35	160	0.25	30	2.86	76.11	1.153
10	0.5	8	0.45	160	0.25	45	2.38	65.90	1.213
11	0.5	12	0.35	140	0.30	60	2.62	55.53	1.540
12	0.5	16	0.40	150	0.20	30	2.82	77.08	1.077
13	0.7	8	0.40	160	0.20	60	2.37	56.36	1.116
14	0.7	12	0.45	140	0.25	30	2.98	74.83	1.199
15	0.7	16	0.35	150	0.30	45	2.89	62.52	1.618
16	0.9	8	0.45	150	0.30	30	2.69	70.48	1.701
17	0.9	12	0.35	160	0.20	45	2.62	68.94	1.014
18	0.9	16	0.40	140	0.25	60	3.13	55.48	1.229

Table 6.8 Experimental results for third trim cutting operation

Sl. No.	Inputs								Responses		
	Pulse on time (T_{ON}: µs)	Servo sensitivity (S_C)	Pulse on time for 1s rim cut {$(T_{ON})_1$: µs}	Wire offset for 1st trim cut {$(WO)_{E1}$: µm}	Pulse on time for 2nd trim cut {$(T_{ON})_2$: µs}	Wire offset for 2nd trim cut {$(WO)_{E2}$: µm}	Pulse on time for 3rd trim cut {$(T_{ON})_3$: µs}	Wire offset for 3rd trim cut {$(WO)_{E3}$: µm}	Effective cutting speed (CS_E: mm/min)	Corner error (C_E: µm)	Surface roughness (R_a: µm)
1	0.5	8	0.35	140	0.20	30	0.05	5	1.96	48.22	0.369
2	0.5	8	0.35	140	0.25	45	0.10	10	2.00	43.72	0.451
3	0.5	8	0.35	140	0.30	60	0.15	15	2.02	20.03	0.625
4	0.5	12	0.40	150	0.20	30	0.05	10	2.28	46.79	0.402
5	0.5	12	0.40	150	0.25	45	0.10	15	2.31	42.34	0.541
6	0.5	12	0.40	150	0.30	60	0.15	5	2.39	23.37	0.721
7	0.5	16	0.45	160	0.20	30	0.05	15	2.46	45.69	0.407
8	0.5	16	0.45	160	0.25	45	0.10	5	2.56	44.52	0.578
9	0.5	16	0.45	160	0.30	60	0.15	10	2.59	24.32	0.657
10	0.7	8	0.40	160	0.20	45	0.15	5	2.12	23.18	0.704
11	0.7	8	0.40	160	0.25	60	0.05	10	2.12	42.20	0.389
12	0.7	8	0.40	160	0.30	30	0.10	15	2.17	39.64	0.493
13	0.7	12	0.45	140	0.20	45	0.15	10	2.49	27.03	0.704
14	0.7	12	0.45	140	0.25	60	0.05	15	2.47	44.89	0.453
15	0.7	12	0.45	140	0.30	30	0.10	5	2.60	44.72	0.585
16	0.7	16	0.35	150	0.20	45	0.15	15	2.41	21.95	0.660
17	0.7	16	0.35	150	0.25	60	0.05	5	2.43	47.39	0.434
18	0.7	16	0.35	150	0.30	30	0.10	10	2.51	43.72	0.518
19	0.9	8	0.45	150	0.20	60	0.10	5	2.25	44.10	0.545
20	0.9	8	0.45	150	0.30	30	0.15	10	2.36	30.74	0.609
21	0.9	8	0.45	150	0.30	45	0.05	15	2.28	45.31	0.480
22	0.9	12	0.35	160	0.20	60	0.10	10	2.27	41.14	0.538
23	0.9	12	0.35	160	0.25	30	0.15	15	2.34	23.95	0.697
24	0.9	12	0.35	160	0.30	45	0.05	5	2.35	44.99	0.549
25	0.9	16	0.40	140	0.20	60	0.10	15	2.60	42.12	0.522
26	0.9	16	0.40	140	0.25	30	0.15	5	2.72	34.48	0.697
27	0.9	16	0.40	140	0.30	45	0.05	10	2.69	48.45	0.515

6.3.2 Influence of process parameters in rough and trim cutting operation

From Figure 6.3a-c, it is observed that pulse on time (T_{ON}) and servo sensitivity (S_C) both are major influencing process factors to determine effective cutting speed (CS_E), corner error (C_E), and surface roughness (R_a) in single pass cutting operation. From Figure 6.3a, it has been observed that cutting speed increases as the increase in pulse on time and servo sensitivity .On the contrary, corner error and surface roughness are decreased as the pulse on time and servo sensitivity decrease. An increase in pulse on time produces intense spark and promotes higher energy pulses, which in turn results in more material removal in the inter electrode gap (IEG) and enhances the cutting speed. Due to this intense sparking at a higher pulse on time, more material will be removed from the corner of the profile being produced, which will deteriorates the corner accuracy. At the same time, crater volume per spark or material removed from each spark also increases. Therefore, the surface roughness also increases with an increase in pulse on time during rough cutting operation. It is further expected from the earlier work (Chapter 5) that an increase in servo sensitivity there will be reduction the gap distance (i.e., IEG). Due to this reduction of inter-electrode gap, the loss of spark energy in the dielectric becomes less. Consequently, there will be more efficient and effective utilisation of spark energy with an increase in servo sensitivity. It is also observed that the trend is the equivalent to pulse on time. For this reason, with an increase in servo sensitivity, there has been an increasing trend in cutting speed, corner error, and surface roughness.

Cutting speed is an important factor that must be maximized during rough cutting operation. It has been observed that pulse parameters settings are always played a crucial role in determining the cutting speed or material removal rate. As the pulse on time increases up to a certain limit, the cutting speed or MRR drastically increases and vice versa. On the other hand, corner inaccuracy (i.e., corner error) and surface finish induced in a single pass (i.e., rough cut) are increased as the pulse on time increases. If the single pass cutting operation has been carried out at a higher pulse parameter setting, more material can be eliminated from the corner and huge undulations can be formed on the work surface. This huge number of corner errors and surface irregularities cannot be eliminated by a single trimming operation. Therefore, the effects of rough cutting process parameters are always reflected in the first trim cutting operation.

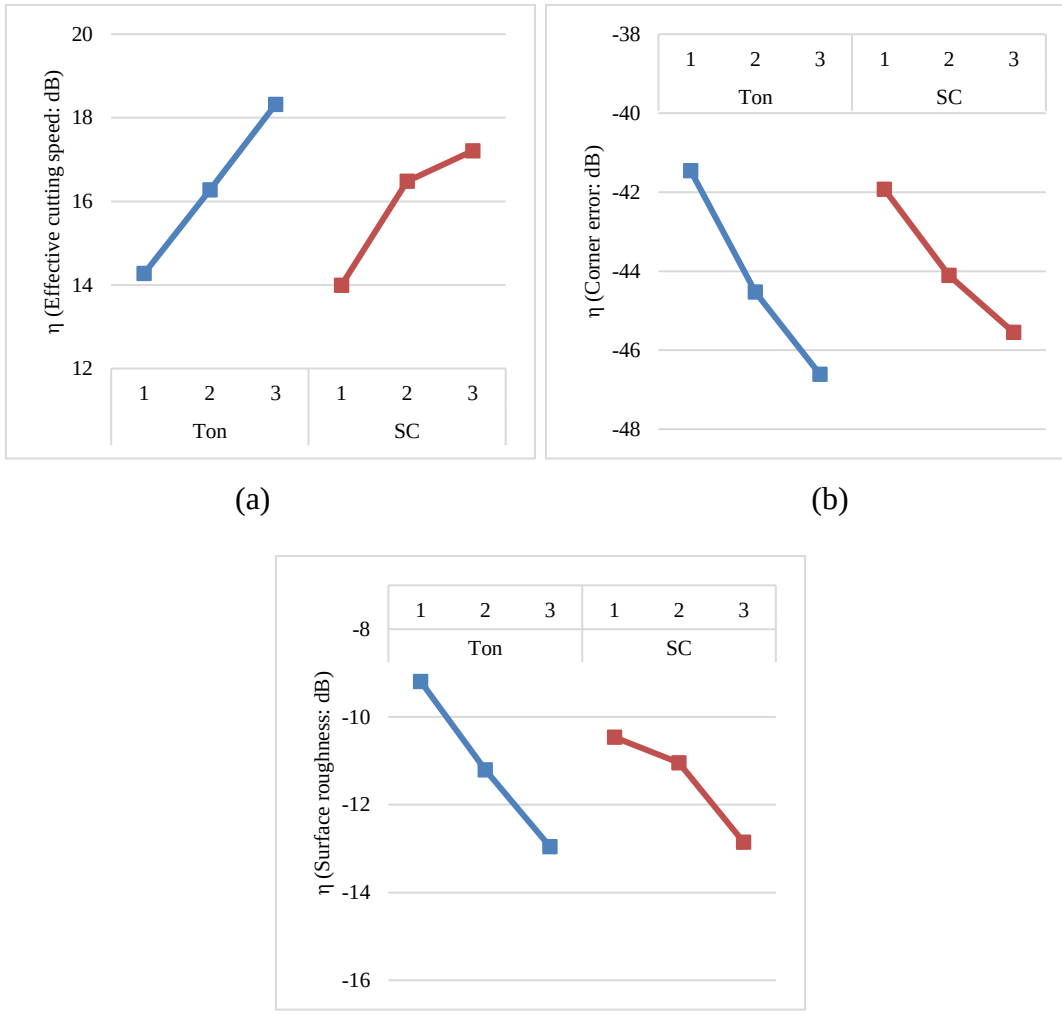

(a) (b)

(c)

Figure 6.3 Effect of rough cutting parameters on (a) effective cutting speed (b) corner error and (c) surface roughness

In a trim cutting operation, the most effective parameters are wire offset and pulse on time. Rough cutting operation revealed the significance of pulse on time. These two significant process parameters are considered for three successive trim cuts at different levels. During the first trim cut, aggressive wire offset values are considered in eliminating the maximum corner error without negotiating the other response criteria. From Figure 6.4a, effective cutting speed, corner error, and surface roughness increase as the pulse on time increases. Effective cutting speed decreases as the wire offset increases, whereas corner accuracy and surface finish improves as the wire offset value increases. Impact of rough cutting parameters (especially pulse on time) on the responses have been observed (shown in Figure 6.4) during the first trim cutting operation. This is happened due to the high pulse parameter setting in the rough cutting operation. After single pass cutting, corner error and surface roughness values are always on the higher side. Only partial elimination of corner errors and surface roughness

can be possible using a single trim cut. Figure 6.4a-c shows the combined effects of rough and first trim cutting parameters on effective cutting speed, corner error, and surface roughness.

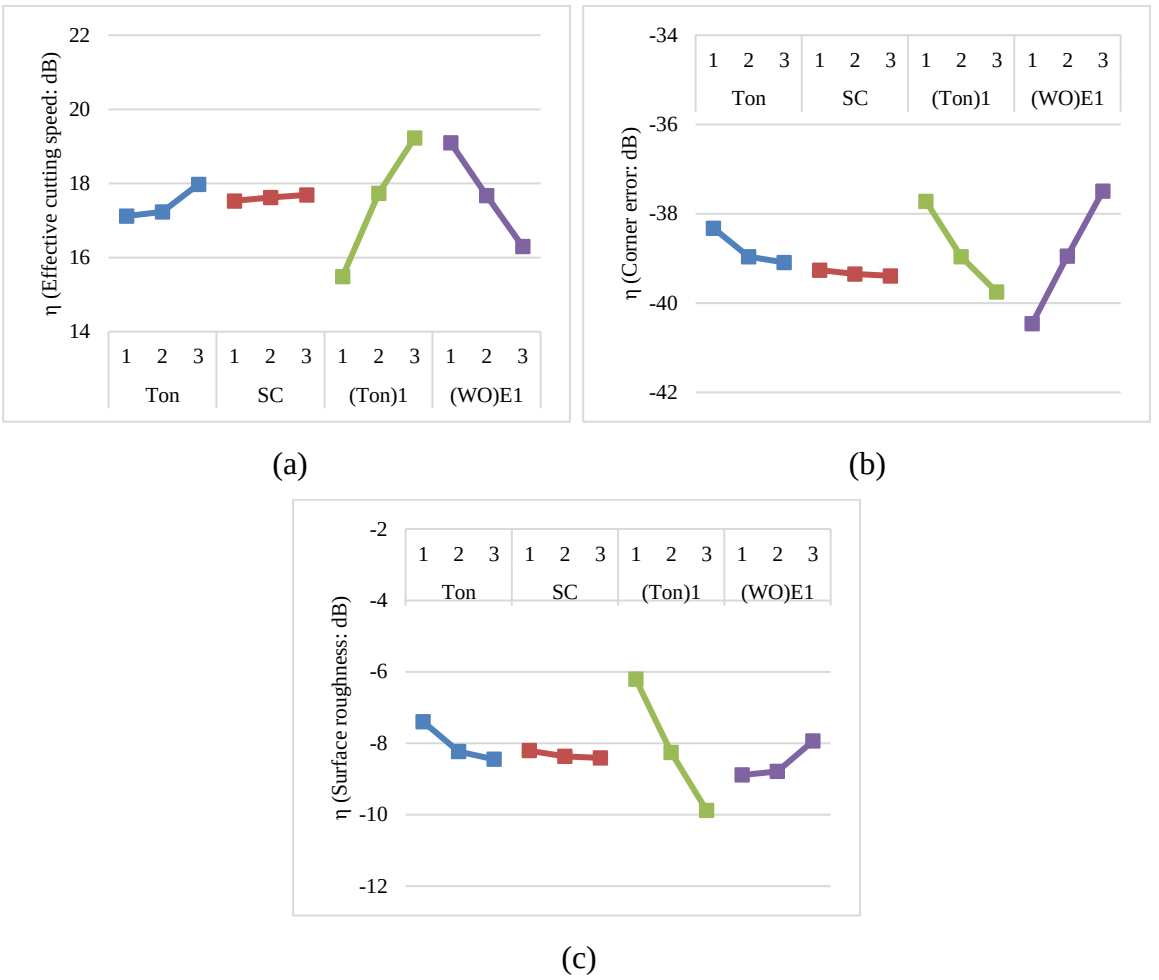

Figure 6.4 Effect of 1st trim cutting parameters on (a) effective cutting speed (b) corner error and (c) surface roughness

Second trim cutting parameters are coupled with rough and first trim cutting parameters to investigate the influence of the three successive cuts (rough & dual trim) on the response factors, i.e., effective cutting speed, corner inaccuracy, and surface finish. It has been observed that the most effective parameter during second trim cutting is pulse on time $(T_{ON})_2$ for effective cutting speed and surface roughness. Whereas wire offset, i.e., $(WO)_{E2}$ of the second trim cutting, is the most dominating parameter to determine the corner error. It has been also observed that the first trim cutting parameters, i.e., $(T_{ON})_1$ & $(WO)_{E1}$, have a significant impact on effective cutting speed, corner error, and surface roughness after the completion of the second trim cutting operation. This is happened due to the fact that corner errors and surface irregularities cannot be fully removed from the machined surface. Here the most important thing is that the corner error and surface roughness decreased as compared to

the first trim cut, but as such influence of rough cutting parameters are observed in the second trim cut. The effect of process parameters during the second trim cutting operation is shown in Figure 6.5.

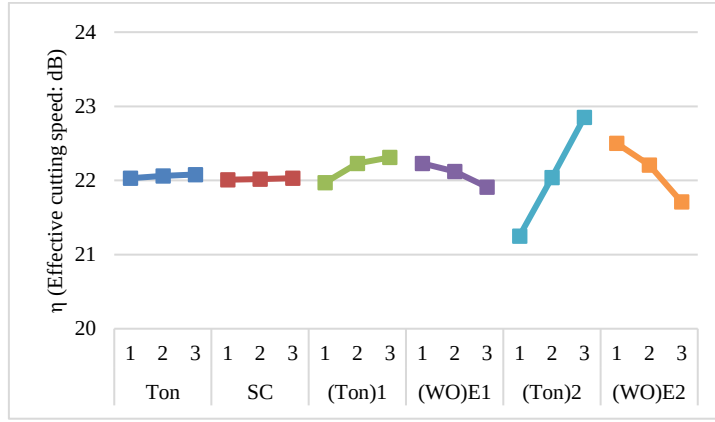

(a)

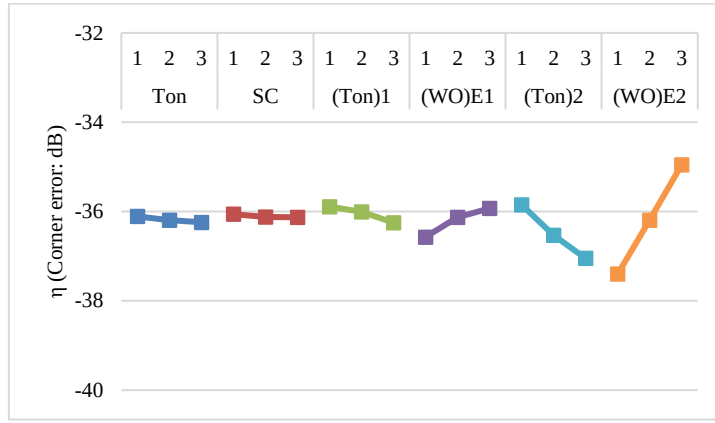

(b)

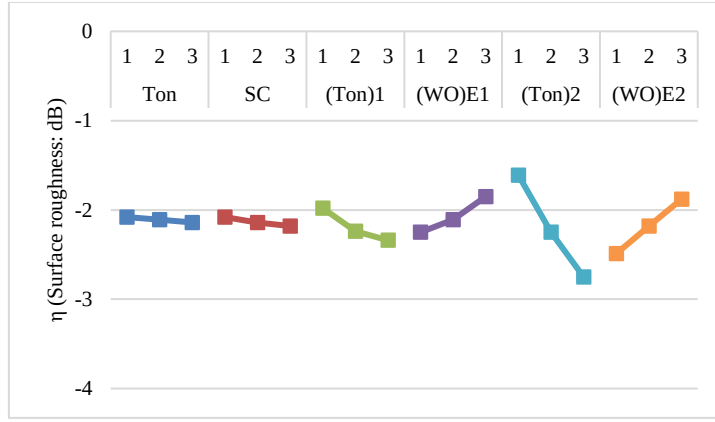

(c)

Figure 6.5 Effect of 2nd trim cutting parameters on (a) effective cutting speed (b) corner error and (c) surface roughness

A third trim cut, or final finish cut, has been carried out to further eliminate the corner errors and surface irregularities present in the job surface. In the final finishing operation, rough, first and second trim cut parameters are blended with third trim cutting parameters. The effects of third trim cut process parameters are the same as for second trim cut parameters and second trim cut parameters have little influence on the third trim cutting operation. It is observed that the third trim cutting pulse on time $(T_{ON})_3$ is the most influential factor to determine the effective cutting speed, whereas wire offset $(WO)_{E3}$ is for corner error. Effective cutting speed, corner error, and surface roughness increase as the third trim cutting pulse on time increases. However, corner error and surface roughness decrease as the third trim cutting wire offset value increases, but effective cutting speed decreases as the wire offset value increases. It is found that the corner accuracy and surface finish are considerably improved after three successive trim cutting operations.

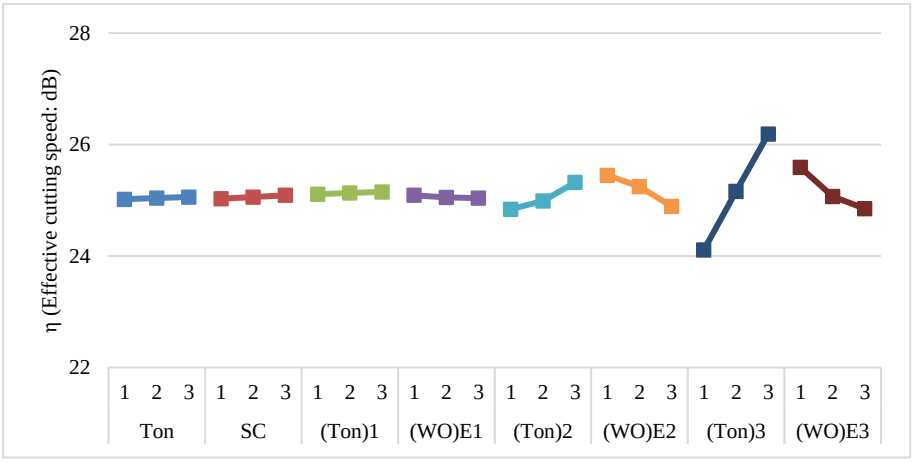

(a)

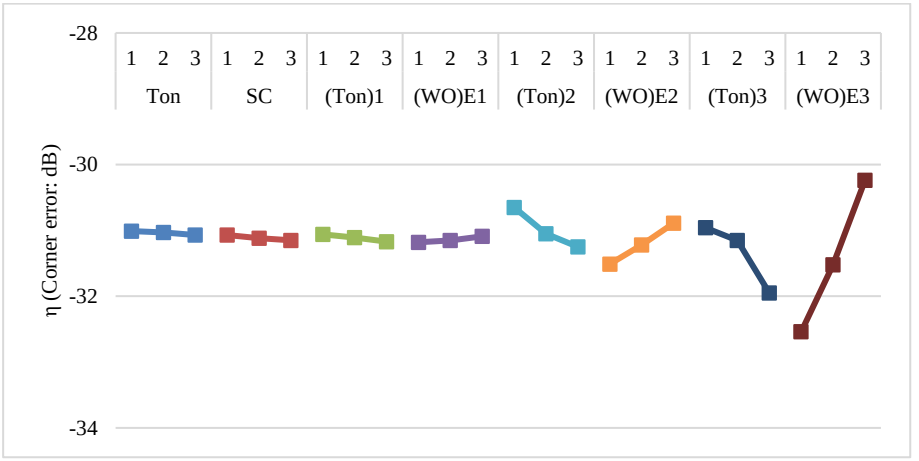

(b)

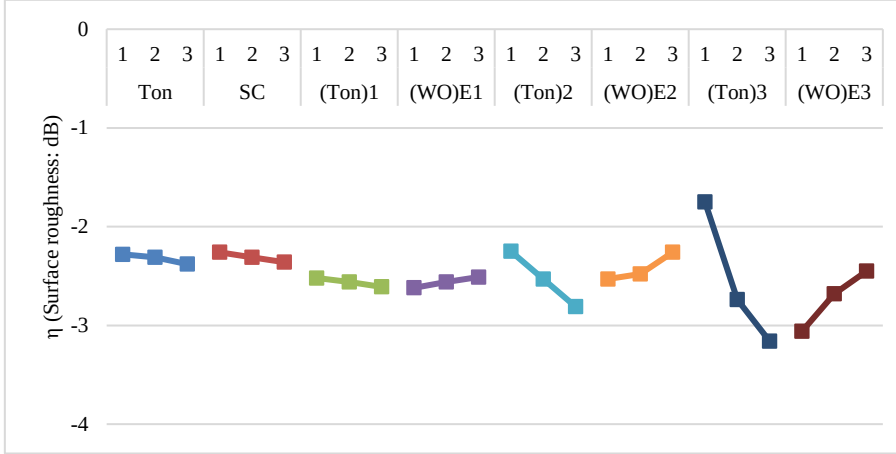

(c)

Figure 6.6 Effect of 3rd trim cutting parameters on (a) effective cutting speed (b) corner error and (c) surface roughness

6.3.3 Modelling of WEDM process in single pass and multipass cutting operation

In order to study the influence of the WEDM parameters a nonlinear regression modelling (quadratic) technique has been used as follows to estimate the parametric effects on the several response criteria:

$$y\,(x) = a+(a_1x_1+a_2x_2+a_3x_3+\ldots\ldots\ldots\ a_mx_m)+(a_4x_1^2+a_5x_2^2+a_6x_3^2+\ldots\ldots\ldots\ a_nx_n^2) \qquad (6.7)$$

Where, a, a_1, a_2 …. a_m, a_n are the constants (coefficient) obtained from the non-linear regression analysis.

$y(x)$ is the response criterion (i.e. effective cutting speed, corner error and surface roughness).

x_1, x_2, x_3 …. x_n are the variable factors for rough and trim cutting operation; such as pulse on time, servo sensitivity, wire offset etc.

Minitab software has been used to establish the mathematical model and to calculate the corresponding coefficient of the obtained model. For better accuracy of the model, insignificant factors are eliminated. The calculated coefficients have been substituted and corresponding relations are given in below:

A. For effective cutting speed

Rough cut

$$y(CS_E) = -2.79 + 6.70\times x_1 + 0.651\times x_2 - 2.58\times x_1^2 - 0.01177\times x_2^2 \qquad (6.8)$$

First trim cut

$y(CS_E) = 3.645 + 0.7500\times x_1 + 0.2500\times x_2 + 27.90\times x_3 - 0.1135\times x_4 - 0.00001\times x_1^2 - 0.005625\times x_2^2 - 30.00\times x_3^2 + 0.000350\times x_4^2$ (6.9)

Second trim cut

$y(CS_E) = -0.53 + 1.625\times x_1 + 0.1533\times x_2 + 8.40\times x_3 - 0.0105\times x_4 + 1.67\times x_5 - 0.00161\times x_6 - 0.833\times x_1^2 - 0.003646\times x_2^2 - 7.33\times x_3^2 + 0.000017\times x_4^2 - 1.33\times x_5^2 + 0.000019\times x_6^2$ (6.10)

Third trim cut

$y(CS_E) = 0.556 + 0.823\times x_1 + 0.11414\times x_2 + 10.53\times x_3 - 0.02949\times x_4 + 2.568\times x_5 - 0.00205\times x_6 + 0.802\times x_7 + 0.00287\times x_8 - 0.3388\times x_1^2 - 0.002618\times x_2^2 - 10.75\times x_3^2 + 0.000088\times x_4^2 - 3.43\times x_5^2 + 0.000014\times x_6^2 - 2.09\times x_7^2 - 0.000316\times x_8^2$ (6.11)

B. For corner error

Rough cut

$y(C_E) = 25.3 + 365.9\times x_1 - 2.29\times x_2 - 223.5\times x_1^2 + 0.1555\times x_2^2$ (6.12)

First trim cut

$y(C_E) = 301.2 - 18.85\times x_1 - 0.4717\times x_2 - 117.8\times x_3 - 1.670\times x_4 + 6.250\times x_1^2 - 0.001875\times x_2^2 + 82.00\times x_3^2 + 0.003900\times x_4^2$ (6.13)

Second trim cut

$y(C_E) = 384.5-40.0\times x_1 + 0.717\times x_2 - 617\times x_3 - 2.03\times x_4 + 9.0\times x_5 - 0.819\times x_6 + 26.94\times x_1^2 - 0.0220\times x_2^2 + 764\times x_3^2 + 0.00685\times x_4^2 - 123\times x_5^2 + 0.00233\times x_6^2$ (6.14)

Third trim cut

$y(C_E) = - 120-47.5\times x_1 - 0.949\times x_2 - 43\times x_3 + 1.97\times x_4 + 392\times x_5 - 0.264\times x_6 + 360.6\times x_7 + 0.559\times x_8 + 37.6\times x_1^2 + 0.0472\times x_2^2 + 79\times x_3^2 - 0.00703\times x_4^2 - 796\times x_5^2 + 0.00168\times x_6^2 - 2818\times x_7^2 - 0.044\times x_8^2$ (6.15)

C. For surface roughness

Rough cut

$y(R_a) = 2.685 + 3.20\times x_1 - 0.1068\times x_2 - 0.988\times x_1^2 + 0.00309\times x_2^2$ (6.16)

First trim cut

$y(R_a) = 1.275 + 1.202\times x_1 + 0.02183\times x_2 + 1.597\times x_3 - 0.01333\times x_4 - 0.5333\times x_1^2 - 0.001333\times x_2^2 + 9.267\times x_3^2 + 0.000027\times x_4^2$ (6.17)

Second trim cut

$y(R_a) = -4.60 + 0.501\times x_1 - 0.0681\times x_2 + 8.86\times x_3 + 0.0848\times x_4 - 21.99\times x_5 - 0.00683\times x_6 - 0.304\times x_1^2 + 0.002599\times x_2^2 - 10.67\times x_3^2 - 0.000282\times x_4^2 + 55.43\times x_5^2 + 0.000078\times x_6^2$ (6.18)

Third trim cut

$$y(R_a) = 1.73 + 0.117\times x_1 + 0.0680\times x_2 + 2.64\times x_3 - 0.0284\times x_4 - 2.77\times x_5 + 0.01680\times x_6 + 0.051\times x_7 - 0.02801\times x_8 - 0.010\times x_1^2 - 0.002629\times x_2^2 - 3.09\times x_3^2 + 0.000096\times x_4^2 + 6.13\times x_5^2 - 0.000181\times x_6^2 + 11.11\times x_7^2 + 0.001231\times x_8^2 \quad (6.19)$$

Where, x_1 & x_2 are the pulse on time (T_{ON}) and servo sensitivity (S_C) during rough cutting operation, x_3 & x_4 are the pulse on time $(T_{ON})_1$ and wire offset $(WO)_{E1}$ during first trim cutting operation, x_5 & x_6 are the pulse on time $(T_{ON})_2$ and wire offset $(WO)_{E2}$ during second trim cutting operation and x_7 & x_8 are the pulse on time $(T_{ON})_3$ and wire offset $(WO)_{E3}$ during third trim cutting operation

It is very important to check the adequacy of the developed mathematical model, because an inappropriate or fake model can lead to a wrong conclusion. By testing the developed model, one can verify whether the model is under fitted or not. For that reason, another set of confirmatory experiments have been conducted to verify the prediction accuracy of the models.

Percentage of prediction error (Shown in Eq. 6.20) based on confirmatory experiments are calculated and exhibited in Table. 6.9 and Table 6.10. It is observed that the predicted results from the mathematical model are very close to the experimental results.

$$\% \text{ prediction error} = \left\{\left|\frac{\text{Experimental value} - \text{Predicted value}}{\text{Experimental value}}\right|\right\} \times 100 \quad (6.20)$$

Table 6.9 Verification experiments for proposed models

	Process parameters								Exp. results		
	T_{ON} (µs)	S_C (-)	$(T_{ON})_1$ (µs)	$(WO)_{E1}$ (µm)	$(T_{ON})_2$ (µs)	$(WO)_{E2}$ (µm)	$(T_{ON})_3$ (µs)	$(WO)_{E3}$ (µm)	CS_E (mm/min)	C_E (µm)	R_a (µm)
	0.5	8	-	-	-	-	-	-	4.37	142.12	3.401
Rough	0.7	12	-	-	-	-	-	-	6.79	166.24	3.494
	0.9	12	-	-	-	-	-	-	7.11	168.25	3.837
	0.5	12	0.4	150	-	-	-	-	7.23	89.15	2.411
Trim-1	0.7	16	0.35	150	-	-	-	-	6.91	88.25	2.201
	0.9	16	0.4	140	-	-	-	-	7.94	90.39	2.832
	0.5	8	0.35	140	0.2	30	-	-	11.71	76.11	1.127
Trim-2	0.7	8	0.35	150	0.25	60	-	-	12.75	54.15	1.151
	0.9	12	0.35	160	0.2	45	-	-	10.97	67.94	1.214
	0.5	8	0.35	140	0.3	60	0.15	15	17.71	21.03	0.559
Trim-3	0.7	12	0.45	140	0.2	45	0.15	10	18.56	26.78	0.681
	0.9	16	0.4	140	0.2	60	0.1	15	17.58	41.82	0.596

Table 6.10 Predicted results and percentage of prediction error

	Exp. results			Predicted values			Percentage (%) prediction error		
	CS_E (mm/min)	C_E (µm)	R_a (µm)	CS_E (mm/min)	C_E (µm)	R_a (µm)	CS_E (mm/min)	C_E (µm)	R_a (µm)
	4.37	142.12	3.401	4.21	139.05	3.287	3.66	2.16	3.35
Rough	6.79	166.24	3.494	7.01	163.34	3.369	3.24	1.74	3.57
	7.11	168.25	3.837	6.87	173.45	4.012	3.37	3.09	4.56
	7.23	89.15	2.411	6.89	86.54	2.378	4.71	2.93	1.36
Trim-1	6.91	88.25	2.201	7.24	85.69	2.305	4.78	2.89	4.72
	7.94	90.39	2.832	8.32	94.05	2.725	4.79	4.05	3.77
	11.71	76.11	1.127	12.16	73.32	1.102	3.85	3.67	2.22
Trim-2	12.75	54.15	1.151	13.15	56.58	1.121	3.12	4.49	2.61
	10.97	67.94	1.214	11.34	70.57	1.258	3.38	3.87	3.62
	17.71	21.03	0.559	18.12	20.35	0.535	2.31	3.23	4.29
Trim-3	18.56	26.78	0.681	17.68	27.84	0.658	4.74	3.96	3.38
	17.58	41.82	0.596	18.22	39.98	0.612	3.64	4.41	2.64

6.3.4 Analysis and optimization of multipass WEDM

The next step after developing the mathematical model is to carry out an optimization of the process parameters using a suitable algorithm. In this case, the main objective is to maximize the effective cutting speed (CS_E), and this is the class of multi objective optimization where three major response factors are known as effective cutting speed (CS_E), corner error (C_E), and surface roughness (R_a). It is already anticipated from our previous research work (Chapter 5) that corner accuracy or surface finish decreases as the machining speed increases. Hence, it is essential to develop a technical approach to create a well-organized trade-off between response parameters. Constrained optimization technique or Pareto algorithm can be used to solve such kind of multi objective optimization problem (Deb: 2012). In this work, Pareto algorithm is used to solve the problem.

To explain the optimization process graphically, results from the algorithm are plotted in Figure 6.7 and Figure 6.8. Only a few significant values are plotted in the figures to obtain an idea of the Pareto algorithm explicitly. A total of twenty optimal solutions corresponding to the input parameters are plotted in two dimensional solution spaces. Each point in the plot represents a specific parameter setting for effective cutting speed, corner error, and surface roughness. In Pareto optimization technique, one can find multiple optimum solutions within a given solution space. In this case, the main objective is to maximize the cutting speed as

well as corner accuracy and surface finish. Here, two pairs of conflicting natures of response parameters have been chosen for optimization, e.g., CS_E vs. C_E and CS_E vs. R_a. A MATLAB programme has been used to find out the most optimal solutions from the set of all experimental data. Using this technique, two different sets of solutions are generated for the two pairs of response parameters, as shown in Figure 6.7 and Figure 6.8. The parameters CS_E vs. C_E and CS_E vs. R_a are considered along the horizontal X-axis and the vertical Y-axis, respectively. The Pareto optimal solutions have been found out. Here, the optimum Pareto results suggest that it is better than any other response at least in respect of one process criterion is taken into account. In this case, there are effective cutting speed (CS_E) or C_E or R_a. These optimum points within the solution space for corner error and surface roughness against effective cutting speed are shown in Figure 6.7 and Figure 6.8. It is evident that from the figures, corner accuracy and surface finish improve as the effective cutting speed is lower. Table 6.11 and Table 6.12 show the optimal process parameter settings and Pareto optimal results for Al 7075 alloy that can be used as guidelines for machining.

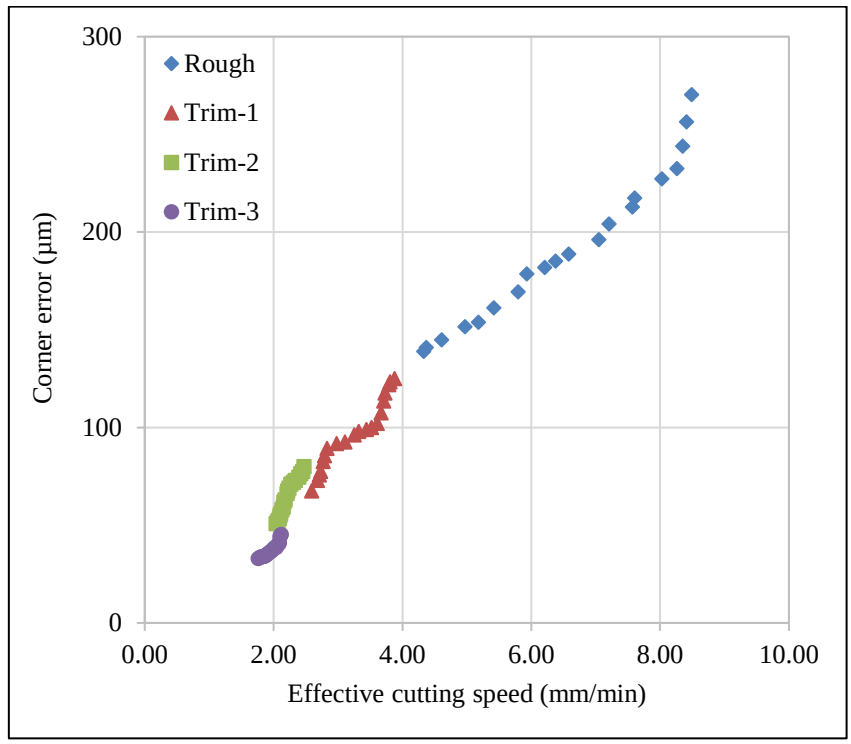

Figure 6.7 Optimal plot of effective cutting speed vs corner error

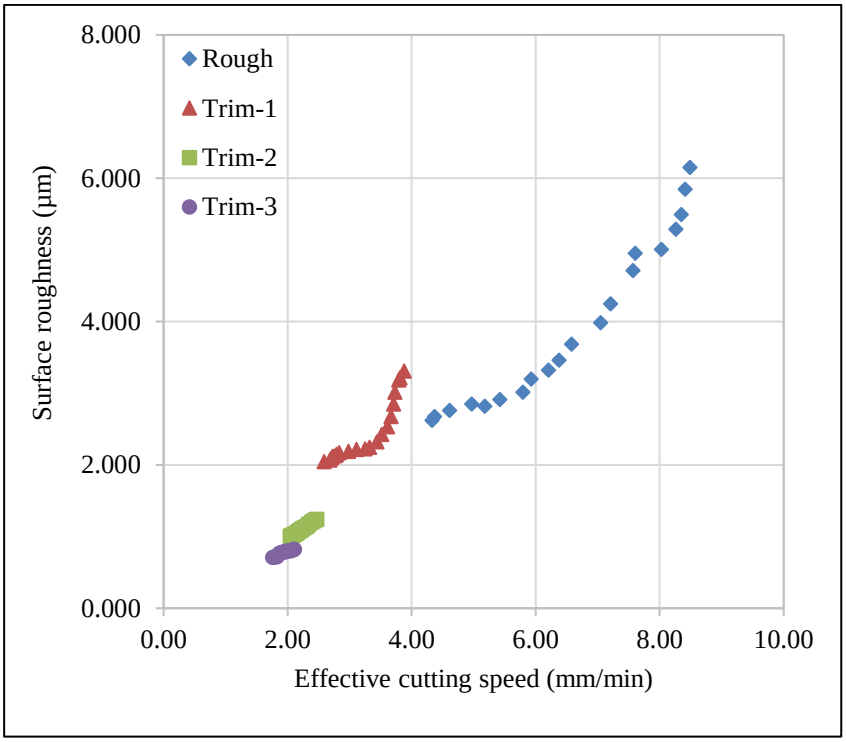

Figure 6.8 Optimal plot of effective cutting speed vs surface roughness

The all non-dominated points within solution space for corner error and surface roughness against effective cutting speed are shown in Figure 6.9 and Figure 6.10. It is observed that from the figures, corner accuracy and surface finish both are increasing as the number of passes increases. Better corner accuracy and surface finish can achieve at the end of final (third trim cut) finish cutting operation. It is observed from Figure 6.9 that if the required corner error between 138 µm to 270 µm, single pass (rough) cutting strategy gives the better results, on the other hand, if the desired corner error value between 138 µm to 73 µm then single (1^{st} trim) trimming strategy gives the superior result with respect to the effective cutting speed. Similarly, if the necessary corner error between 73 µm to 50 µm, then double (2^{nd} trim) trimming strategy gives the better results otherwise it is better strategy to select the triple (3^{rd} trim) trimming operation when the required corner error lies 50 µm to 32 µm. By analysed the optimal results, three critical corner error values i.e. 138 µm, 73 µm and 50 µm are obtained from three types of cutting condition i.e. rough & 1^{st} trim, 1^{st} trim & 2^{nd} trim, 2^{nd} trim & 3^{rd} trim. If the productivity i.e. cutting velocity is prime importance then rough cutting (single pass) strategy always gives the better result, but if the accuracy or precision becomes

more importance then multiple trim cutting (1st or 2nd or 3rd trimming) strategy should be the best choice depending upon the specific requirement.

Again, from the optimal plot of surface roughness (Shown in Figure 6.10) for all three successive trim cuts followed by rough cut, it is observed that the better surface finish can be achieved at the end of third trim cutting operation. From Figure 6.10, it is observed that if the required surface roughness value between 2.618 µm to 6.150 µm, single (rough) pass cutting strategy gives the better result otherwise, if the required surface roughness value less than 2.618 µm and up to 2.042 µm, then single (1st trimming) trim cutting strategy is preferable with respect to the effective cutting speed. Likewise, if the required surface finish is less than 2.042 µm and up to 1.086 µm, then double (2nd trimming) trim cutting strategy gives better results. Now, if the desired surface roughness value between 1.086 µm to 0.592 µm then triple (3rd trimming) trim cutting strategy is a best choice. Thus, here three different critical surface roughness values i.e. 2.618 µm, 2.042 µm and 1.086 µm are obtained from three pair of cutting condition (i.e. rough & 1st trim, 1st trim & 2nd trim, 2nd trim & 3rd trim).

Now for example, if the required corner error and surface roughness values below a certain critical limit i.e. 138 µm and 2.618 µm respectively, then single trim cutting strategy should be used. If the C_E and R_a values are less than or equals to 73 µm and 2.042 µm then double trim cutting strategy should be a better choice for improved production. In both cases, effective cutting speeds are found to be 3.61 mm/min and 2.59 mm/min respectively. It is found that the effective cutting speed decreases as the number of passes increases. When accuracy and surface finish are more important than trim cutting strategy is a better choice in WEDM. It is anticipated that from the combined optimal results (rough & trim), corner error and surface roughness values are always high in single pass (rough) cutting. Both are decreases as the number of pass increases. Overall combined Pareto optimal solutions of single pass and multipass cutting operations are given in Table 6.12 and the optimal parameter combinations are given in Table 6.11. These combined tables (Table 6.11 & Table 6.12) with all optimum parametric combinations is extremely useful for selecting the economic machining strategy for efficient machining of Al 7075.

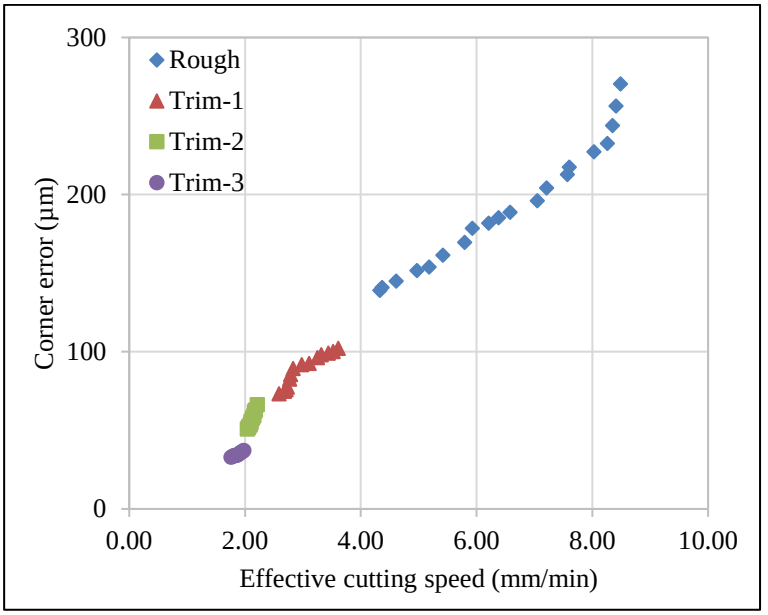

Figure 6.9 Variation of effective cutting speed with corner error in multipass cutting operations.

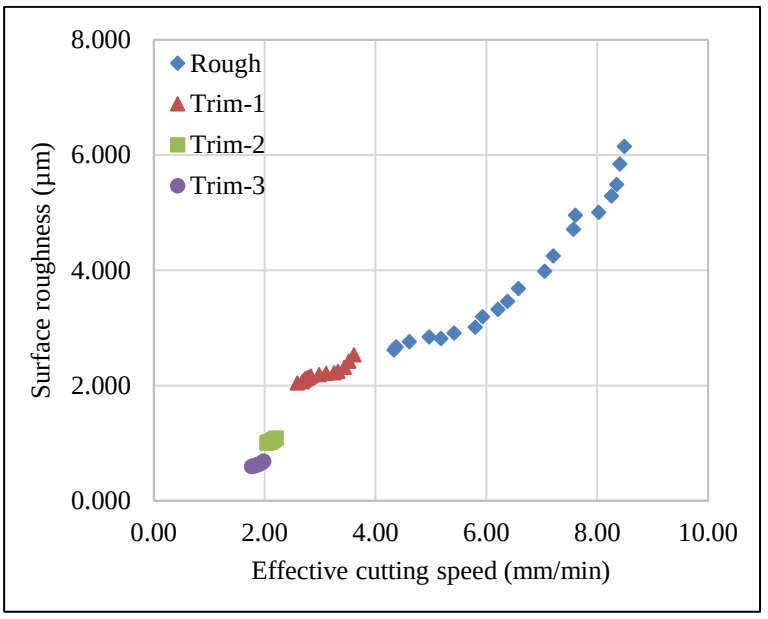

Figure 6.10 Variation of effective cutting speed with surface roughness in multipass cutting operations.

Table 6.11 Optimal parameter combination for rough and trim cutting

	Rough		Trim-1		Trim-2		Trim-3	
Sl. No.	T_{ON}: µs	S_C: -	$(T_{on})_1$: µs	$(WO)_{E1}$: µm	$(T_{on})_2$: µs	$(WO)_{E2}$: µm	$(T_{on})_3$: µs	$(WO)_{E3}$: µm
1	0.5	8	0.35	140	0.25	40	0.1	10
2	0.5	8	0.35	145	0.25	35	0.1	10
3	0.55	9	0.35	150	0.25	30	0.05	10
4	0.6	9	0.35	155	0.25	35	0.05	10
5	0.65	9	0.35	160	0.2	40	0.15	5
6	0.75	8	0.35	140	0.2	45	0.1	5
7	0.8	10	0.35	145	0.2	50	0.05	5
8	0.8	11	0.4	150	0.2	55	0.05	15
9	0.7	12	0.4	155	0.2	60	0.15	15
10	0.75	10	0.4	160	0.2	30	0.15	15
11	0.85	8	0.4	140	0.3	35	0.15	15
12	0.9	8	0.4	145	0.3	40	0.05	15
13	0.9	10	0.4	150	0.3	45	0.05	15
14	0.85	9	0.45	155	0.3	50	0.05	10
15	0.85	10	0.45	160	0.3	55	0.15	10
16	0.75	12	0.45	145	0.3	60	0.1	10
17	0.85	10	0.45	145	0.3	45	0.1	15
18	0.85	11	0.45	150	0.3	50	0.15	15
19	0.9	11	0.45	160	0.3	55	0.15	15
20	0.9	12	0.45	160	0.3	60	0.15	15

Table 6.12 Pareto optimal results for Al 7075

Sl. No.	Effective cutting speed (CS_E: mm/min)				Corner error (C_E: µm)				Surface roughness (R_a: µm)			
	Rough	Trim-1	Trim-2	Trim-3	Rough	Trim-1	Trim-2	Trim-3	Rough	Trim-1	Trim-2	Trim-3
1	4.33	2.59	2.04	1.76	138.89	67.57	50.76	32.12	2.618	2.042	1.002	0.708
2	4.37	2.68	2.06	1.79	140.85	72.99	51.55	33.21	2.673	2.066	1.009	0.714
3	4.61	2.71	2.07	1.81	144.93	75.76	52.36	33.51	2.759	2.097	1.015	0.717
4	4.97	2.73	2.09	1.83	151.52	77.52	53.48	33.78	2.847	2.118	1.018	0.719
5	5.18	2.77	2.1	1.86	153.85	82.64	54.95	34.13	2.816	2.129	1.026	0.761
6	5.42	2.79	2.11	1.87	161.29	85.47	55.87	34.56	2.911	2.147	1.030	0.768
7	5.80	2.83	2.13	1.89	169.49	89.29	57.80	34.87	3.011	2.169	1.040	0.771
8	5.93	2.98	2.15	1.91	178.57	91.74	59.17	35.46	3.197	2.187	1.048	0.779
9	6.21	3.11	2.16	1.93	181.82	92.59	61.73	35.74	3.321	2.213	1.061	0.782
10	6.38	3.25	2.18	1.95	185.19	96.15	62.89	36.36	3.461	2.223	1.074	0.786

Sl. No.	Effective cutting speed (CS_E: mm/min)				Corner error (C_E: µm)				Surface roughness (R_a: µm)			
	Rough	Trim-1	Trim-2	Trim-3	Rough	Trim-1	Trim-2	Trim-3	Rough	Trim-1	Trim-2	Trim-3
11	6.58	3.32	2.21	1.97	188.68	98.04	66.23	36.91	3.683	2.246	1.086	0.791
12	7.05	3.44	2.22	1.98	196.08	99.01	67.57	37.19	3.981	2.319	1.096	0.797
13	7.21	3.52	2.24	2.01	204.08	100.00	68.97	38.31	4.248	2.424	1.107	0.798
14	7.57	3.61	2.27	2.04	212.77	102.04	70.92	38.94	4.710	2.531	1.122	0.801
15	7.61	3.67	2.31	2.06	217.39	107.53	71.94	39.54	4.953	2.673	1.144	0.803
16	8.03	3.71	2.34	2.08	230.54	113.64	72.99	40.25	5.008	2.847	1.174	0.812
17	8.26	3.73	2.39	2.09	236.25	117.65	74.63	41.29	5.288	3.011	1.201	0.817
18	8.35	3.79	2.42	2.10	243.25	121.95	76.34	42.64	5.491	3.183	1.217	0.819
19	8.41	3.81	2.45	2.11	245.12	123.46	77.52	43.68	5.845	3.213	1.231	0.822
20	8.49	3.88	2.47	2.12	246.32	125	80.00	44.87	6.150	3.310	1.241	0.825

6.4 Improvement of corner accuracy and surface finish for multipass cutting in WEDM

For analysis, average corner error and surface roughness values are considered for the improvement of corner accuracy and surface finish. Average values of responses are calculated from the Pareto optimal chart given in Table 6.12. In order to compare the cutting speed in different cutting conditions (i.e., trim cut followed by rough cut), the average value of "effective cutting speed" is considered. Average effective cutting speed for rough and trim cutting conditions are 6.54 mm/min, 3.02 mm/min, 2.12 mm/min and 1.88 mm/min respectively. It has been observed that from Figure 6.11, effective cutting speed significantly decreases as the number of passes increases (i.e., total length of cut increases). On the other hand, average corner error and surface roughness decrease after each pass (shown in Figure 6.12 and Figure 6.13). From Figure 6.12, it is observed that the average corner error in rough cutting condition is 192.79 µm, whereas in three different trim cuts it becomes 88.45 µm, 56.98 µm, and 34.94 µm. The improvement of corner accuracy after the first trim cut is 54%. This is happening due to aggressive wire offset and moderate pulse parameter setting during the first trim cutting operation. Corner accuracy after the second trim cut improves by 36% compared to the first trim cut and after final finish cut, improves by 39% compared to the second trim cut. Figure 6.13 shows the average surface roughness in different cutting conditions. The average surface roughness values for rough and trim cuts are 3.948 µm, 2.207 µm, 1.037 µm, and 0.634 µm. Surface finish improves by 44% after first trim cut in respect of rough cut, 53% after second trim cut in respect of first trim cut and 39% after the final finish cut in respect of second trim cut. Surface finish improvement after first trim cut is

less, but the rate of improvement after the second and third trim cuts is more. This is happening due to the fact that the pulse parameter setting during first trim cutting is moderate, but in the case of second and third cuts, it is low. Overall improvement of corner accuracy and surface finish after three successive three trim cuts with respect to the rough cut are 82% and 84%. Corner error measurement in different cutting conditions i.e. rough and three trim cuts are shown in Figure 6.14 - Figure 6.17.

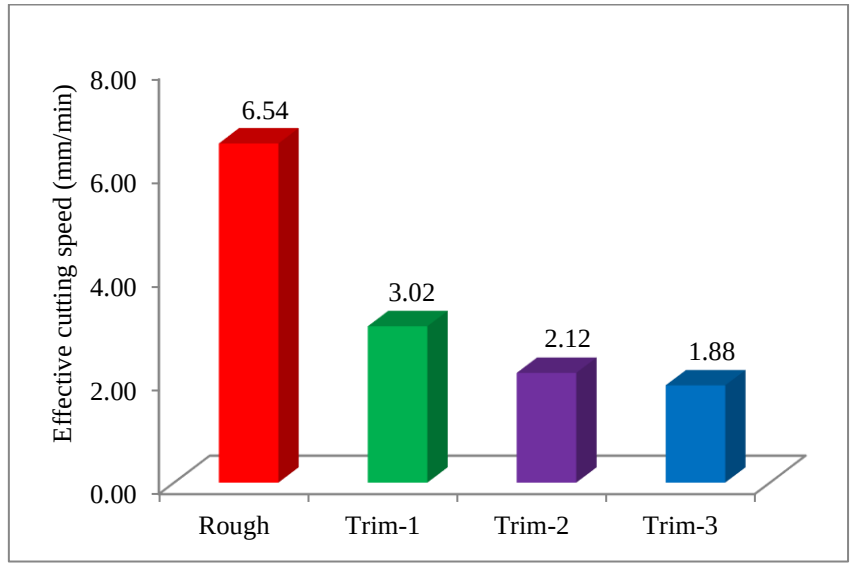

Figure 6.11 Effective cutting speed in different cutting condition

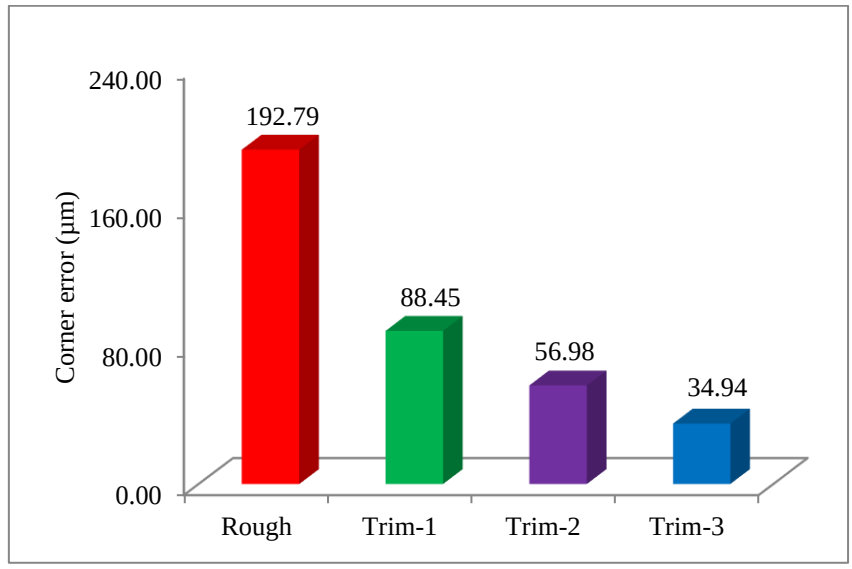

Figure 6.12 Corner error in different cutting condition

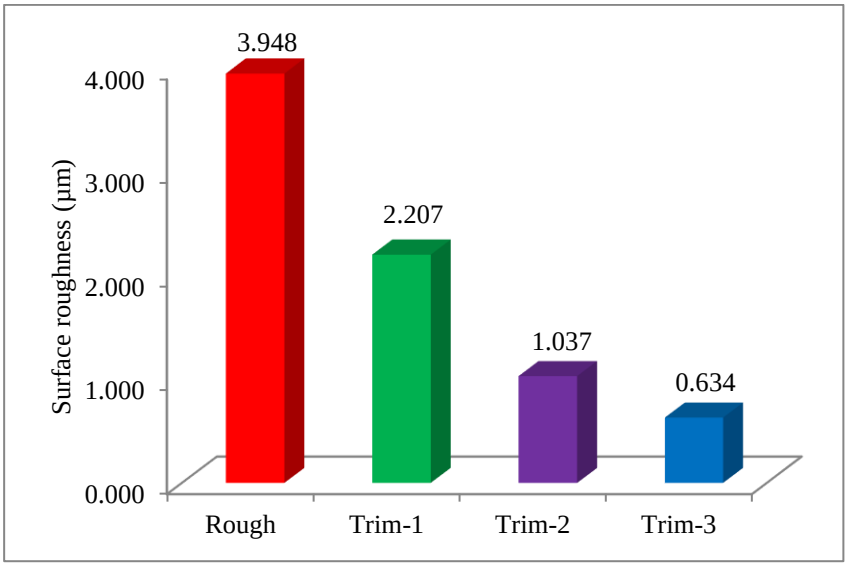

Figure 6.13 Surface roughness in different cutting condition

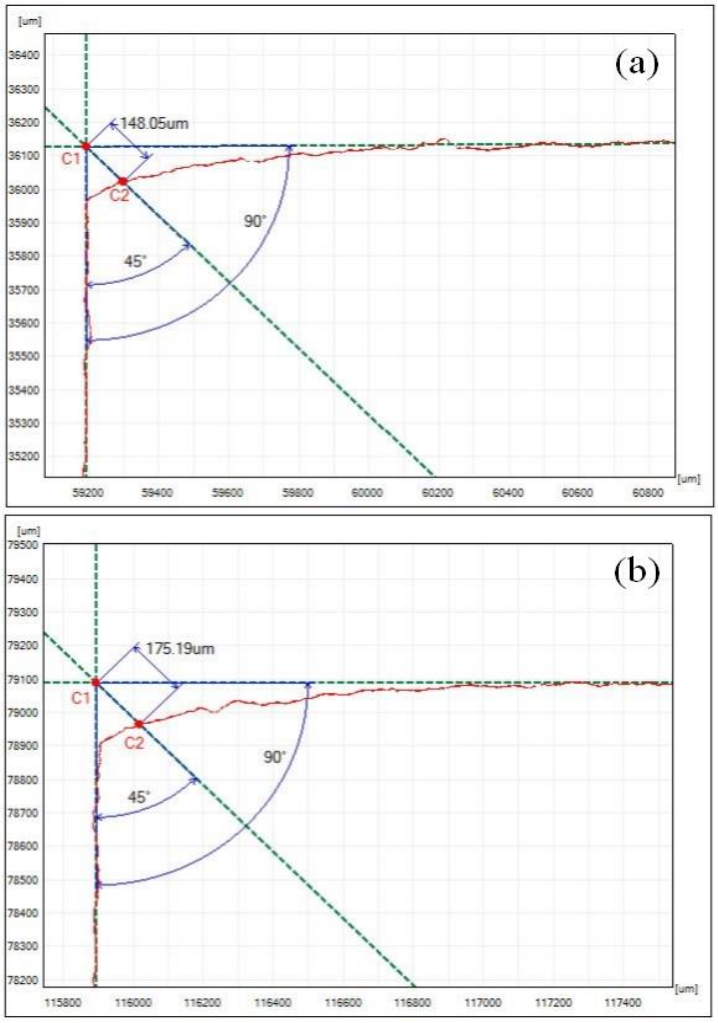

Figure 6.14 Measurement of corner error in rough cut profile (a) T_{ON} = 0.5 µs, (WO) = 0 (b) T_{ON} = 0.9 µs, (WO) = 0.

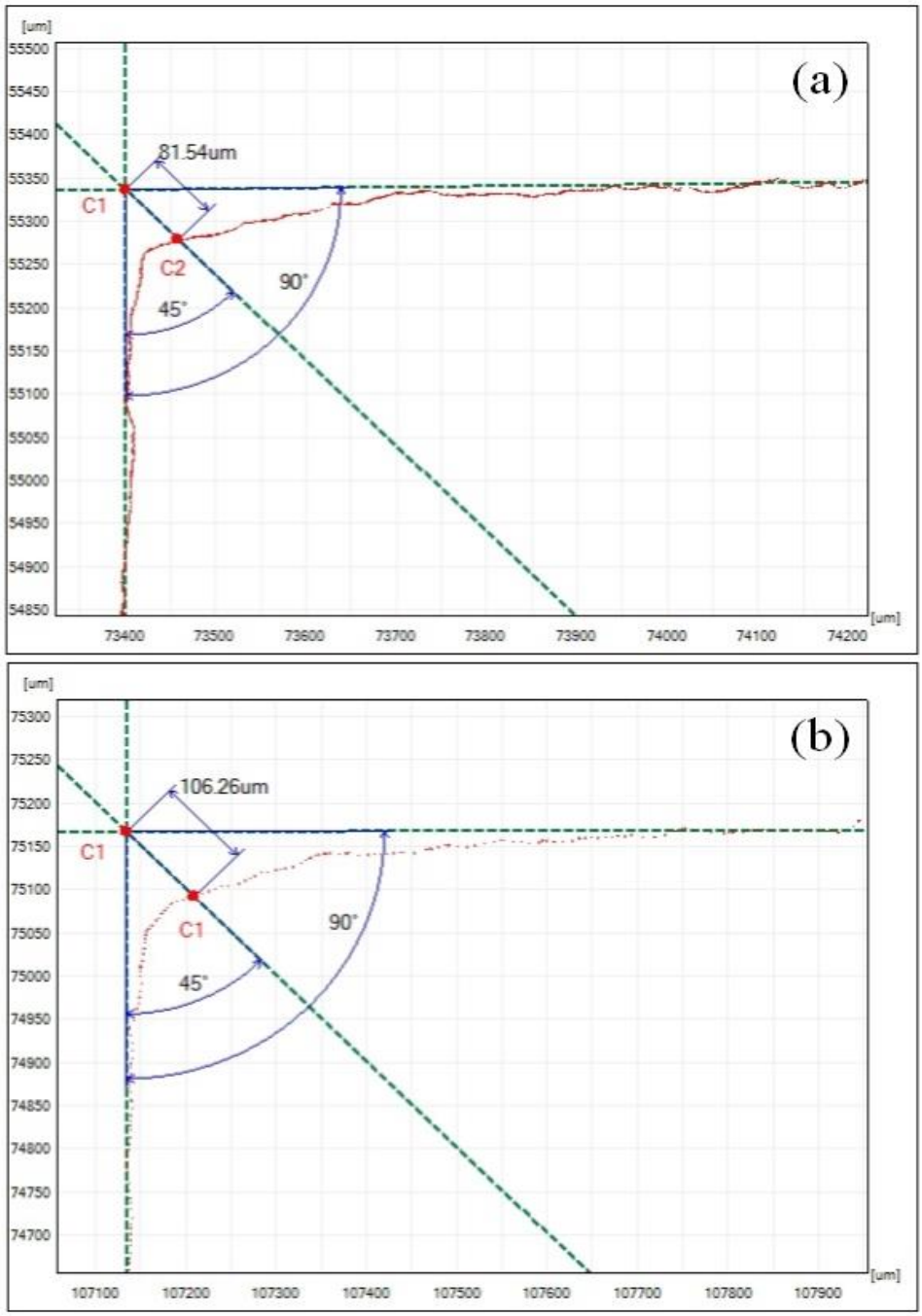

Figure 6.15 Measurement of corner error in 1st trim cut profile (a) $(T_{ON})_1$ = 0.35 µs, $(WO)_{E1}$ = 160 µm (b) $(T_{ON})_1$ = 0.45 µs, $(WO)_{E1}$ = 140 µm.

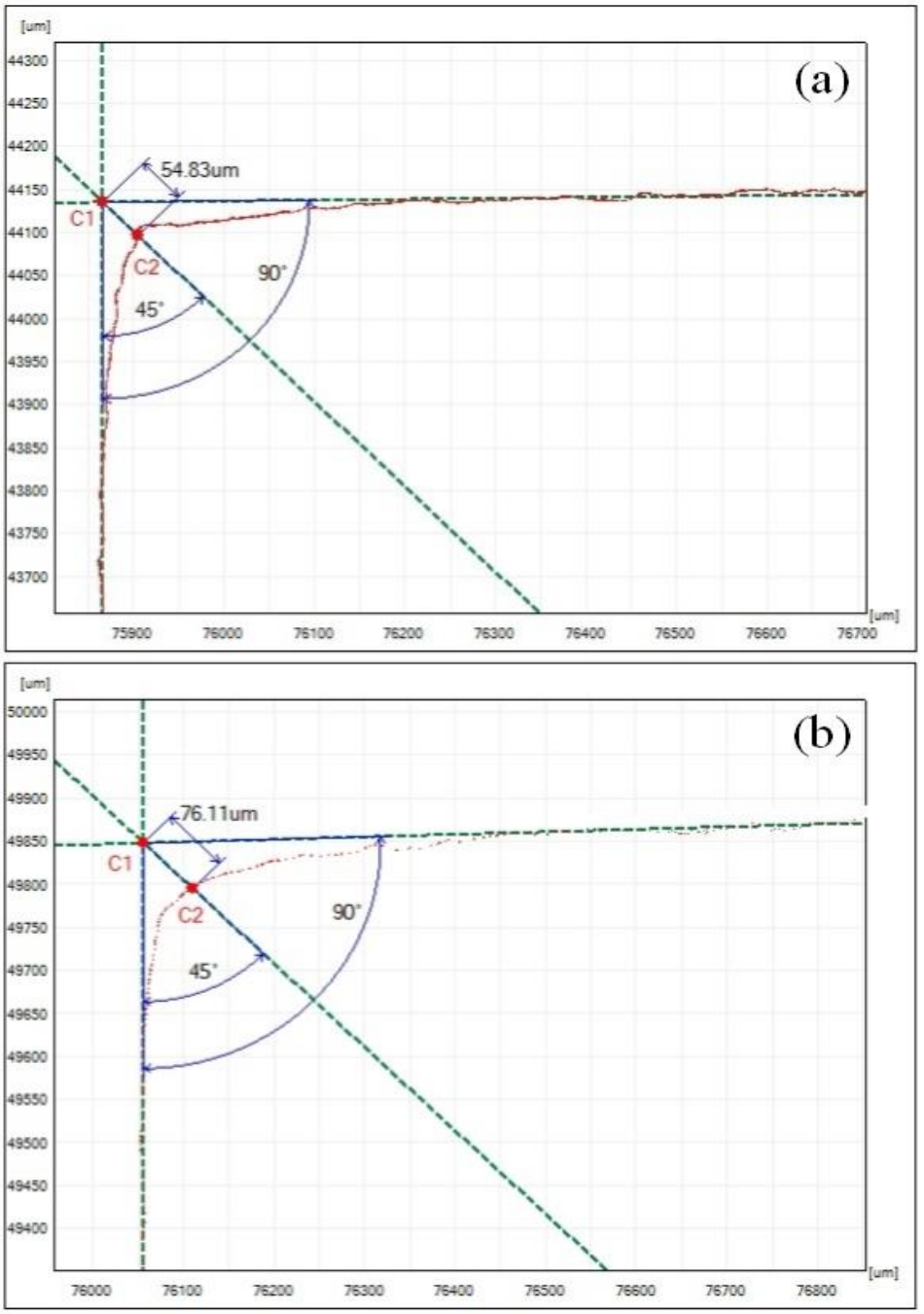

Figure 6.16 Measurement of corner error in 2nd trim cut profile (a) $(T_{ON})_2$ = 0.2 µs, $(WO)_{E2}$ = 60 µm (b) $(T_{ON})_2$ = 0.3 µs, $(WO)_{E2}$ = 30 µm.

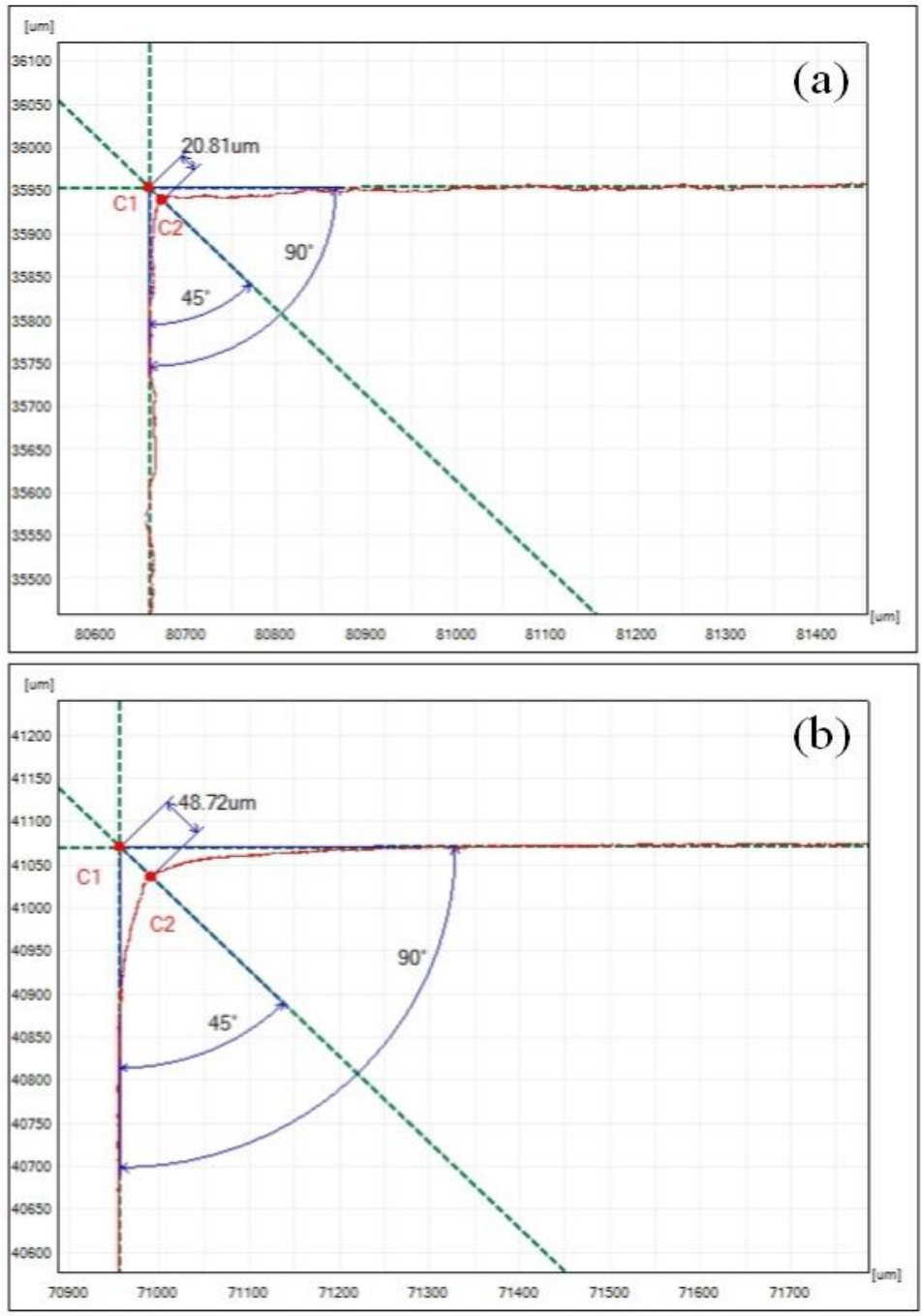

Figure 6.17 Measurement of corner error in 3rd trim cut profile (a) $(T_{ON})_3$ = 0.05 µs, $(WO)_{E3}$ = 15 µm (b) $(T_{ON})_3$ = 0.15 µs, $(WO)_{E3}$ = 5 µm.

6.5 Analysis of surface features produced by single pass and multipass cutting operation

Machining of Al 7075 using WEDM has not been clearly investigated so far. Analysis and investigation of surface texture after machining of this alloy is not available in the past literature. It is therefore very essential to create a relationship between the surface roughness under rough and trim cutting conditions. Improvement of surface finish when the trim or

finish cutting operation is imposed over the rough cut surface. The machining parameters setting in single pass cutting are incorporated into three successive multipass cutting during the experimental run.

6.5.1 SEM analysis

SEM image analysis has been conducted on the specimen surface. A Zeiss scanning electron microscope is utilised to inspect the characteristics of the machined surface. SEM micrographs of rough and trim cut surfaces are shown in Figure 6.18 - Figure 6.21. A series of sample preparations have been carried out before capturing the SEM image. Initially, the specimen is dehydrated by incubation in a series of ethanol or acetone solutions. Solvent concentration (Hexa-methyl-disilazane) is gradually increased so that the moisture or vaporised water particles are gently removed without specimen shrinkage. After drying process, specimens are placed in the SEM chamber and then a vacuum is created to capture images. The SEM micrographs are captured at 1000X magnification power.

SEM analysis has been carried out on the Al 7075 rough cut surface to inspect the topography of the machined surface. A photographic view of the work surface machining at T_{ON} = 0.9 µs and S_C = 16 parameter settings is shown in Figure 6.18. The rough cut machined surface is subjected to different surface irregularities such as craters, micro voids, recast materials, spalling, etc. The formation of such irregularities on the job surface is a result of discharge action, electrode material and type of dielectric used. WEDM can reach temperatures ranging from 10000°C - 12000°C. At this high temperature, several types of metallurgical changes occurred on the surface. The job surface rapidly melted as the temperature raised and re-solidified due to the cooling action by the dielectric liquid. At this high temperature, a huge amount of thermal stress arises in the melting zone and successive solidification causes intense metallurgical damage in the machining area. In a particular area, certain grain boundary flaws and cracks are visible, which are common in thermal machining. Fatigue strength of the machining product is often drastically reduced. From Figure 6.18, it has been observed that large craters and re-solidified materials are present in the machining zone. As the pulse on time increases, the discharge power per pulse also increases, which enhance the material removal rate and cutting speed. As the removal of material increases, crater volume per unit area also increases. As a result, wide craters and lumps of re-solidified or recast materials are formed in the machining zone. Apart from that, micro voids and spalls are also visible. This is happening due to the bubble formation and re-hardening of molten metals in the machining zone.

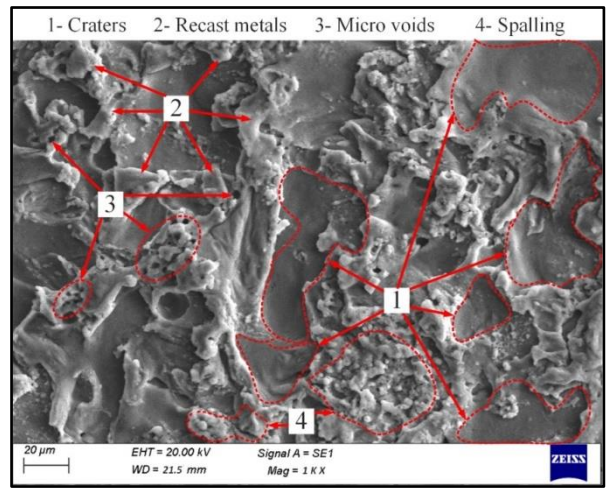

Figure 6.18 SEM image of rough cut surface.

A SEM image of the first trim cut surface is shown in Figure 6.19. After completion of the rough cutting operation, the electrode is traced back along the same path with a certain amount of wire offset. Three different sets of wire offsets, such as 140 µm, 150 µm, and 160 µm, are considered during the first trim cutting operation. These wire offsets are not only provided to eliminate the dimensional error but also to remove the undulations present in the rough cut surface. The machined surface's microstructure reveals a noticeable reduction in crater size. It is also observed that the melted and re-deposited materials are significantly reduced. Naturally, in trim cutting operations, pulse power parameter settings must be on the lower side to remove the least amount of material. As the machining is carried out in less aggressive parameter settings, presence of craters, re-melted deposited materials and micro voids are observed, but the dimensions of these irregularities are small, as shown in Figure 6.19. Due to these low parameter settings, discharge power per spark is less and, as a result, the amount of material removed per spark is also less.

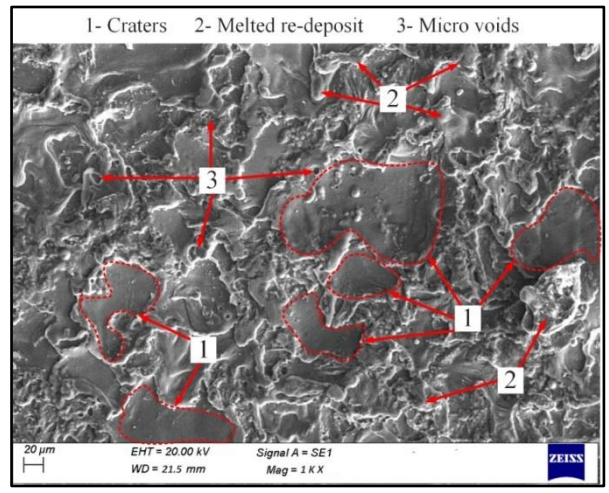

Figure 6.19 SEM image of 1st trim cut surface

After the second trim cutting operation, it has been observed that the machined surface is full of small hillocks, small diameter craters, and porosity. During second trim cutting, pulse on time is taken as 0.20 µs, 0.25 µs, and 0.30 µs with the wire offset of 30 µm, 45 µm, and 60 µm. The lower pulse parameter setting gives small discharge power during sparking, which decreases the material removal rate and enhances the surface quality and corner accuracy. Surface irregularities after the first trim cut are partially removed by the second trim cutting. A micrograph of the second trim cut surface is shown in Figure 6.20. It has been observed that the recast material is uniformly distributed throughout the machined surface. These re-solidified materials form small hillocks like structures and cause porosity by bubble formation while machining.

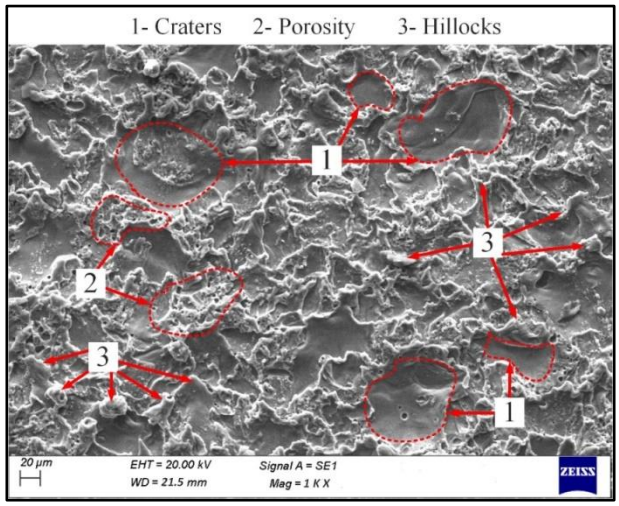

Figure 6.20 SEM image of 2nd trim cut surface.

A SEM image of the final (third) trim cut surface is shown in Figure 6.21. The presence of small debris is visible on the machined surface in the form of white spots, and it is evident that the surface is full of recast aluminium material. In addition, the existence of multiple scratches, small diameter craters and micro pores are found along the surface. This may be due to the repeating wire travel through the machining area. However, it is interesting to see that there are no such cracks visible on the workpiece as the aluminium is a soft and malleable material. The finish trim cutting operation is carried out at a low pulse parameter setting as the prime objective is to minimize the dimensional error and surface roughness as much as possible. Values of the pulse on time are considered as 0.05 µs, 0.10 µs and 0.15 µs, whereas another input parameter (wire offset) is taken as 5 µm, 10 µm and 15 µm. This pulse parameter setting provides small discharge power while machining and as a result, material removal rate decreases but surface quality improves considerably.

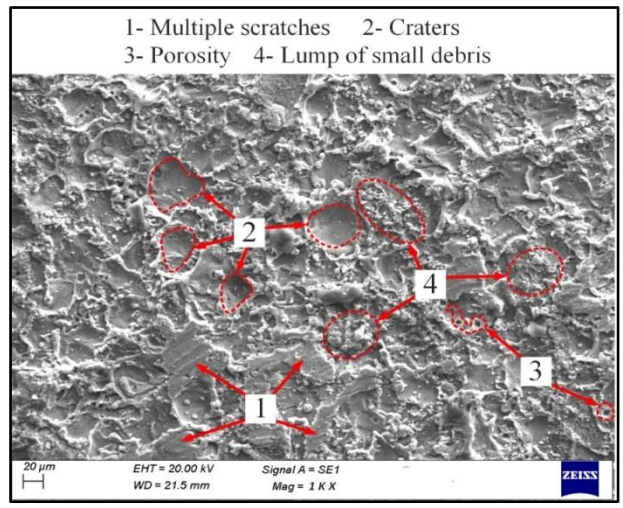

Figure 6.21 SEM image of 3rd trim cut surface.

6.5.2 CCI analysis

The 3D image of the rough cut surface captured by the CCI microscope is shown in Figure 6.22. The CCI image demonstrates the formation of wide discharge craters, deep holes, nuggets, straits, and micro-globules present on the machined surface. During rough cutting operations, pulse parameter settings are always on the higher side as productivity is of prime importance. Due to these aggressive pulse parameter settings, discharge power in each pulse is also high, which leads to more melting of materials and increase the formation of molten metal droplets, wide craters, and deep holes.

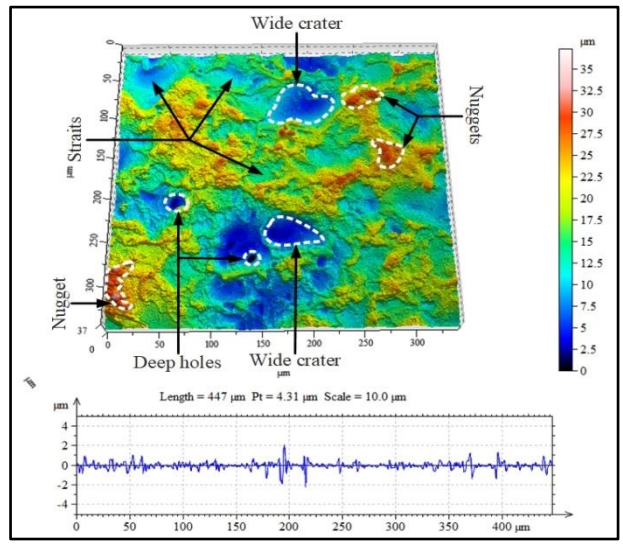

Figure 6.22 CCI image of rough cut surface.

Figure 6.23 shows the 3D topography of the first trim cut surface. There is no significant virtual difference in the 3D stereogram of the rough and first trim cut surface. The wide

craters and deep holes (gas holes) on the surface are typical structures developed due to the melting, recasting, and gas generation while machining.

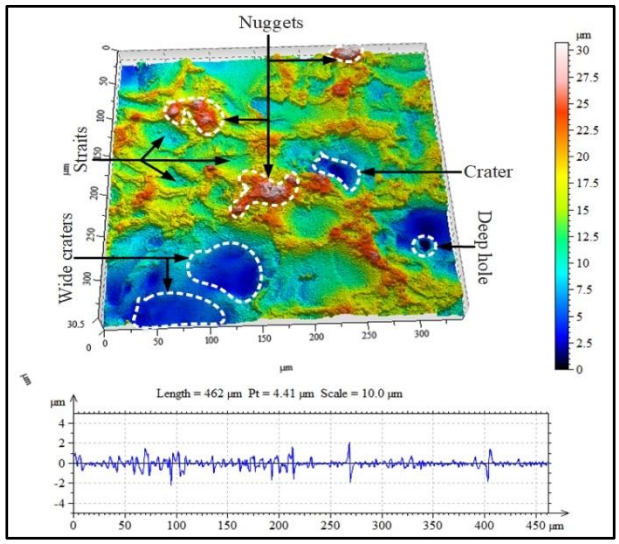

Figure 6.23 CCI image of 1st trim cut surface.

Some interesting observations have been made from the 3D stereogram image of the second trim cut surface (Shown in Figure 6.24). Different surface irregularities like deep craters, nuggets, and straits are present on the machined surface. Energy per pulse is low during the second trim cutting operation. That's why wide craters and straits are not found on the surface. Only a few deep craters are observed on the machined surface. This is happening due to the fact that pulse parameter and wire offset values are significantly low during the second trim cutting operation.

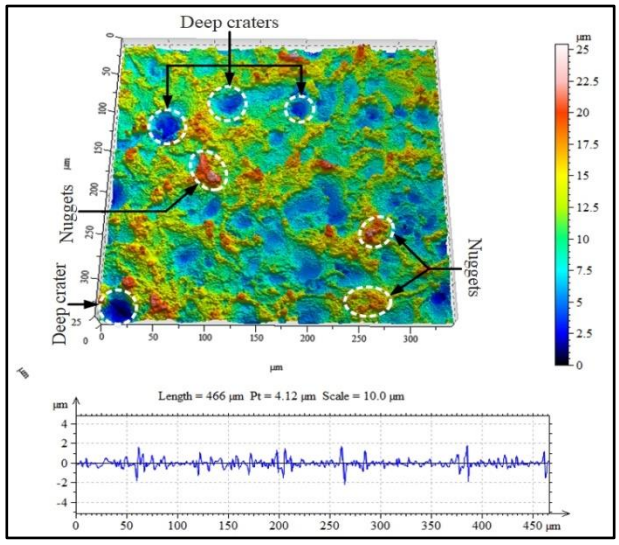

Figure 6.24 CCI image of 2nd trim cut surface.

The micro voids, or deep holes, are formed by the electrical discharge with a low intensity of energy. The nuggets or nodules are uniformly distributed in the machining zone, which is formed due to the re-solidification of molten metals. The droplet like shape of the nuggets indicates that the surface energy of the nodules is minimized during solidification of metal. Pulse parameter setting and wire offset value during final finish cutting are very low; T_{ON} varies from 0.05-0.15 µs and $(WO)_{E3}$ varies from 5-15 µm. As the pulse parameter setting is on the lower side, the energy intensity in each discharge is also low, and hence rapid melting of huge amounts of material isn't occur. For that reason, wide craters and lumps of big debris are not found in the machining area; only small voids and nuggets are noted. Figure 6.25 shows a representative CCI plot of the final trim cut surface.

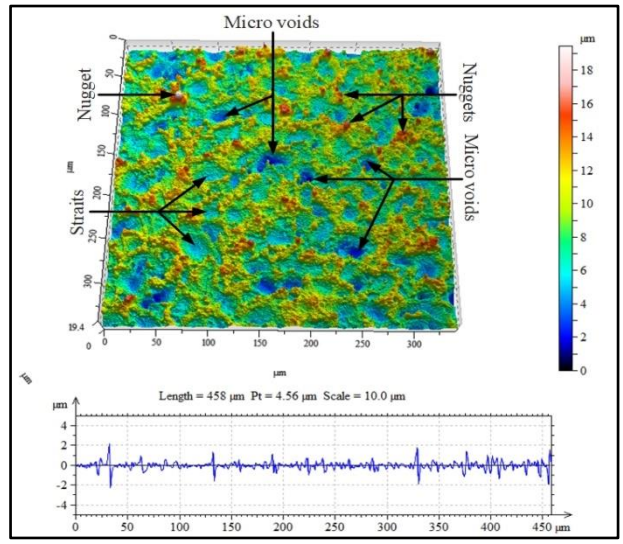

Figure 6.25 CCI image of 3rd trim cut surface.

6.5.3 EDS analysis

An energy dispersive spectroscopy (EDS) related to the SEM has been performed to investigate the elemental composition of the machined surface. During machining, elements from wire electrode and dielectric liquid are diffused into the workpiece. Figure 6.26 and Figure 6.27 represent the EDS pattern of the main (rough) cut and first trim cut surface of Al 7075 workpiece. It has been observed that foreign components like carbon (C) and oxygen (O) are highly deposited on the work surface after machining. In this research, commercial wires (electrode) are used for machining. This wire electrode is coated with tungsten carbide material for better performance. Carbon components are probably diffused from the coating of the electrode. Another two foreign elements, copper (Cu) and sodium (Na), also decompose on the surface and are diffused from the core of the electrode and dielectric fluid.

Deposition of such foreign elements on the surface takes place due to the reaction between the dielectric liquid and the workpiece while machining. As the concentration of salt (NaCl) increases in the dielectric to maintain the conductivity, the dissolved salt becomes more stable and can burn in the dielectric liquid. This burning process occurs at a high temperature in the inter electrode gap. At high temperatures, NaCl reacts with water and forms different kinds of sodium and chlorine oxides. Similarly, at this high temperature, copper melts and evaporates from the wire, reacts with molten metal released from the workpiece, and deposits on the machined surface.

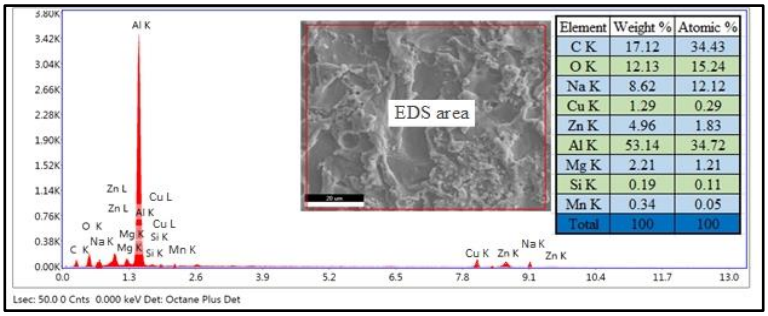

Element	Weight %	Atomic %
C K	17.12	34.43
O K	12.13	15.24
Na K	8.62	12.12
Cu K	1.29	0.29
Zn K	4.96	1.83
Al K	53.14	34.72
Mg K	2.21	1.21
Si K	0.19	0.11
Mn K	0.34	0.05
Total	100	100

Figure 6.26 EDS pattern and elemental composition of rough cut surface.

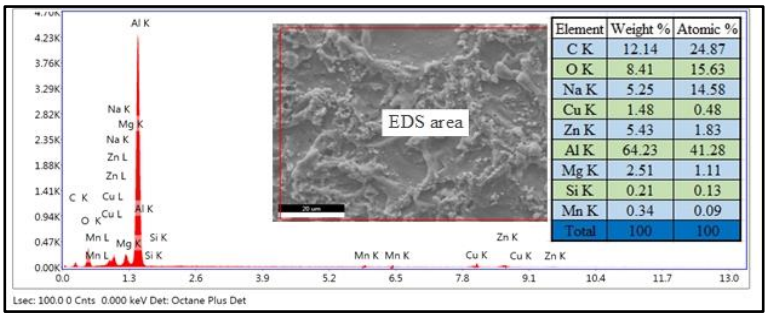

Element	Weight %	Atomic %
C K	12.14	24.87
O K	8.41	15.63
Na K	5.25	14.58
Cu K	1.48	0.48
Zn K	5.43	1.83
Al K	64.23	41.28
Mg K	2.51	1.11
Si K	0.21	0.13
Mn K	0.34	0.09
Total	100	100

Figure 6.27 EDS pattern and elemental composition of 1st trim cut surface.

The presence of aluminium (Al) is detected on the second and third trim cut surfaces, which are more than the rough and first trim cut surfaces. This is happening due to less diffusion of material from the workpiece as the discharge power is low during the second and third trim cutting operations. The amount of foreign elements like C, O, and Na presence on the second and third trim cut surfaces are less. The main reason is that power used in soft trimming (low wire off set value) operation is very low. Although the workpiece material is melted and incompletely reacted with dissolved sodium, a little amount is deposited on the work surface. On the other hand, the presences of metallic components are increased as the melting and vaporisation temperatures of these materials are high. The EDS spectrum and elemental

composition percentage of the second and third rim cut surfaces are shown in Figures 6.28 and Figure 6.29.

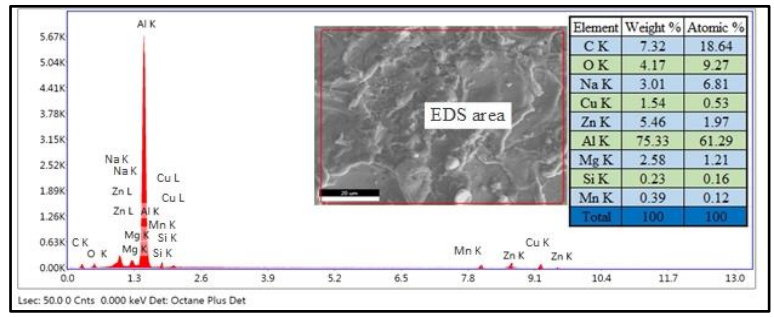

Element	Weight %	Atomic %
C K	7.32	18.64
O K	4.17	9.27
Na K	3.01	6.81
Cu K	1.54	0.53
Zn K	5.46	1.97
Al K	75.33	61.29
Mg K	2.58	1.21
Si K	0.23	0.16
Mn K	0.39	0.12
Total	100	100

Figure 6.28 EDS pattern and elemental composition of 2nd trim cut surface.

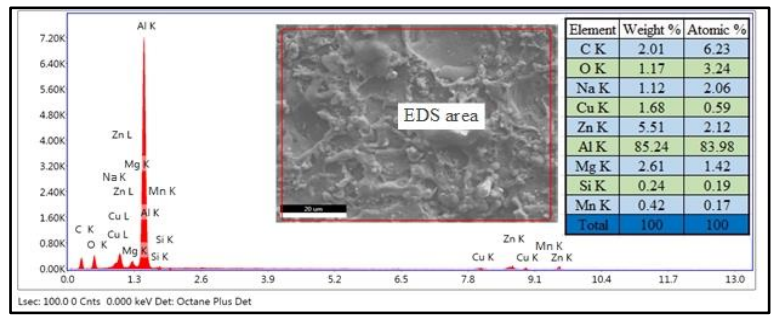

Element	Weight %	Atomic %
C K	2.01	6.23
O K	1.17	3.24
Na K	1.12	2.06
Cu K	1.68	0.59
Zn K	5.51	2.12
Al K	85.24	83.98
Mg K	2.61	1.42
Si K	0.24	0.19
Mn K	0.42	0.17
Total	100	100

Figure 6.29 EDS pattern and elemental composition of 3rd rim cut surface.

6.5 Conclusions from the set of experiments

Strategies for rough and trim cutting operations have been developed in the present modular set of experiments. The improvements of corner accuracy and surface finish through trim cutting operations have been studied on Al 7075. It is noted that the number of passes improves the corner accuracy and surface finish. It is also observed that the accuracy and finish are not only dependent on the number of passes but also considerably influenced by the trim cutting process parameters. From the experimental results of rough cutting operation, it is observed that corner error, surface roughness, and effective cutting speed are strongly influenced by pulse on time (T_{ON}) and servo sensitivity (S_c). Responses are increasing as the pulse on time and servo sensitivity increases. However, in case of a single trimming operation, trim cut parameters such as pulse on time $(T_{ON})_1$ and wire offset $(WO)_{E1}$ are more effective in determining the corner error, surface roughness and effective cutting speed.

Corner error and effective cutting speed are significantly influenced by $(T_{ON})_1$ and $(WO)_{E1}$, whereas surface roughness value impacts by $(T_{ON})_1$ only. With an increase in pulse on time, cutting speed increases, but corner accuracy and surface finish deteriorate. The same trend is observed in the second trimming operation also. In second trim cutting operation, effective cutting speed increases as the pulse on time for the second trim cut i.e. $(T_{ON})_2$ increases. On the other hand, corner accuracy and surface finish are improved as the wire offset value for second trim cut $(WO)_{E2}$ increases. It is also observed that for surface roughness, increasing the wire offset value gives a better trimming action. In all cases, the third trim cutting pulse on time $(T_{ON})_3$ and wire offset $(WO)_{E3}$ are very sensitive to determine corner error and surface roughness along with effective cutting speed. It is concluded that the trim cutting process parameters are more significant to determine response factors like corner accuracy and surface finish.

Thus, it is impossible to maximize the effective cutting speed, corner accuracy and surface finish simultaneously. To handle such intricacy, Pareto optimization technique is employed for rough and three successive trim cutting operations. After analysing the experimental results, two different Pareto optimal solutions sets are separately calculated for corner error and surface roughness. Three critical corner error values such as 138 µm, 73 µm, and 50 µm are obtained from the three types of cutting operation (i.e. rough & 1^{st} trim, 1^{st} trim & 2^{nd} trim, 2^{nd} trim & 3^{rd} trim). Similarly, three different critical surface roughness values such as 2.618 µm, 2.042 µm and 1.086 µm are also obtained from the experimental study. It is observed that if the required corner error is 138 µm - 270 µm, single pass (rough) cutting strategy gives the better results, on the other hand, if the desired corner error value 138 µm - 73 µm then single trimming operation always gives the superior result. Similarly, if the necessary corner error 73 µm - 50 µm, then double trimming strategy gives the better results otherwise it is better strategy to select the triple trimming operation when the required corner error lies 50 µm - 32 µm. On the other hand, if the required surface roughness value 2.618 µm - 6.150 µm, single (rough) pass cutting strategy gives the better result otherwise, if the required surface roughness value less than 2.042 µm - 2.618 µm, then single trim cutting strategy is preferable with respect to the effective cutting speed. Likewise, if the required

surface finish is 1.086 µm - 2.042 µm, then double trimming strategy gives better results. Now, if the desired surface roughness value 0.592 µm - 1.086 µm then triples trim cutting strategy is a best choice. It is found that when required corner error is 152 µm then rough cutting operation give the better result with an effective cutting speed of 4.97 mm/min. Now, if the required corner error and surface roughness values are 152 µm and 2.2 µm then single trimming operation gives the best result in a given effective cutting speed of 3.11 mm/min. It is recommended to select the lower cutting speed to get the better surface finish with respect to a given corner error. Generally, in the trim cutting operation, corner accuracy and surface finish are prime importance and it is clearly found that triple trimming strategy yields the best results. It is found that after the three successive trim cutting, corner accuracy improved by 82% whereas surface finish improved by 84%, which are satisfactory.

Chapter-7

Summary and General Conclusions

7.1 Summary and general conclusions

Present research has been carried out on modelling and optimization of wire electro discharge machining (WEDM) of Al 7075 alloy. The quantitative and qualitative improvements in corner accuracy and surface finish while maintaining the productivity have been studied in this research. Based upon extensive experimental investigation and subsequent analysis and optimization of the WEDM process, the following observations are made:

I. The pilot experiment was carried out at three different levels of conductivity settings i.e., 4 µS/cm, 12 µS/cm and 22 µS/cm to select the ranges of variable process parameters in a single pass cutting operation of Al 7075. It was noted that the process parameters settings for pulse on time are from 0.5 µs to 0.9 µs, arc on time is from 0.2 µs to 0.4 µs, pulse off time is from 14 µs to 34 µs, arc off time is from 10 µs to 30 µs, servo sensitivity is from 1 to 3, wire tension is from 0.8 kg to 1.6 kg and servo voltage is from 10 volt to 20 volt.

II. Three different sets of experiments were carried out at three different levels of conductivity settings (i.e. 4 µS/cm, 12 µS/cm & 22 µS/cm) to find the appropriate dielectric conductivity that was effective and suitable for optimal machining of Al 7075 in single pass cutting. Four independent process parameters such as open circuit voltage, pulse on time, pulse frequency and servo sensitivity were selected for experimentations. The level value of independent parameters was different in each conductivity setting. The Pareto optimization technique was implemented for all three levels of conductivity separately. Twenty sets of Pareto optimal solutions in each conductivity setting (i.e., 4, 12, and 22 µS/cm) were searched out from all possible combinations. From the experimental results, it was found that (unlike steel, where the optimum conductivity is 22 µS/cm) the 12 µS/cm conductivity setting gives the maximum cutting speed in a single pass cutting operation. However, the better surface finish and corner accuracy can be achieved at 4 µS/cm conductivity setting at the expense of (slower) cutting speed in rough cutting operations.

III. To further improve the corner accuracy and surface finish, multipass cutting of Al 7075 was employed. The findings from the single pass cutting operation of Al 7075 at

12 µS/cm conductivity setting were used for subsequent multipass cutting operation. Three different trim cutting strategies namely single, double, and triple trim cut, were carried out after the rough cutting operation. From the experimental results, it was observed that corner error, surface roughness, and cutting speed were strongly influenced by trim cutting process parameters, i.e., pulse on time and wire offset. It was further noted that surface roughness was not influenced by rough cutting parameters, but at the same time, corner error strongly depends on them. It was observed that corner error, surface roughness, and cutting speed increases as the trim cutting pulse on time was increased. On the other hand, corner accuracy and surface finish were improved, but cutting speed reduced as the wire offset value was increased.

IV. The Pareto optimization technique was employed on three different trim cutting strategies separately by introducing the new concept of effective cutting speed. Four different sets of Pareto optimal solutions were obtained in four different cutting conditions, i.e., rough cut alone and single, double, and triple trim cut separately.

V. An integrated Pareto optimization technique was carried out by combining single pass and multipass cutting to select the best machining strategy. After analysing the experimental results of multipass cutting operation, three critical corner error (138 µm, 73 µm, & 50 µm) and surface roughness (2.618 µm, 2.042 µm & 1.086 µm) values were obtained from the four types of cutting operations (i.e. rough cut and single, double & triple pass trimming). It was observed that from the optimized results, if the required corner error (C_E) or surface roughness (R_a) were more than 138 µm or 2.618 µm and up to 246 µm or 6.150 µm then rough cutting strategy can give the better result, on the other hand, if the required C_E and R_a values were less than of 138 µm or 2.618 µm and up to a limit 73 µm or 2.042 µm then single trimming operation can give the superior result. Similarly, if the required C_E and R_a values were less than of single trimming results (i.e. 73 µm or 2.042 µm) and up to 50 µm or 1.086 µm, then double trimming strategy can gives the best results. Now, if the desired C_E and R_a value less than of double trim cutting results (i.e. 50 µm or 1.086 µm) and up to 32 µm or 0.592 µm then triple trimming strategy will be the best choice.

VI. Based upon the Pareto optimized results, average corner error and surface roughness were calculated. It was observed that, from the calculated results, corner accuracy and

surface finish improved by 54% and 44% after a single trimming operation. On the other hand, corner accuracy and surface finish improved by 36% and 53% after the double trimming operation. Similarly, at the end of final finishing (after triple trim cut) operation, corner accuracy and surface finish were improved by 39%. The overall improvements in corner accuracy and surface finish after three successive trim cuts followed by rough cut were 82% and 84% respectively. It was noted that the corner accuracy and surface finish were not significantly improves by single trimming operation but remarkable improvements were observed after double and triple trimming operation.

VII. Surface characteristics analysis was carried out on rough and trim cut surfaces. Using SEM image analysis, it was observed that the formed craters were wider and deeper in the rough cut surface but the size of craters became smaller as the number of trim cuts increased. Only a few small craters and micro voids were observed at the end of the final trim cutting (triple trimming) operation. Similarly, from CCI surface analysis, wide craters and nuggets were observed in the rough cut surface, but mostly disappeared at the end of the triple trimming operation.

The present research work can be used directly for effective, efficient, and economical machining of Al 7075 material for industrial applications. Here, there are still some future scopes of research in this field. The effects of process parameters on wettability, HAZ, recast layer thickness and tribological behaviour can be further investigated. Besides, this proposed new integrated optimization techniques utilizing the concept of effective cutting speed may be used for other materials as well as other advanced machining processes.

Bibliography

Rajurkar K. P. and Wang W. M. (1997) 'Improvement of EDM Performance with Advanced Monitoring and Control Systems', Journal of Manufacturing Science and Engineering, Vol. 119(4B), pp. 770-775.

Puri A. B., and Bhattacharyya B. (2003) 'Modelling and analysis of the wire-tool vibration in wire-cut EDM', Journal of Materials Processing Technology, Vol. 141 (3), pp. 295-301.

Yan M. T., Huang C. W., Fang C. C., and Chang C. X. (2004) 'Development of a prototype Micro-Wire-EDM machine', Journal of Materials Processing Technology, Vol. 149 (1-3), pp. 99-105.

Kumar A., Maheshwari S., Sharma C., and Beri N. (2010) 'Research Developments in Additives Mixed Electrical Discharge Machining (AEDM): A State of Art Review' Materials and Manufacturing Processes, Vol. 25(10) pp. 1166-1180.

Kumar A., Kumar V. and Kumar J. (2012) 'A State of Art in Development of Wire Electrodes for High Performance Wire Cut EDM' International Conference on Advancements and Futuristic Trends in Mechanical and Materials Engineering, Punjab Technical University, Kapurthala, Punjab, India.

Ayesta I., Izquierdo B., Flaño O., Sánchez J. A., Albizuri J., and Avilés R. (2016) 'Influence of the WEDM process on the fatigue behavior of Inconel® 718', International Journal of Fatigue, Vol. 92 (1), pp. 220-233.

Zhang Y., Zhang Z., Zhang G. and Li W. (2020) 'Reduction of Energy Consumption and Thermal Deformation in WEDM by Magnetic Field Assisted Technology', International Journal of Precision Engineering and Manufacturing-Green Technology, Vol. 7, pp. 391–404.

Kavimani V., Prakash K. S., Thankachan T., Nagaraja S., Jeevanantham A. K. and Jhon J. P. (2020) WEDM Parameter Optimization for Silicon@r-GO/Magneisum Composite Using Taguchi Based GRA Coupled PCA', Silicon, Vol. 12 pp. 1161–1175.

Chaudhari R., Vora J. J., Parikh D. M., Wankhede V. and Khanna S. (2020) 'Multi-response Optimization of WEDM Parameters Using an Integrated Approach of RSM–GRA

Analysis for Pure Titanium', Journal of The Institution of Engineers (India): Series D, Vol. 101(1) pp. 117–126.

Devarasiddappa D., Chandrasekaran M. and Arunachalam R. (2020) 'Experimental investigation and parametric optimization for minimizing surface roughness during WEDM of Ti6Al4V alloy using modified TLBO algorithm', Journal of the Brazilian Society of Mechanical Sciences and Engineering, Vol. 42, pp. 128.

Chaudhari R., Vora J. J., Patel V., López de Lacalle L. N. and Parikh D.M. (2020) 'Effect of WEDM Process Parameters on Surface Morphology of Nitinol Shape Memory Alloy', Materials, Vol. 13, pp. 4943.

Sharma P., Chakradhar D. and Narendranath S. (2021) 'Measurement of WEDM performance characteristics of aero-engine alloy using RSM-based TLBO algorithm', Measurement, Vol. 179, pp. 109483.

Ishfaq K., Zahoor S., Khan S. A., Rehman M., Alfaify A. and Anwar S. (2021) 'Minimizing the corner errors (top and bottom) at optimized cutting rate and surface finish during WEDM of Al6061' Engineering Science and Technology, an International Journal, Vol. 24, pp. 1027-1041.

Sibalija T. V., Kumar S., Patel G. C.M. and Jagadish (2021) 'A soft computing-based study on WEDM optimization in processing Inconel 625' Neural Computing and Applications, Vol. 33, pp. 11985–12006.

ZHANG Y., ZHANG G., ZHANG Z., ZHANG Y., and HUANG Y. (2022) 'Effect of assisted transverse magnetic field on distortion behavior of thin-walled components in WEDM process', Chinese Journal of Aeronautics, Vol. 35 (2), pp. 291-307.

Wang J., Sánchez J. A., Izquierdo B., and Ayesta I. (2023) 'Effect of discharge accumulation on wire breakage in WEDM process', International Journal of Advanced Manufacturing Technology, Vol. 125, pp. 1343–1353.

Liao Y. S., Huang J. T. and Su H. C. (1996) 'A study on the machining-parameters optimization of wire electrical discharge machining', Journal of Materials Processing Technology, Vol. 71(3), pp. 487-493.

Prohaszka J., Mamalis A. G. and Vaxevanidis N. M. (1997) 'The effect of electrode material on machinability in wire electro-discharge machining', Journal of Materials Processing Technology, Vol. 69 (1–3), pp. 233-237.

Borsellino C., Filice L., Ruisi V. F. and Micari F. (1999) 'A Study on the Correlations between Machining Parameters and Specimen Quality in WEDM', Advanced Manufacturing Systems and Technology, International Centre for Mechanical Sciences book series (CISM, volume 406).

Gökler M. I. and Ozanözgü A. M. (2000) 'Experimental investigation of effects of cutting parameters on surface roughness in the WEDM process' International Journal of Machine Tools and Manufacture, Vol. 40 (13), pp. 1831-1848.

Kim C. H. and Kruth J. P. (2001) 'Influence of the electrical conductivity of dielectric on WEDM of sintered carbide' KSME International Journal, Vol. 15, pp. 1676–1682.

Guo Z. N., Wang X., Huang Z. G. and Yue T. M. (2002) 'Experimental investigation into shaping particle-reinforced material by WEDM-HS' Journal of Materials Processing Technology, Vol. 129 (1–3), pp. 56-59.

Tosun N. and Cogun C. (2003) 'An investigation on wire wear in WEDM', Journal of Materials Processing Technology, Vol. 134 (3), pp. 273-278.

Kozak J., Rajurkar K. P. and Chandarana N. (2004) 'Machining of low electrical conductive materials by wire electrical discharge machining (WEDM)', Journal of Materials Processing Technology, Vol. 149 (1–3), pp. 266-271.

Sarkar S. Mitra S. and Bhattacharyya B. (2005) 'Parametric analysis and optimization of wire electrical discharge machining of γ-titanium aluminide alloy', Journal of Materials Processing Technology, Vol. 159 (3), pp. 286-294.

Ozdemir N. and Ozek C. (2006) 'An investigation on machinability of nodular cast iron by WEDM', International Journal of Advanced Manufacturing Technology, Vol. 28, pp. 869-872.

Han F., Zhang J. and Soichiro I. (2007) 'Corner error simulation of rough cutting in wire EDM', Precision Engineering, Vol. 31 (4), pp. 331-336.

Aspinwall D. K., Soo S. L., Berrisford A. E. and Walder G. (2008) 'Workpiece surface roughness and integrity after WEDM of Ti–6Al–4V and Inconel 718 using minimum damage generator technology', CIRP Annals, Vol. 57 (1), 2008, pp. 187-190.

Somashekhar K. P., Ramachandran N. and Mathew J. (2010) 'Material removal characteristics of microslot (kerf) geometry in μ-WEDM on aluminum', The International Journal of Advanced Manufacturing Technology, Vol. 51, pp. 611–626.

Shah A., Mufti N. A., Rakwal D. and Bamberg E. (2011) 'Material Removal Rate, Kerf, and Surface Roughness of Tungsten Carbide Machined with Wire Electrical Discharge Machining', Journal of Materials Engineering and Performance, Vol. 20, pp. 71–76.

Selvakumar G., Sornalatha G., Sarkar S. and Mitra S. (2014) 'Experimental investigation and multi-objective optimization of wire electrical discharge machining (WEDM) of 5083 aluminum alloy', Transactions of Nonferrous Metals Society of China, Vol. 24 (2), pp. 373-379.

Sharma N., Khanna R. and Gupta R. D. (2015) 'WEDM process variables investigation for HSLA by response surface methodology and genetic algorithm', Engineering Science and Technology, an International Journal, Vol. 18 (2), pp. 171-177.

Yu H., Lian Z., Wan Y., Weng Z., Xu J. and Yu Z. (2015) 'Fabrication of durable superamphiphobic aluminum alloy surfaces with anisotropic sliding by HS-WEDM and solution immersion processes', Surface and Coatings Technology, Vol. 275, pp. 112-119.

Soundararajan R., Ramesh A., Mohanraj N. and Parthasarathi N. (2016) 'An investigation of material removal rate and surface roughness of squeeze casted A413 alloy on WEDM by multi response optimization using RSM', Journal of Alloys and Compounds, Vol. 685, pp. 533-545.

Kumar P. and Parkash R. (2016) 'Experimental investigation and optimization of EDM process parameters for machining of aluminum boron carbide (Al–B4C) composite', Vol. 20 (2), pp. 330-348.

Samanta A., Sekh M. and Sarkar S. (2016) 'Influence of different control strategies in wire electrical discharge machining of varying height job', International Journal of Advanced Manufacturing Technology, Vol. 100, pp. 1299–1309.

Gong Y., Sun Y., Wen X., Wang C. and Gao Q. (2017) 'Experimental study on surface integrity of Ti-6Al-4V machined by LS-WEDM' International Journal of Advanced Manufacturing Technology, Vol. 88, pp. 197-207.

Nain S. S., Garg D. and Kumar S. (2018) 'Evaluation and analysis of cutting speed, wire wear ration and dimensional deviation of wire electrical discharge machining of super alloy udimet-L605 using support vector machine and grey relational analysis' Advances in manufacturing, Vol. 6, pp. 225-246.

Bisaria H. and Shandilya P. (2019) 'Experimental investigation on wire electric discharge machining (WEDM) of Nimonic C-263 superalloy' Materials and Manufacturing Processes, Vol. 34(1), pp. 83-92.

Phate M. R., Toney S. B. and Phate V. R. (2019) 'Analysis of Machining Parameters in WEDM of Al/SiCp20 MMC Using Taguchi-Based Grey-Fuzzy Approach' Modelling and Simulation in Engineering, Vol. 2019, Article ID: 1483169, 13 pages.

Mandal K., Bose D., Mitra S. and Sarkar S. (2020) 'Experimental investigation of process parameters in WEDM of Al 7075 alloy', Manufacturing Review, 7, 30.

Straka L., Pite J. and Čorný I. (2021) 'Influence of the main technological parameters and material properties of the workpiece on the geometrical accuracy of the machined surface at WEDM' International Journal of Advanced Manufacturing Technology, Vol. 115, pp. 3065-3087.

Chen Z., Zhou H., Yan Z., Han F. and Yan H. (2021) 'Machining characteristics of 65 vol.% SiCp/Al composite in micro-WEDM' Ceramics International, Vol. 47, pp. 13533-13543.

Spedding T. A. and Wang Z. Q. (1997) 'Parametric optimization and surface characterization of wire electrical discharge machining process', Precision Engineering, Vol. 20 (1), pp. 5-15.

Liao Y. S., Huang J. T. and Su H. C. (1997) 'A study on the machining-parameters optimization of wire electrical discharge machining', Vol. 71 (3), pp. 487-493.

Spedding T. A. and Wang Z. Q. (1997a) 'Study on modeling of wire EDM processes, Journal of Materials Processing Technology, Vol. 69, pp. 8-28.

Han F., Kunieda M., Sendai T. and Imai Y. (2002) 'High precision simulation of WEDM using parametric programming', CIRP Annals, Vol. 51 (1), pp. 165-168.

Tosun N. (2003) 'The Effect of the Cutting Parameters on Performance of WEDM', KSME International Journal, Vol. 17 (6) pp. 816-824.

Tosun N., Cogun C. and Tosun G. (2004) 'A study on kerf and material removal rate in wire electrical discharge machining based on Taguchi method', Journal of Materials Processing Technology, Vol. 152 (3), pp. 316–322.

Hewiy M. S., El-Taweel T. A. and El-Safty M. F. (2005) 'Modelling the machining parameters of wire electrical discharge machining of Inconel 601 using RSM', Journal of Materials Processing Technology, Vol. 169 (2), pp. 328-336.

Ho K. H., Newman S. T. and Allen R. D. (2005) 'STEP-NC compliant information modelling for wire electrical discharge machining component manufacture', Proceedings of the Institution of Mechanical Engineers, Part B: Journal of Engineering Manufacture, Vol. 219 (10), pp. 777-784.

Sarkar S., Mitra S. and Bhattacharyya B. (2005) 'Wire electrical discharge machining of gamma titanium aluminide for optimum process criteria yield in single pass cutting operation', International Journal of Manufacturing Technology and Management, Vol. 7 (2-4), pp. 207-223.

Chiang K. T. and Chang F. P. (2006) 'Optimization of the WEDM process of particle-reinforced material with multiple performance characteristics using grey relational analysis', Journal of Materials Processing Technology, Vol. 180 (1-3), pp. 96-101.

Mahapatra S. S. and Patnaik A. (2006) 'Parametric Optimization of Wire Electrical Discharge Machining (WEDM) Process using Taguchi Method', Journal of the Brazilian Society of Mechanical Sciences and Engineering, Vol. 28 (4), pp. 422-429.

Ramakrishnan R. and Karunamoorthy L. (2008) 'Modeling and multi-response optimization of Inconel 718 on machining of CNC WEDM process', Journal of Materials Processing Technology, Vol. 207 (1-3), pp. 343-349.

Prasad D. V. S. S. S. and Kishna A. G. (2009) 'Empirical modeling and optimization of wire electrical discharge machining', International Journal of Advanced Manufacturing Technology, Vol. 43, pp. 914-925.

Chen H. C., Lin J. C., Yang Y. K. and Tsai C. H. (2010) 'Optimization of wire electrical discharge machining for pure tungsten using a neural network integrated simulated annealing approach, Expert systems with applications, Vol. 37, pp. 7147-7153.

Sarkar S., Ghosh K., Mitra S. and Bhattacharyya B. (2010) 'An Integrated Approach to Optimization of WEDM Combining Single-Pass and Multipass Cutting Operation', Materials and Manufacturing Processes, Vol. 25 (8), pp. 799-807.

Sadeghi M., Razavi H., Esmaeilzadeh A. and Kolahan F. (2011) 'Optimization of cutting conditions in WEDM process using regression modelling and Tabu-search algorithm', Proceedings of the Institution of Mechanical Engineers, Part B: Journal of Engineering Manufacture, Vol. 225 (10), pp. 1825-1834.

Goswami A. and Kumar J. (2014) 'Optimization in wire-cut EDM of Nimonic-80A using Taguchi's approach and utility concept', Engineering Science and Technology, an International Journal, Vol. 17 (4), pp. 236-246.

Rao T. B. and Krishna A. G. (2014) 'Selection of optimal process parameters in WEDM while machining Al 7075/SiCp metal matrix composites' International Journal of Advanced Manufacturing Technology, Vol. 73, pp. 299-314.

Lal S. Kumar S, Khan Z. A. and Siddiquee (2015) 'Multi-response optimization of wire electrical discharge machining process parameters for Al 7075/Al2O3/SiC hybride composite using Taguchi-based grey relational analysis' Proceedings of the Institution of Mechanical Engineers, Part B: Journal of Engineering Manufacture, Vol. 229, pp. 229-237.

Kumar V., Kumar V. and Jangra K. K. (2015) 'An experimental analysis and optimization of machining rate and surface characteristics in WEDM of Monel-400 using RSM and desirability approach', Journal of Industrial Engineering International, Vol. 11, pp. 297–307.

Gopalakrishnan R. and John E. R. D. (2017) 'Experimental Investigation and Multi Response Optimization of WEDM Process of AA7075 Metal Matrix Composites Using Particle Swarm Optimization', International Journal of Intelligent Engineering and Systems, Vol.10, No.4.

Kumar H., Manna A. and Kumar R. (2018) 'Modeling and desirability approach-based multi-response optimization of WEDM parameters in machining of aluminum metal matrix composite', Journal of the Brazilian Society of Mechanical Sciences and Engineering, 40, 458.

Mandal K., Sarkar S., Mitra S. and Bose D. (2019) 'Multi-Attribute Optimization in WEDM of Light Metal Alloy', Materials Today: Proceedings, Vol. 18, pp. 3492–3500.

Phate M. R. and Toney S. B. (2019) 'Modeling and prediction of WEDM performance parameters for Ai/SiCp MMC using dimensional analysis and artificial neural network', Engineering Science and Technology, an International Journal, Vol. 22, pp. 468-476.

Thangaraj M., Annamalai R., Moiduddin K., Alkindi M., Ramalingam S. and Alghamdi O. (2020) 'Enhancing the Surface Quality of Micro Titanium Alloy Specimen in WEDM Process by Adopting TGRA-Based Optimization', Materials, 13(6), 1440.

Mandal K., Sarkar S., Mitra S. and Bose D. (2020) 'Parametric analysis and GRA approach in WEDM of Al 7075 alloy, Materials Today: Proceedings, Vol. 26, pp. 660–664.

Chaudhari R., Vora J. J., Prabu S. S. M. Palani I. A., Patel V. K. and Parikh D. M. (2021) 'Pareto optimization of WEDM process parameters for machining a NiTi shape memory alloy using a combined approach of RSM and heat transfer search algorithm', Advances in Manufacturing Vol. 9, pp. 64–80.

Goyal A., Gautam N. and Pathak V. K. (2021) 'An adaptive neuro-fuzzy and NSGA-II-based hybrid approach for modelling and multi-objective optimization of WEDM quality characteristics during machining titanium alloy', Neural Computing and Applications, Vol. 33 pp. 16659–16674.

Hsue W. J., Liao Y. S. and Lua S. S. (1999) 'Fundamental geometry analysis of wire electrical discharge machining in corner cutting', International Journal of Machine Tools and Manufacture, Vol. 39 (4), pp. 651-667.

Lin C. T., Chung I. F. and Huang S. Y. (2001) 'Improvement of machining accuracy by fuzzy logic at corner parts for wire-EDM', Fuzzy Sets and Systems, Vol. 122 (3), pp. 499-511.

Kunieda M. and Furudate C. (2001) ‘High Precision Finish Cutting by Dry WEDM’, CIRP Annals, Vol. 50 (1), pp. 121-124.

Han F., Kunieda M., Sendai T. and Imai Y. (2002) ‘High precision simulation of WEDM using parametric programming’, CIRP Annals, Vol. 51 (1), pp. 165-168.

Puri A. B. and Bhattacharyya B. (2003) ‘An analysis and optimisation of the geometrical inaccuracy due to wire lag phenomenon in WEDM’, International Journal of Machine Tools and Manufacture, Volume 43 (2), pp. 151-159.

Sato T. and Shibata J. (2004) ‘Entrance mark control on precision WEDM’, Journal of Materials Processing Technology, Vol. 149 (1–3), pp. 129-133.

Yan M. T. and Huang P. H. (2004) ‘Accuracy improvement of wire-EDM by real-time wire tension control’, International Journal of Machine Tools and Manufacture, Vol. 44 (7–8), pp. 807-814.

Sanchez J. A., Lacalle L. N. L. D. and Lamikiz A. (2004) ‘A computer-aided system for the optimization of the accuracy of the wire electro-discharge machining process’, International Journal of Computer Integrated Manufacturing, Vol. 17 (5), pp. 413-420.

Takino H., Ichonohe T., Tanimoto K., Yamaguchi S., Nomura K. and Kunieda M. (2005) ‘High quality cutting of polished single-crystal silicon by wire electrical discharge machining’, Precision Engineering, Vol. 29 (4), pp. 423-430.

Sanchez J. A., Rodil J. L., Herrero A., Lacalle L. N. L. D. and Lamikiz A. (2007) ‘On the influence of cutting speed limitation on the accuracy of wire-EDM corner-cutting’, Journal of Materials Processing Technology, Vol. 182 (1-3), pp. 574-579.

Han F., Zhang J. and Soichiro I. (2007) ‘Corner error simulation of rough cutting in wire EDM’, Precision Engineering, Volume 31 (4), pp. 331-336.

Dodun O., Gonçalves-Coelho A. M., Slătineanu L. and Nagîţ G. (2009) ‘Using wire electrical discharge machining for improved corner cutting accuracy of thin parts, International Journal of Advanced Manufacturing Technology, Vol. 41, Article number: 858.

Lin P. D. and Liao T. T. (2009) ‘An effective-wire-radius compensation scheme for enhancing the precision of wire-cut electrical discharge machines’, International Journal of Advanced Manufacturing Technology, Vol. 40, pp. 324–331.

Wang W., Liu Z. D., Tian Z. J., Huang Y. H. and Liu Z. X. (2009) 'High efficiency slicing of low resistance silicon ingot by wire electrolytic-spark hybrid machining', Journal of Materials Processing Technology, Vol. 209 (7), pp. 3149-3155.

Sarkar S., Sekh M., Mitra S. and Bhattacharyya B. (2011) 'A novel method of determination of wire lag for enhanced profile accuracy in WEDM', Precision Engineering, Vol. 35 (2), pp. 339-347.

Hoang K. T. and Yang S. H. (2012) 'A study on the effect of different vibration-assisted methods in micro-WEDM', Journal of Materials Processing Technology, Vol. 213 (9) pp. 1616-1622.

Amineh S. K., Tehrani A. F. and Mohammadi A. (2013) 'Improving the surface quality in wire electrical discharge machined specimens by removing the recast layer using magnetic abrasive finishing method', International Journal of Advanced Manufacturing Technology, Vol. 66, pp. 1793–1803.

Bobbili R., Madhu V. and Gogia A. K. (2013) ' Effect of wire-EDM machining parameters on surface roughness and material removal rate of high strength armor steel, Materials and Manufacturing Processes, Vol. 28, pp. 364-368.

Maher I., Sarhan A. A. D. and Hamdi M. (2015) 'Review of improvements in wire electrode properties for longer working time and utilization in wire EDM machining' International Journal of Advanced Manufacturing Technology, Vol. 76 pp. 329–351.

Selvakumar G., Jiju K. B., Sarkar S. and Mitra S. (2016) 'Enhancing die corner accuracy through trim cut in WEDM', International Journal of Advanced Manufacturing Technology, Vol. 83, pp. 791–803.

Werner A. (2016) 'Method for enhanced accuracy in machining curvilinear profiles on wire-cut electrical discharge machines', Precision Engineering, Vol. 44, pp. 75-80.

Mouralova K., Matouseka R., Kovar J., Mach J., Klakurkova L. and Bednar J. (2016) 'Analyzing the surface layer after WEDM depending on the parameters of a machine for the 16MnCr5 steel', Measurement, Vol. 94, pp. 771-779.

Chen H., Zhao W. S., Xi X. C., Chen M. and Liang W. (2017) 'Non-circular parametric curve and curved surface interpolation and tool compensation for WEDM based on unit arc length increment method', International Journal of Advanced Manufacturing Technology, Vol. 88 pp. 1257–1266.

Mouralova K., Kovar J., Klakurkova L., Bednar J., Benes L. and Zahradnicek R. (2018) 'Analysis of surface morphology and topography of pure aluminium machined using WEDM', Measurement, Vol. 114, pp. 169-176.

Singh M. A., Sarma D. K. Hanzel O., Sedlacek J. and Sajgalik P. (2018) 'Surfacee characteristics and erosion phenomena in WEDM of alumina composites' Materials and Manufacturing Processes, Vol. 33, pp. 1815-1821.

Mandal K., Sarkar S., Mitra S. and Bose D. (2019) 'Surface roughness and surface topography evaluation of Al 6065-T6 alloy using wire electro discharge machining (wire EDM)' Advances in Materials and Processing Technologies, Vol. 6(1), pp. 75-83.

Farooq M. U., Ali M. A., He Y., Khan A. M., Pruncu C. I., Kashif M., Ahmed N. and Asif N. (2020) 'Curved profiles machining of Ti6l4V alloy through WEDM: investigations on geometrical errors', Journal of Materials Research and Technology, Vol. 9 (6), pp. 16186-16201.

Kirwin R. M., Moller J. C. and Jahan M. P. (2021) 'Modification and adaptation of wire lag model based on surface feed for improving accuracy in wire EDM of Ti-6Al-4V alloy' International Journal of Advanced Manufacturing Technology, Vol. 117, pp. 2909–2920.

Sharma P., Chakradhar D. and Narendranath S. (2021) 'Precision manufacturing of turbine wheel slots by trim-offset approach of WEDM' Precision Engineering, Vol. 71, pp. 293-303.

Phadke, M.S. (1989) 'Quality Engineering Using Robust Design' Prentice Hall International Edition, Englewood Cliffs, New Jersy, ISBN: 0137451679.

Cochran W. G. and Cox G. M. (1992) 'Experimental Designs' Asia Publishing House, Second Edition, ISBN: 978-0-471-54567-5.

Deb K. (2012) "Optimization for Engineering Design: Algorithms and Examples", Printec Hall of India Private Limited, Second Edition, ISBN: 978-81-203-4678-9.